Control Signal Transmission through Power Supply Cables

of a 3-Phase PWM Motor

by

Jose A. Mendez

Submitted to the Department of Electrical Engineering and Computer Science

in Partial Fulfillment of the Requirements of the Degree of

Master of Engineering in Electrical Engineering and Computer Science

at the Massachusetts Institute of Technology

February 4, 2006

Author_____
Department of Electrical Engineering and Computer Science
February 4, 2006

Certified by_____
Dr. Chathan M. Cooke
Thesis Supervisor

Accepted by_____
Arthur C. Smith
Chairman, Department Committee on Graduate Theses

Control Signal Transmission through Power Supply Cables

of a 3-Phase PWM Motor

by

Jose A. Mendez

Submitted to the

Department of Electrical engineering and Computer Science

February 4, 2006

In Partial Fulfillment of the Requirements for the Degree of
Master of Engineering in Electrical Engineering and Computer Science

ABSTRACT

Modern process control systems often employ accurate position or speed controlled PWM motors, which require feedback data for the drive control loop. Current methods require an independently shielded cable for feedback data transmission. This is due to the fact that high-voltage PWM signals could easily interfere with the feedback signals, which are typically one or more orders of magnitude smaller than typical PWM signals. We propose a "zero-wire" solution, in which the additional feedback cable used is eliminated, and the feedback data is sent simultaneously with the PWM signals in the same motor power conductors. In this study, we first analyzed the characteristics of typical feedback and PWM signals. Additionally, a standard representative motor drive cable was carefully measured and analyzed for its wave transport characteristics. The results lead us to select an RF modulation approach in which we modulate the data signals to 900MHz. The data signals are injected and extracted from the power conductors using feed-through capacitors and high-pass filters. To test the performance of our approach, we build a model system in which simulated PWM signals were applied to a 30m motor power cable fitted with data couplers and 900MHz RF RS232 data modems for modulation. Tests with different cables and attenuation were performed and data error rates measured. The error rates for strong RF signals, RSSI (Received Signal Strength Indicator) values higher than -60dBm, were limited by RF modem performance to 0.01%. Error rates did not increase with or without PWM power signals when RSSI values were over -80dBm. A design for transmission of DC power for motor feedback electronics is presented, in which we choose an intermediate frequency carrier at 1MHz to transmit power. The 1MHz signals are injected and extracted through the same feed-through capacitors using band-pass filters. Measurements and simulation have shown that the new feedback data transport system design developed in this project is effective and feasible.

Acknowledgements:

I would like to thank my thesis advisor, Dr. Chathan M. Cooke. If not for his constant encouragement, wealth of knowledge and technical expertise, this project would not have been possible.

I would also like to extend thanks to our sponsor company, Danaher-Motion®, who provided us with all the financial support we required.

INDEX:

1. INTRODUCTION

1.1 Overview

This chapter includes a short presentation of the main issues and tradeoffs for this study which concerns data transport for servo motor control. A new improved approach is proposed and compared to present day systems. The goals for this new work and the organization of this project are also presented.

1.2. The Servo-Motor System

There are four basic components in an electrical servo-motor system. First, we need a controllable power source, the drive, which yields the variable power signals that provide power to the motor. Secondly, we have a means of transferring the power signals from the drive to the motor, i.e. a power cable. Thirdly, we require a way of measuring and controlling the motor itself, a feedback system. This feedback system, residing at the motor end measures motor status variables and relays the information back to the drive. Finally, we have, of course, the motor itself. These mechanisms are used in a myriad of applications, from food and packaging industries and electronic component manufacturers to heavy industrial applications like precision metal cutting machines. It is this great variety of applications which produces servo motor systems with requirements which vary widely (to the extent of producing specs which differ by orders of magnitude). The wide variety of applications and conditions make for a very interesting field of research.

1.3. Current Solution: Extra Feedback Cable

A substantial problem with servo motor systems is that interference between power and feedback signals is common. While power signals can range from 120V up to the kV range, feedback signals are generally below the 10V range. Furthermore, power signals use PWM (pulse width modulation), which include fast transitions and thus, substantial high frequency content. For these reasons, power and feedback signals must be electrically and magnetically isolated from each other. This conflicts with the fact that feedback and power signals must travel through similar paths, and thus physical separation is not practical. The current solution for this problem is to use two separate heavily shielded cables (or a "bundled" solution, which includes two separately shielded cables wrapped together in a larger diameter cable). This implies added costs and sizing problems. Appendix I provides a compilation of present day specifications and requirements. This is the problem we will asses and investigate.

1.4. Zero-Wire Solution

To solve the problem of feedback transmission we propose getting rid of the extra feedback cable altogether to explore the possibility of sending the feedback data concurrently with the same power signals in the same conductor. For the purposes of this investigation, we will focus on using all the conductors in the power cable in parallel for feedback transmission with the shielding used as a common ground. Some other options which were not studied include, for example, transmitting feedback information using two of the power cables as a balanced differential pair. This solution could help in suppressing interference and ground loop problems.

1.5. Thesis Goals and Organization

The main goals of this investigation are:

1. Characterize typical PWM and feedback signals in time and frequency domain
2. Measure the characteristics (high frequency) of a typical, affordable 3-phase PWM motor power cable
3. Use a modulation technique (and carrier frequency) to separate the feedback signals from the PWM signals in the frequency domain
4. Design passive coupling circuits to inject and extract feedback signals without affecting PWM signal transmission
5. Create a model system to simulate real PWM signals
6. Design for transmission of DC power for motor feedback electronics
7. Test our system for reliability
8. Propose options for further investigation

Regarding the thesis organization, after this first chapter, the introduction, which serves as a quick background of the issues and the direction of this investigation, we offer a chapter on theory and background. This chapter contains theoretical principles and background from which the system will be developed. Chapter three introduces the devices and apparatus that will be used for measurement and testing. Furthermore, this chapter will also include diagrams of the different experimental setups used for testing and data acquisition. Chapter four presents results, data, plus analysis and preliminary conclusions. Finally, chapter five includes concluding remarks and proposed directions for future work and investigation.

2. THEORY AND BACKGROUND

2.1. Information Transmission in Noisy Environments

2.1.1. Introduction

As power requirements for information transmission decrease, so does the ratio between information signal power and noise signal power. This imposes challenges for reliable, error-free information transmission. The sources of this noise can be anything from random environmental noise, such as that caused by thermal fluctuations to interference or "jamming" caused by other nearby transmitters. A simple unidirectional information transmission setup can be modeled as shown in figure 1 below:

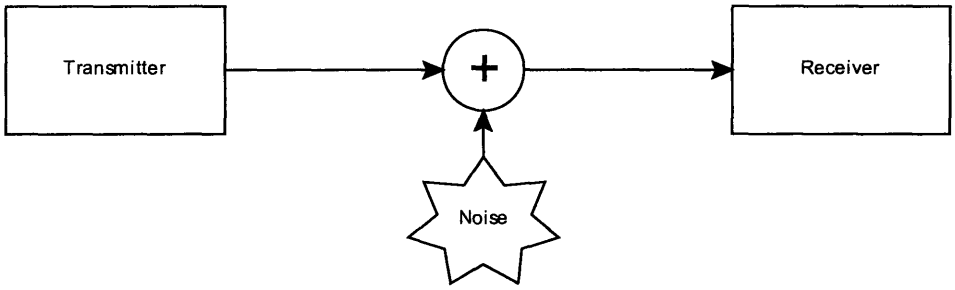

Information transmission through a noisy channel
figure 1.

The problem arises when the added noise signal power in the transmission channel is comparable to the transmitted signal power. In this case, the receiver would not be able to differentiate between information signals and induced noise signals, making the communication slow or unreliable. Of course, there are many existing solutions created to overcome this problem. Because our main purpose is to create a robust system to transmit information in the presence of motor signals, which for our purposes, can be

thought of as channel-added noise, we will briefly discuss some of the existing solutions to communication in noisy environments.

2.1.2. Noise rejection by frequency band separation

What are we specifically referring to when we talk about channel noise? Channel noise is, in its simplest terms, anything that arrives at the receiver end which was not transmitted. This includes, among other things, everything from random thermal fluctuations, signal pickup from other transmission sources, and even unaccounted nonlinearities in the transmission channel. If we look at all these noise sources in the frequency domain, they can range from white noise, with an ideally constant spectral density at all frequencies, to Gaussian noise with bell-shaped spectral density characteristics. This immediately brings the idea of separating the noise from the signal by simply deliberately choosing transmission frequencies in which the noise levels are low.

2.1.2.1. Principles of operation

Suppose we could somehow determine the frequency fn at which a certain band-limited noise source exists, for example, in the case of our motor, this noise would just correspond to the spectral content of the motor power signals. Then, we could choose a frequency ft such that the transmission frequency band does not interfere with the noise frequency band. The general idea of this frequency band separation is shown on figure 2:

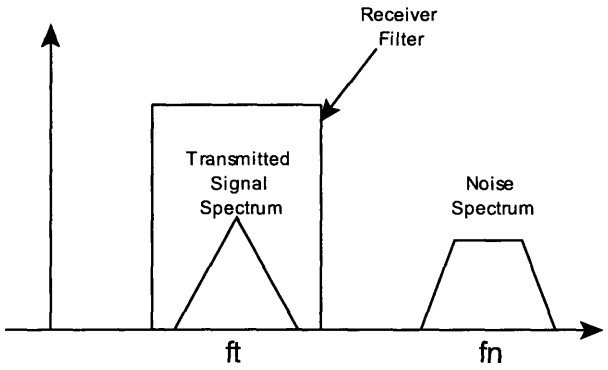

Noise rejection by frequency band separation
figure 2.

The idea is to send a band-limited information signal at a different center frequency of that of the noise signal. Then, both signals are sent concurrently on the transmission channel. Given that we chose a center frequency for the transmission signal that is sufficiently apart from the noise frequency, the signals will not overlap in the frequency domain. Then, we can obtain our wanted signal by simply passing the received signal, noise+data through a band-pass filter centered at our transmission frequency.

This static procedure would work perfectly in a situation in which the band-limited spectral content and central frequency of the noise is predictable or well defined. Unfortunately, this is not usually the case. For example, if one is attempting to transmit information with a mobile platform, the relative strengths, frequencies and distributions of the interfering noise signals may vary greatly. This is exactly the case for cellular phone technology. To illustrate some current solutions to this dilemma, let's look at some existing examples.

2.1.2.2. Existing Examples: Cell-phones, Wi-Fi, Spread Spectrum

Few existing technologies have to deal with varying noise and interference as efficiently and transparently as the cellular phone. During a call, a user may move closer or further from sources of interference, for example, base stations or other users. The

quality of the transmission channel might also vary greatly, with changing line-of-sight distances and wildly changing multi-path communication. How do cell phones and other interference prone wireless technologies (such as Wi-Fi) solve this problem? The currently prevalent solution is based on a technique which was conceived in the 1940's called frequency hopping.

Frequency hopping (now usually called "spread spectrum") is a technique of communication which addresses the problems of interference and jamming. Initially considered as a way to overcome deliberate jamming of communication channels during war times, it consists on rapidly changing the center frequency of the transmitted signal. By hopping around different frequencies, the energy of the transmitted signal is spread out in the frequency domain, thus reducing the effect of sources of interference at specific frequencies.

For example, say we are attempting to transmit information at a center frequency of 100MHz. If we use narrowband transmission, any source of noise operating at a frequency of 100MHz (an FM radio station, for example), would add up directly to our transmitted signal, thus increasing our probability of error. If this same signal is instead transmitted using frequency hopping methods, although the received signal at 100MHz would be corrupted, the information received at other frequencies would not. Thus, this type of wide-band transmission attains better noise and interference rejection at the cost of utilizing a larger portion of the frequency spectrum (higher bandwidth). Variations of this spread spectrum transmission principle exist in practically any currently existing cellular phone and Wi-Fi wireless broadband technology.

This spread spectrum technology can be used more efficiently by refining the frequency-selecting algorithm. We have several options for determining how we are going to change the transmission frequency. One option is to set a certain pattern of frequencies and program this into both the transmitter and receiver. This way, we start with a certain frequency, after some determined time, move to another frequency and so on, repeating the pattern indefinitely. Another option is to select a random sequence as our frequency transmission list. Finally, one could use a more sophisticated method, in which we first determine a relatively "quiet" piece of the spectrum and then send our precious information in that frequency. This technique is used by the HPA (home plug alliance) protocol, an Ethernet over power lines system which will be discussed with more detail on section 2.2.3.

So, we have discussed existing methods for rejecting band-limited interference noise sources, even if those are dynamic in frequency and power. The important term we need to address next is "band-limited". What about noise sources that are clearly not band limited, such as white noise? Is there a way to deal with inherently wide-band noise, optimizing our noise rejection?

2.1.3. Noise rejection by modulation

A very useful technique we can exploit to make our communication systems more robust and resistant to noise is modulation. In short, modulation is the action of taking some information signal and transforming it utilizing a given reversible algorithm such that the original signal can be recovered by applying the reverse of the algorithm. The principles of modulation and sample modulation techniques will be covered with more

detail on section 2.7. Using different principles of modulation, one can change an original data stream into a set of chosen symbols. These symbols can be represented in the transmitted signal in different ways, such as, signal amplitudes, frequency or phase. This allows us to choose modulation schemes which deliberately avoid the effects of noise by choosing symbols with sufficiently distinct representations, such that a transmitted symbol is not received as a different symbol due to noise.

2.2. Current Electrical Solutions for Data over Power

2.2.1. Introduction

The idea of utilizing existing power transmission infrastructure to transmit electrical information is not new. In the last few decades, several technologies have emerged for transmission and detection of high-frequency information carrying signals through power cables in the presence of high-voltage power signals at respectable data rates and long transmission distances. Because our purpose is to transmit data signals in the presence of high voltage power signals, it is of interest to briefly discuss some of the existing technologies to get a basic idea of how to approach our problem.

Of course, existing Ethernet over power technologies deal with power signals which are ideally sinusoidal, with a center frequency close to 60MHz. These signals, thus have very well behaved spectral content, with almost no high-frequency components. In the case of our PWM signals, which are ideally square waves with a fundamental frequency close to 10KHz, the spectral content should spread out to higher frequencies. Thus, although the basics are similar, transmission of information in the presence of high-voltage, well defined signals, our problem is a little more complicated, with power signals that spread out in the frequency domain. Given these considerations,

let's look briefly at some of the current solutions for information transmission over power lines.

2.2.2. BPL (broadband over power lines) technologies

BPL refers to broadband over power lines, an idea which has recently developed momentum as an alternative for communication to rural areas, where power networks exist but construction of new communication networks would be too inefficient or expensive. A similar system, PLC, which stands for power line carrier has been used for many years by power utility companies for control and monitoring of remote equipment and stations. This technology uses carrier frequencies ranging from 150KHz to 490KHz in the US and from 30KHz to 150KHz in Europe for communication [12, 14]. One of the main problems that arises by using these frequency ranges is that there is significant EMI and radio signal pickup, as long power line cables, which are not manufactured for high speed or high frequency signal transmission, serve as super long antennas. This, coupled with the fact that the transmission frequencies are relatively low, result in low throughput rates which, although suitable for some monitoring and control systems, are unacceptable for high speed data transmission.

The proposed BPL protocol would use higher frequencies, between 2MHz and 80MHz. Because high power cables are not designed to carry high frequency signals efficiently, repeaters must be placed every couple of hundred meters of power line to re-amplify and relay the information down the line. Another problem which arises with this information transmission scheme is the presence of transformers and relay stations in the power network. The frequency response of high power takedown transformers has a very

low magnitude for high signal frequencies, as they are ideally designed to transmit at frequencies in the order of 60Hz. For this reason, BPL networks are proposed to work only as localized networks. In such a setup, the main information hub is located at the high voltage to medium voltage substation. Here, the information is modulated up to the desired transmission frequency and coupled into the medium voltage line through magnetic coupling.

Magnetic coupling works by transmitting a signal from one cable to another through the mutual inductance of the cables. A simple magnetic coupler is a high frequency transformer. Signals are transmitted through the transformer although there is no direct electrical connection between the terminals. This allows us to couple in information-carrying high frequency signals without loading our circuitry with high voltage power signals. These signals are then sent down the medium voltage power lines.

The next barrier is the step down transformer which reduces the voltage from medium voltage to household voltage levels. There are several proposed solutions for overcoming the inefficient high frequency behavior of the transformers. The first is just to boost up the power of the information signal such that it survives the journey through the transformer. Although this is a simple enough solution, it is not very efficient. The other option is bypassing the transformer altogether. This can be achieved by magnetically coupling in and out at the input and output side of the transformer in a similar manner in which we originally injected the signal at the substation, thus effectively eliminating the transformer problem entirely. The last proposed solution is to use the step down transformer stations as Wi-Fi towers. A Wi-Fi transmitter is attached

at each take down transformer station and then individual users connect through the network wirelessly through the station.

Although all these ideas seem reasonable and feasible, they do not come with their own set of drawbacks, mainly EM radiation. As previously stated, power line conductors are not shielded, therefore, they will radiate eagerly when excited with high frequency signals. Wide implementation of this technology could cause serious interference problems for short wave (HAMs) and other radios. Currently, regulations are being constructed to address this problem.

2.2.3. Home Plug (HPA) compliant

While BPL attempts transmission of Ethernet over medium voltage power lines over very long distances, there are several other technologies which exploit the power networks already available at homes and offices. HPA, which stands for HomePlug Alliance is one of the dominating protocols in this area. The technology is similar to that of BPL, except of course, that the voltage power signals that are present in user-end power drops are less than a decade below those of the medium voltage power signals BPL is designed to operate with. One of the issues that HPA is specifically designed to deal with is drastic changes in power line network conditions. In a normal household, the properties of the power network depend heavily on many uncontrollable factors such as which appliances are running at which times. For example, devices such as electric power drills and vacuum cleaners are great sources of static which degrade the quality of the communication line. According to specifications, HPA network devices avoid these pitfalls by using a form of frequency hopping by "listening" to the power network and

determining a relatively quiet frequency to transmit information. With the use of these techniques, HPA networks are able to routinely achieve broadband Ethernet speeds of up to 14Mbps under normal working environments.

Although these technologies solve a problem which is in some ways similar to ours, our solution must, furthermore, have short delay times (less than 10us). Delay is not considered an issue for most computer networking environments, but in our case, long delays are not acceptable, as we are designing for motor feedback control which must react quickly to any changes in the conditions.

2.3. Motor Feeder Cable Characteristics

2.3.1. Introduction

On previous sections we have addressed the problems of information transmission in noisy environments. In the following sections we will focus on the issue of the quality of our proposed conductor, the motor power feeder cable. These motor power cables are designed to transmit high voltage power signals, in which high frequency information is not essential. For this reason, motor power cables have poor high frequency characteristics as compared to, for example, a coaxial cable. This is going to be one of the main problems to be addressed during the development of the proposed solution.

2.3.2. Physical structure of motor power cables

We will focus our research in 3-phase PWM power cables as our test system utilizes a 3-phase PWM motor. Although this might seem as a very specific case, the results are applicable to other situations, as the main issues to be encountered will be very

similar. The general structure of a 3-phase, 4-wire PWM power cable is shown in figure 3.

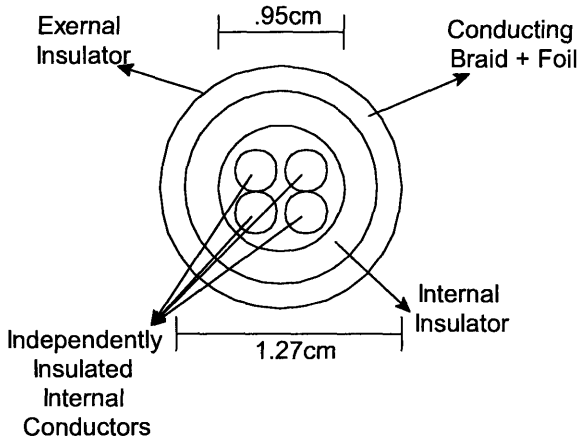

Cross-sectional view of 4-conductor motor feeder cable for a 3-phase motor
Figure 3.

The structure of a general 4 conductor motor feeder cable is as follows. Four individual insulated cables are at the center of the conductor, 3 cables for the 3 phases of the motor and an additional cable for ground. These four cables are bundled together at the center of the cable and wrapped with a conducting foil and braided metal shield which is usually tied to ground. This structure is in turn wrapped in a final insulating material. The reason for the shielding in this cable might appear confusing at first. If this cable is designed for transmission of high voltage power signals, why should we care about shielding the signals against EMI interference? After all, the signal levels in this cable will routinely exceed 100V. The truth is that this shielding is not intended to protect the power signals from EMI interference, but designed to prevent EMI radiation from the PWM signals to the outside world. Current solutions for feedback control of these motors require an additional cable for transmission of the feedback signals. In general, this feedback cable will be installed such that it lies in the same pathway as the power

cable, and a short distance from it. Thus, to prevent harmonics emanating from the power cable to couple in to our feedback signals, power cables are usually well shielded.

The final note on the physical structure of these power cables is that they can vary in length from a few meters to hundreds of meters. Some 3-phase motors are utilized in environments in which the motor and the drive system need to be physically separated, either because of specifics of production (such as harsh operating conditions at the motor end) or because of the advantages resulting from the economies of scale of centralizing the drive system of several motors that need to be controlled simultaneously. Therefore, some of these motor feeder cables can be substantially long, something that we must take into account for our solution.

2.3.3. Literature review on power cable performance

Although power cables are not necessarily designed for high frequency signal transmission, they are designed for transmission of relatively fast transients, as those present in PWM signals. Because this rise time is directly related to bandwidth, there is some literature about characteristics of motor cables at frequencies higher than the usual PWM frequencies of 10KHz. All of the studies and papers found dealing with this topic characterize the power cable up to frequencies in the order of 1MHz.

2.3.3.1. Frequency-domain characterization

The following figure, extracted from Moreira [10], shows the calculated characteristic impedance of an unshielded, 4 wire cable. The characteristic impedance was measured here by tying together two of the conductors and measuring the impedance between these two conductors and a third one. The fourth conductor was tied to ground.

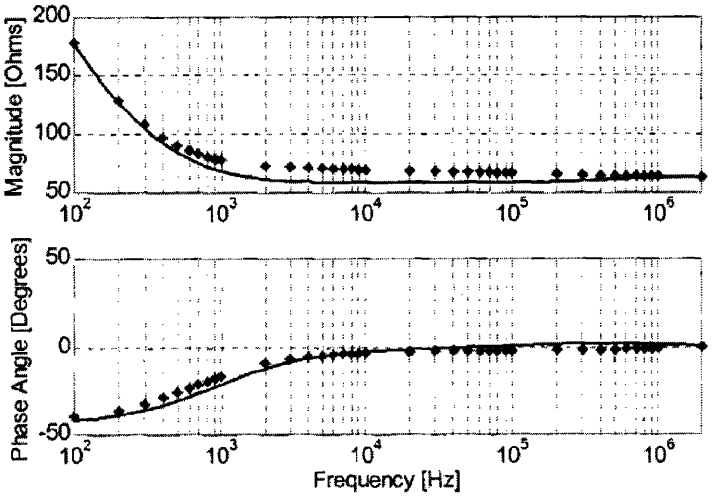

Measured characteristic impedance; 4-wire cable, 2-wires to 3rd wire, 4th wire tied to gnd [10]
Figure 4.

Although this test only covers frequencies up to 2MHz, we can see the beginning of some of the problems we expect to face at higher frequencies. The signal losses of the cable increase rapidly as frequency increases. Thus, we would expect that for very high transmission frequencies the power cable will have very low effective transmission (very lossy) and decreasing our high frequency transfer response magnitude.

2.3.3.2. Cable reflections and oscillations

Another motor feeder cable characteristic that has been studied in literature is voltage ringing and overshoot at the motor end. An example from Moreira of this overshoot and ringing is shown below in figure 5

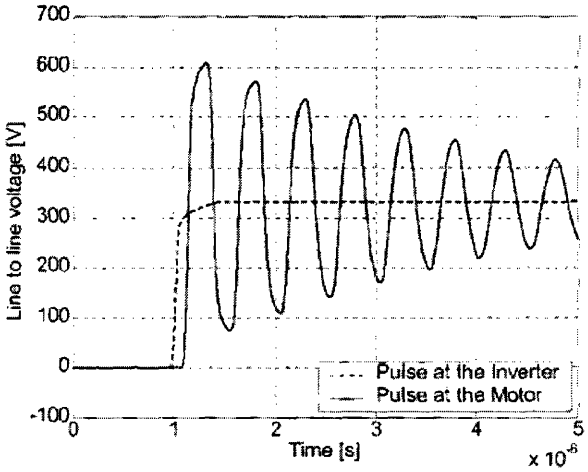

Motor power signal overshoot and ring at the motor end [10]
Figure 5.

In this example, the PWM signal at the motor end oscillates with an initial amplitude which is double the amplitude of the transmitted signal and a frequency of about 2MHz. This high frequency oscillation can be explained as a result of signal reflections at the motor end caused by impedance mismatch between the cable and the motor. The topics of signal reflections, transmission lines and impedance mismatch will be addressed in section 2.5.

Although this short literature review gives us some insight on what the characteristics of the power cable might be at low frequencies, we need to better understand conductor frequency-dependent non idealities which might become significant factors of signal loss as the transmission frequency increases.

2.4. High Frequency Conductor Losses

2.4.1. Introduction

As we increase our frequencies of interest, many of our low frequency lumped circuit assumptions start to break down. For example, what is a lossless wire at low

frequencies behaves inductively at higher frequencies. Furthermore, if we keep increasing the frequency to even higher levels, wires start introducing non-negligible losses into our system. In the following sections, we will investigate these frequency dependent non idealities of conductors to better predict and analyze how our power cable behaves at very high frequencies.

2.4.2. The skin effect

Skin effect is the term given to a phenomenon in which the series impedance of a conductor appears to increase with increasing frequency. To clarify this point, let's begin by recalling what factors constitute our calculations for series impedance. The low frequency resistance per unit length of a conductor is given by the well known equation:

$$R_0 = \frac{1}{A_c \sigma}$$

Where Ac is the effective cross sectional area of the conductor and sigma is the conductivity of the material from which the conductor is constructed. The skin effect comes into play by decreasing the quantity Ac, the effective cross sectional area. Even though the physical cross sectional area of the conductor is fixed and given by the physical dimensions of such conductor, the *effective* cross sectional area is a function of frequency. This frequency dependent Ac gives rise to the skin effect.

2.4.2.1. Description of the skin effect

In it's simplest terms, skin effect is caused by internal magnetic fields in the conductor inducing reverse currents to rapidly changing signals at the center of the conductor and adding in-phase currents at the edges. Refer to figure 6 below.

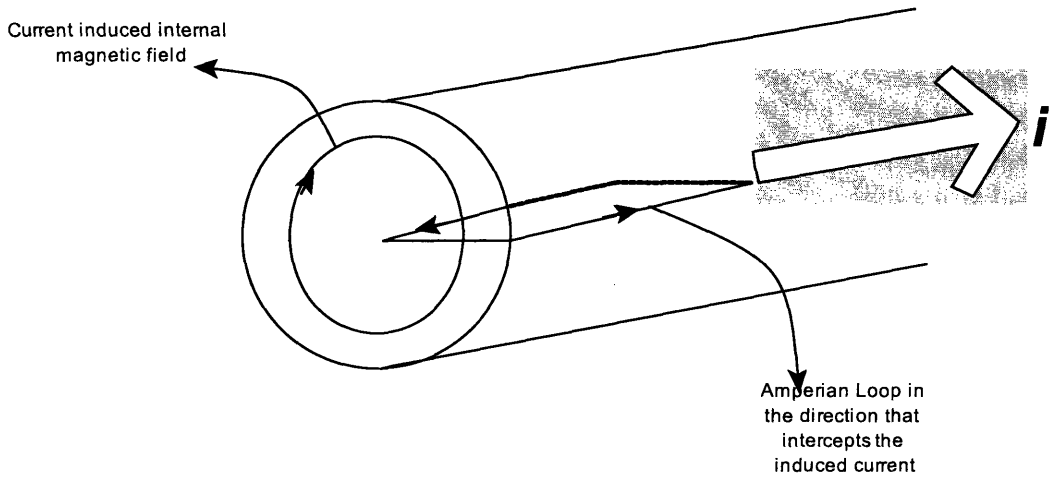

The skin effect
figure 6.

Suppose we have a current in the direction shown by the large arrow in the diagram. Then, we know that:

$$\oint_C B \cdot ds = \mu_0 I_{encl}$$

,where B is the magnetic field, u0 is the permeability of free space and Iencl is the current which flows through the closed surface. Therefore, the direction of the magnetic field induced by the current going into the cable as shown will be clockwise. If we construct an amperian loop as shown, positive magnetic flux is defined by the RHR as going upwards. Then, we recall that:

$$\oint_C E \cdot ds = -\frac{\partial}{\partial t} \oiint_S B \cdot dA$$

,where E is the induced electric field around the closed curve. The expression at the right hand side simply refers to the change in magnetic flux (negative) with respect to time through the closed surface S. To comprehend how skin effect works, imagine that the input current "I" is sinusoidal and of high frequency. If the current into the conductor is increasing, the induced magnetic field is increasing and thus, there is a net negative

change in magnetic flux through the amperian loop. Because the induced electric field is the *negative* of the change in magnetic flux, the induced current will be in the same direction as the amperian loop, as shown. The net result is that there is an induced current through the center of the conductor that is in *opposite* direction of the conductor current, while there is an induced current at the surface of the conductor which is in the same direction as the conductor current. Therefore, as we increase the frequency (which increases the magnetic flux time derivative), more and more of the current will flow through the edge of the conductor, as the induced currents will effectively cancel the currents closer to the center. Figure 7 below shows the progression of effective conductive cross sectional area as we increase frequency.

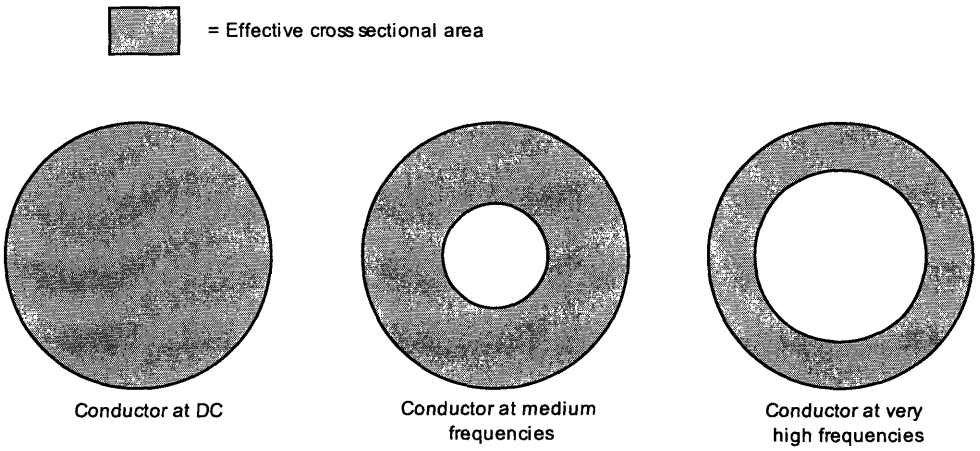

Reduction of effective cross sectional area due to skin effect figure 7.

2.4.2.2. Mathematical model

Now that we have discussed the basics of what causes skin effect and how increasing frequency increases effective series impedance, we can go into some existing mathematical models to describe this behavior more precisely. There are many mathematical models for skin effect, with varying levels of depth and complexity. To

choose which of these models we will explore, we need to remember why we are investigating the skin effect. Our main purpose is to determine whether or not skin effect will be an important contribution to signal attenuation in our cable, and, if it is, how will this attenuation change with increasing frequency.

Literature agrees that, given a certain degree of approximation, the effective increase in series resistance due to the skin effect is proportional to the square root of frequency. A way to understand where this term comes from is by introducing a term commonly used when addressing skin effect: the skin depth. The skin depth, normally denoted by the Greek letter lowercase delta; δ is the thickness of the effective conductive area at a given frequency, and is given by [8]:

$$\delta = \sqrt{\frac{1}{\pi \mu_0 \sigma f}} = \sqrt{\frac{\rho}{\pi \mu_0 f}}$$

To see where the square root impedance dependence arises, recall that the effective cross sectional area is given roughly by:

$$A_c = \pi (r + \delta)^2 - \pi r^2$$

which, after some manipulation, simplifies to:

$$A_c = 2\pi r\delta + \pi \delta^2$$

In the regions where skin effect is substantial, the skin depth, by definition must be small compared to the radius of the dead zone, thus, we can neglect the second order term, concluding that the effective series resistance is approximated by the simple equation [8]:

$$R = \frac{1}{A_c \sigma} = \frac{1}{2\pi r \sigma \sqrt{\frac{1}{\pi \mu_0 \sigma f}}} = \frac{\sqrt{\mu_0 f}}{2r\sqrt{\pi \sigma}}$$

which shows the monotonically increasing dependence of series resistance on the square root of frequency, as claimed by literature.

Of more importance than the absolute series resistance is the ratio of series resistance at a certain high frequency to the series resistance at DC. After all, we care about the cable having higher losses at high frequencies *as compared to* the losses at DC. This ratio is given by:

$$\frac{R(f)}{R_{DC}} = \frac{\frac{\sqrt{\mu_0 f}}{2r\sqrt{\pi\sigma}}}{\frac{1}{\pi r^2 \sigma}} = \frac{r\sqrt{\pi\mu_0\sigma f}}{2}$$

One important thing to note about this last equation is that the series resistance ratio (and thus the signal attenuation) at high frequencies is higher for cables with greater radii. This is to be expected, as there is more effective cross sectional area to be lost more quickly due to skin effect for a thicker cable. This is the reason why most high speed cables are very thin. Motor power cables have to be designed with the constraint that they must be able to efficiently carry high currents, which, unfortunately for our high speed transmission hopes, means that these cables are relatively thick for RF frequencies. Therefore, we expect skin effect to be a significant contributor to signal attenuation at higher frequencies.

2.4.3. Dielectric loss

At very high frequencies, other types of signal loss mechanisms become significant. The most notable is dielectric loss. Dielectric loss is the collective term given to any kind of signal attenuation which is caused by power dissipation in the insulating dielectric that separates the interior conductor from the exterior shield. The

two main causes of dielectric loss, dipole relaxation and conduction loss will be reviewed.

2.4.3.1. Conduction losses

Conduction losses are present at all frequencies, and refer to the fact that there are no ideal insulators in the real world. With modern materials and signal levels, though, conduction losses tend to be small. In general, conduction losses are significant when dielectrics are operating in breakdown region, where the electric field present in the dielectric is strong enough to rip electrons off the molecules of the dielectric thus producing conduction. Because we are not investigating the behavior of the cable at extremely high voltage levels, conduction losses can be neglected.

2.4.3.2. Dipole relaxation

A mechanism for dielectric loss that we might need to take into account, though, is dipole relaxation, as its effect is monotonically increasing with frequency. As shown in figure 8, a dielectric is an insulating material which is composed of molecules that polarize under the effects of an electric field. When an electric field is applied, these molecules will experience an electrostatic force forcing them to align with the field.

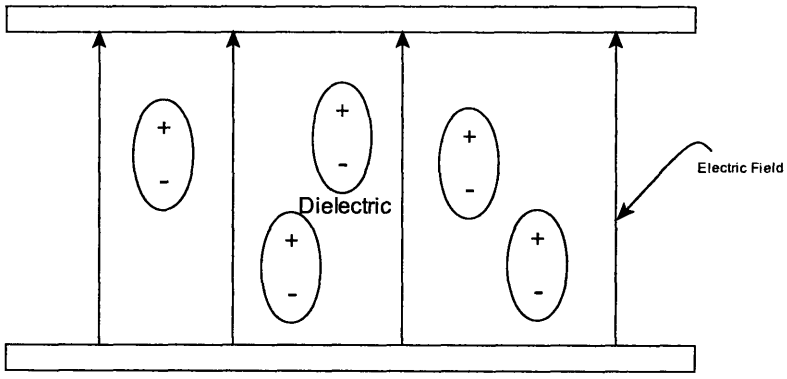

Dielectric polarized molecules align with electric field figure 8.

The source for loss arises when this static figure is changed into a more dynamic one. Suppose that instead of applying a simple constant electric field we apply a rapidly changing field. Sometime during the transition between positive and negative electric field the molecules must rotate and realign, as shown in figure 9. Because this transition cannot occur instantaneously, the molecules must temporarily arrange themselves in a higher energy state before they realign with the electric field. This extra energy is then dissipated in the dielectric mostly as intermolecular friction and heat.

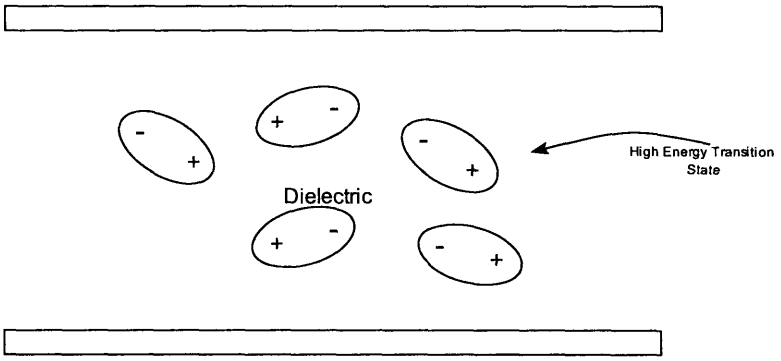

Intermediate high-energy transition state from positive to negative electric field figure 9.

At very high frequencies and signal power levels the dielectric dissipation loss can be quite significant. Microwave ovens, for example, work exploiting dielectric loss.

2.5. Transmission Line Theory

2.5.1. Introduction

A transmission line is a structure used to transfer energy from one point to another. More specifically, in the world of electrical engineering transmission line refers to a structure which guides electromagnetic energy from one point to another. Some examples of transmission lines include coaxial cables, waveguides, and PCB buses. In the mathematical sense, as long as there is a signal return path, any signal transmission

system is a transmission line. Thus, any electrical transmission system must be a transmission line, as KCL dictates that there shall always be a return path. Two examples of commonly used transmission line structures are shown in figure 10.

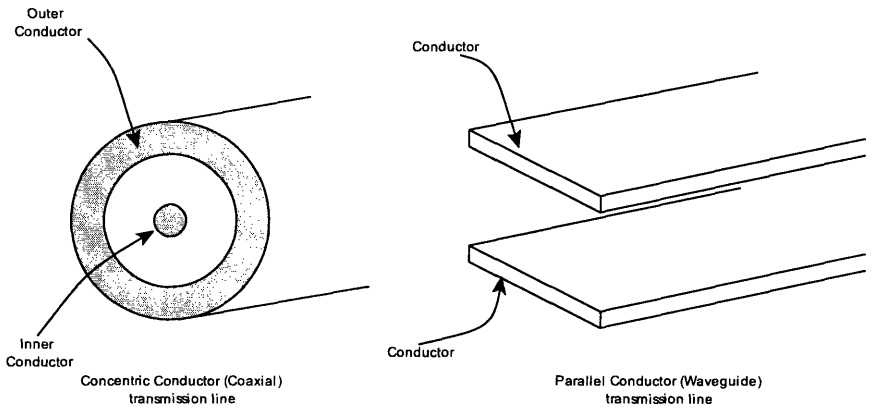

Popular transmission line structures
figure 10.

Our system of interest, the motor power cable is in fact a version of the coaxial transmission line, except with four inner conductors instead of just one. In the following sections we will develop electrical and mathematical models for these structures, focusing on the extraction of key parameters such as characteristic impedance and propagation speed. Furthermore, we will explore high-frequency considerations and different regions of operation.

2.5.2. Ideal (lossless) transmission lines

As a first step, we will develop and analyze a model for a transmission line in which the conductors are assumed to be perfectly conducting, with zero resistivity. Although this might seem to be an oversimplification, the model we will develop predicts real behaviors very accurately for moderate to low signal speeds.

2.5.2.1. Lumped-element model

Our first step in developing a model for the transmission line is taking the physical structure and representing it with discrete circuit components. Suppose we take a transmission line and divide it lengthwise in individual segments of length dL.

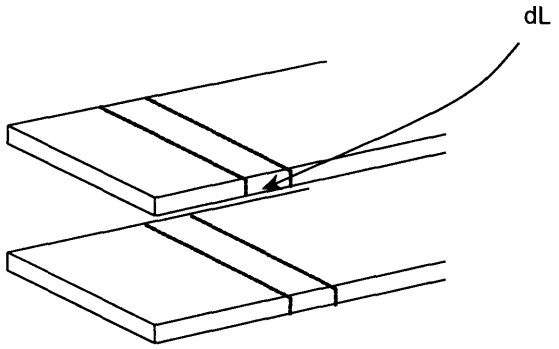

Differential piece of transmission line for lumped element model figure 11.

Each of these segments can be modeled by two elements. There is some finite self inductance due to the fact that the conductor is of a finite length dL. Furthermore, there is parallel plate capacitance between the two conductors. Therefore, each segment dL can be modeled simply by an inductor in series with a shunt capacitor. Our full transmission line is just an infinite chain of such circuits:

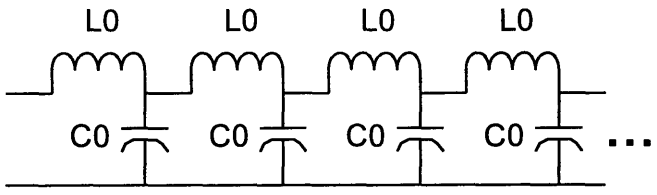

Lumped element model for an ideal transmission line figure 12.

2.5.2.2. General transmission line equations

Now that we have a general lumped model for our transmission line, we can attack this problem with common circuit solving techniques. Take some piece of transmission line of length dL:

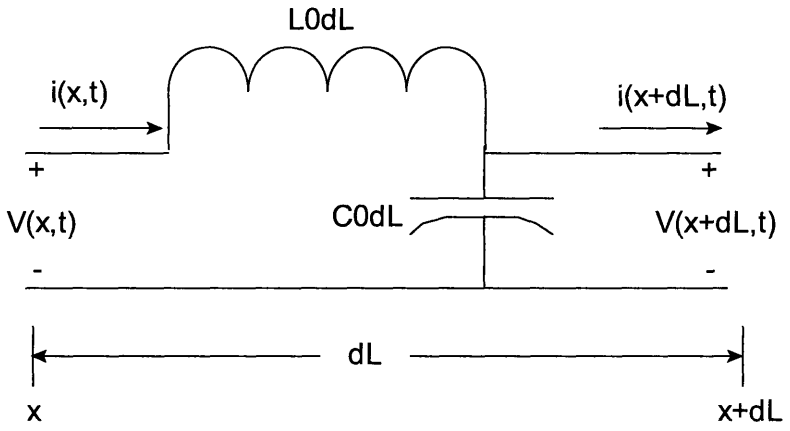

Incremental piece of transmission line
figure 13.

Let i(x,t) and v(x,t) be the voltages and currents in the branches at some position x down the transmission line and at some instant in time, t. L0 and C0 are inductance and capacitance per unit length respectively. Now, apply KVL and KCL on the circuit above to obtain:

$$V(x,t) - L_0 dL \frac{\partial i(x,t)}{\partial t} - C_0 dL \frac{\partial V(x+dL,t)}{\partial t} = 0$$

$$i(x,t) - C_0 dL \frac{\partial V(x+dL,t)}{\partial t} - i(x+dL,t) = 0$$

Rearranging these equations and letting dL go to 0, we obtain:

$$\frac{i(x,t)-i(x+dL,t)}{dL}=C_0\frac{\partial V(x+dL,t)}{\partial t}\Rightarrow-\frac{\partial i(x,t)}{\partial L}=C_0\frac{\partial V(x,t)}{\partial t}$$
$$\frac{V(x,t)-V(x+dL,t)}{dL}=L_0\frac{\partial i(x,t)}{\partial t}\Rightarrow-\frac{\partial V(x,t)}{\partial L}=L_0\frac{\partial i(x,t)}{\partial t}$$

These last two equations are called the general transmission line equations, as they uniquely define the voltage and current at every point of the transmission line.

2.5.2.3. Characteristic impedance

Suppose we have an infinitely long transmission line. We know it's capacitance per unit length C0 and inductance per unit length L0. What equivalent real resistance could be used to substitute the load this impedance line would present? Although finding the impedance of the transmission line might at first seem like a mathematically involved calculation (it is an infinite network), the number crunching is reduced substantially if we use a simple mathematical trick. Suppose the equivalent impedance of the infinite network is Z0. If we add an additional L0 and C0, the impedance should not change, as the initial network already had an infinite chain of these structures. Furthermore, this new network is exactly the same as the original network, and thus, it must have the same impedance, Z0.

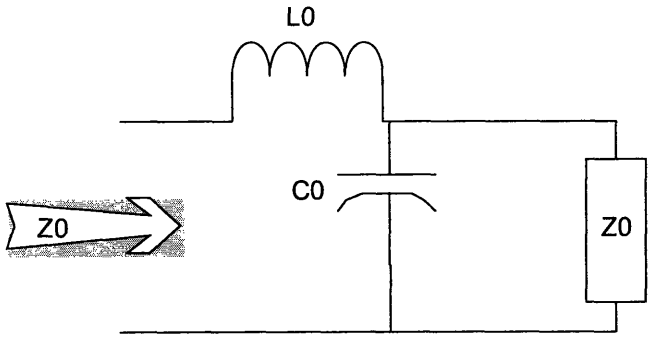

Adding an inductor capacitor pair to the transmission line does not change equivalent impedance
figure 14.

Using impedance analysis:

$$Z_0 = L_0 s + \frac{1}{C_0 s} \| Z_0 \Rightarrow$$

$$Z_0 = \sqrt{\frac{L_0}{C_0}}$$

This parameter is called the characteristic impedance of the line, and is the equivalent load that will be presented at the input end if the transmission line is very long compared to the speed of the injected signal. The characteristic impedance of an ideal transmission line is purely real.

2.5.2.4. Propagation speed

The propagation speed of the signals down the transmission line is given by:

$$v = \frac{1}{\sqrt{L_0 C_0}}$$

This equation is analogous to the equation for the speed of electromagnetic waves in free space (the speed of light), in which the permeability of free space and the permittivity of free space substitute L0 and C0 respectively.

We, therefore, have two independent equations relating the intrinsic characteristic values L0 and C0 to easily measurable quantities, the characteristic impedance Z0 and the propagation speed, v. Thus, given knowledge of any two of these quantities, we can determine the remaining two.

2.5.3. Real (lossy) transmission lines

Now that we have a good idea of how an ideal transmission line works, let's try to analyze the nuances of real transmission lines, especially real transmission lines at high

frequencies. As frequency increases several factors, such as skin effect and dielectric loss (discussed in more detail in section 2.4) cause regular conductors to behave in non-ideal fashion. Because a transmission line is nothing more than two conductors with some dielectric material between them, it is plausible that the same frequency dependent non idealities that affected single wire conductors will also play a factor in transmission lines. As discussed previously, skin effect is characterized by increasing series resistance, while dielectric loss is characterized by increasing shunt conductance. Thus, we can model these non idealities as well as other imperfections by adding some elements to our ideal model. We can then approach this model in a manner similar to our ideal case.

2.5.3.1. Lumped-element model

Skin effect has the effect of increasing the series resistance of the conductor by decreasing it's effective cross sectional area. Thus, we can model this effect by adding a resistor in series to our model. Dielectric loss, on the other hand, has the effect of shorting out the two conductors at high frequencies. This points towards adding a shunt conductance that models this effect. The modified lumped element model is shown below in figure 15.

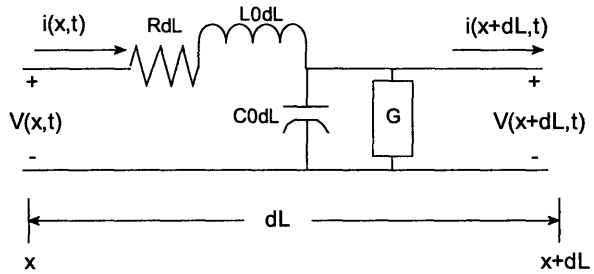

Incremental piece of real transmission line with parasitic series resistance and shunt conductance
figure 15.

Our new lumped model is very similar to the ideal one, with the addition of a series resistance to model non-zero resistive loss in the conductor and a conductance to model signal loss due to dielectric shunting.

2.5.3.2. Characteristic impedance

An easy way to obtain the characteristic impedance of the real transmission line is to simply substitute the impedance of the resistance plus the inductance for the inductance and the impedance of the capacitance in parallel with the conductance for the capacitance. The resulting equation is:

$$Z_0 = \sqrt{\frac{R + L_0 s}{G + C_0 s}} = \sqrt{\frac{R + L_0 jw}{G + C_0 jw}}$$

The most important difference to note is that, depending on the relative magnitudes of the series resistance and conductance as compared to the impedance of the series inductance and shunt capacitance, the transmission line characteristic impedance is no longer frequency independent.

2.5.3.3. General transmission line equations, propagation and attenuation constants

The general transmission line equations are derived in the same manner as for the ideal case, resulting in:

$$v(x,t) - i(x,t)RdL - L_0 dL\frac{\partial i(x,t)}{\partial t} - v(x+dL,t) = 0$$

$$i(x,t) - C_0 dL\frac{\partial V(x+dL,t)}{\partial t} - GdLv(x+dL,t) - i(x+dL,t) = 0$$

which, letting dL approach 0 yield:

$$-\frac{\partial v(x,t)}{\partial L} = Ri(x,t) + L_0 \frac{\partial i(x,t)}{\partial t}$$
$$-\frac{\partial i(x,t)}{\partial L} = Gv(x,t) + C_0 \frac{\partial v(x,t)}{\partial t}$$

By assuming that the voltage and current waveforms are sinusoidal in nature, one can obtain the propagation and attenuation constants:

$$\gamma = \sqrt{(R + jwL)(G + jwC)};$$
$$\gamma = \alpha + j\beta$$

The attenuation constant alpha is the real part of the propagation constant. This real part produces an evanescence in the wave transmission, thus reducing the wave energy as it travels through the line, and it is generally measured, as all the other parameters presented so far, per unit length.

2.5.4. Finite transmission lines in TEM mode

So far we have addressed transmission lines of an infinite length. Not only is this a purely theoretical construct, but infinite transmission lines defeat the main purpose why we study transmission lines at all. In an infinite transmission line, any signal injected into one end will travel forever down the line, never to be recovered. Although we could waste power sending signals down infinite transmission lines in the name of science, it is much more interesting to be able to measure and compare signals at the input and output terminals of a real, finite, terminated transmission line. In the following sections, we will develop a model to analyze transmission and reception of signals through finite transmission lines, taking into account the effects of different termination impedances.

2.5.4.1. Introduction to TEM

The lumped transmission line model in which we have based all our analysis so far implies an important assumption that we must address now. In our proposed model, there is shunt per length capacitance, but no series capacitance. In the same manner, there is series per length inductance, but no shunt inductance. This implies that, for example, that the magnitude of the electric field in the direction of the wave propagation must always be 0. If this was not the case, then we would need some equivalent series capacitance to model this field. In the same way, we cannot have any magnetic field in the direction of the wave motion. This specific mode of operation, in which the magnitude of both the magnetic and electric field in the direction of wave propagation is always 0 is called TEM. More specifically, TEM stands for transverse electro-magnetic, mode in which the magnetic and electric fields are always orthogonal to the direction of motion. Furthermore, we can argue that the magnetic field and electric field are orthogonal to each other as they are for electromagnetic waves. Therefore, for a transmission line in TEM mode the electric field is orthogonal to the magnetic field which is orthogonal to the direction of wave propagation.

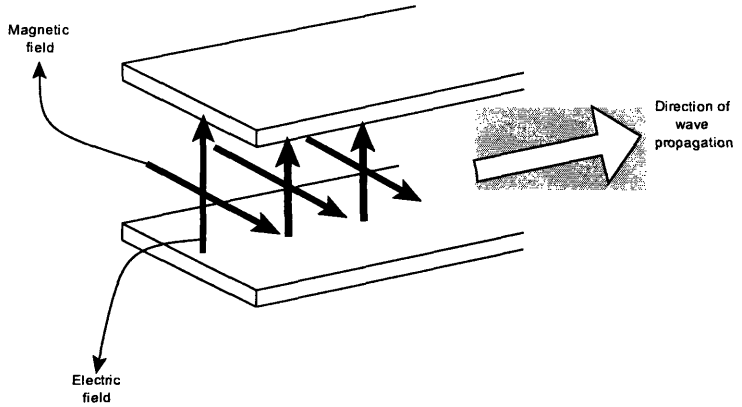

Electro-magnetic fields in a transmission line in TEM mode figure 16.

Figure 16 above shows a transmission line being excited in TEM mode. As previously stated, the magnetic and electric fields are orthogonal to the direction of propagation and to each other. Furthermore, the direction of propagation is given by the cross product of the electric and magnetic fields; ExB.

2.5.4.2. Reflection coefficient

Suppose we excite a finite transmission line in TEM mode. What happens to the signal once it arrives at the other end of the transmission line? Figure 17 shows the propagation of a voltage pulse down a finite transmission line terminated in some arbitrary impedance ZL.

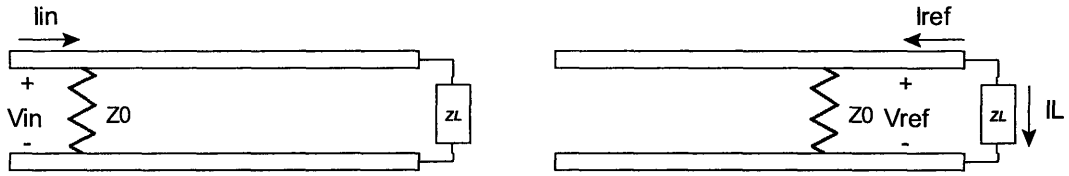

Voltage pulse traveling down a finite, terminated transmission line figure 18.

A voltage pulse, Vin is applied at the input end of the finite transmission line. The current Iin that this pulse will induce is set by the characteristic impedance of the line:

$$I_{in} = \frac{V_{in}}{Z_0}$$

When the voltage pulse arrives at the line termination impedance ZL, this impedance will force a new voltage/current ratio according to Ohm's law. Because current flow must be conserved, the remaining current that ZL does not sink must be reflected back to the transmission line. The ratio between the magnitude of the reflected voltage pulse to the incident voltage source is given by the reflection coefficient, denoted by uppercase gamma:

$$\Gamma = \frac{Z_L - Z_0}{Z_L + Z_0}$$

To understand the intuitive meaning of this expression, suppose ZL=infinity, or in other words, the load end is left open circuited. In this case, the reflection coefficient is 1. What this means is that all of the energy of the transmitted pulse is reflected back from the load. If instead we short-circuit the load end; ZL=0, the reflection coefficient is -1. What this means is that the traveling wave arrives at the load end, finds the short circuit and continues traveling on the opposite conductor of the transmission line. Because we had already defined as positive voltage the difference between the voltage at one conductor minus the voltage at the other, this kind of transmission results in just a sign reversal, as predicted by the reflection coefficient. Finally, if we set the termination impedance equal to the characteristic impedance of the transmission line, the reflection coefficient is zero. In this condition, the transmission line is said to be "matched". Because the load impedance forces the same voltage/current ratio as the transmission line, all of the energy of the pulse is transmitted to the load and dissipated there, thus, there is no wave reflection. This leads to an experimental way of determining the characteristic impedance of an arbitrary finite transmission line. Using a pulse generator, one can send voltage pulses down a transmission line. Then, change the load impedance while observing the voltage vs. time waveforms at the load end. The characteristic impedance of the line is then just the impedance at the load that results in no reflections at the load end. This technique will be essential to developing our transmission line model of the motor power cable.

Although it is not desired for most practical purposes, the reflection coefficient does not need to be purely real. For example, suppose that the load impedance is not

purely resistive but a network which contains both passive and reactive components. Because the load impedance is frequency dependent, the reflection coefficient will also be frequency dependent. This is generally not desired because it implies that different frequencies will be transferred and reflected in different magnitudes. For waveforms that are rich in harmonics, such as square waves or triangle waves, this causes distortion, which, depending on the degree of frequency dependence of the load impedance, could prove to be unacceptable.

In our case, because we are attempting to couple our high frequency signals in and out of the cable using capacitors, we have to deal with the problem of frequency dependent reflection coefficients. We will approach the problem of our detector as a pure impedance-matching problem, without diving into the minutia of how our detector works. Therefore, suppose we are given the transmission line termination shown in figure 19 below:

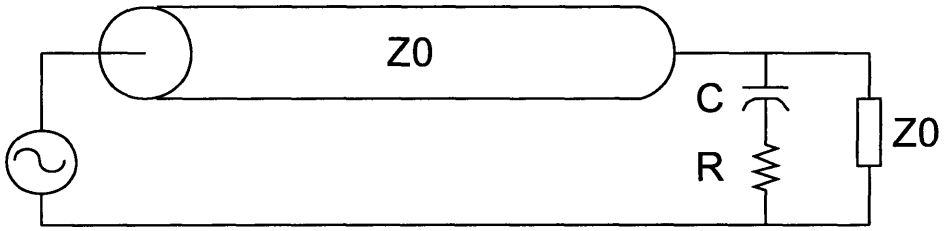

Transmission line with an additional capacitive termination
figure 19.

The load impedance is inherently frequency dependent. This is easy to comprehend if one considers what happens for high and low frequency components. For very low frequencies, the impedance of the capacitor is very large, so the load impedance approaches that of the matched impedance, Z0. For very high frequencies, the impedance

of the capacitor is very small, so the load impedance approaches the parallel combination of Z0 and R, which is always less than Z0.

2.5.4.3. Constant-impedance termination network

Now, suppose that we wanted to minimize distortion caused by this frequency dependent load. One solution is to use an inductor-resistor string to balance out the decreasing impedance of the capacitor-resistor string. The proposed circuit is shown on figure 20:

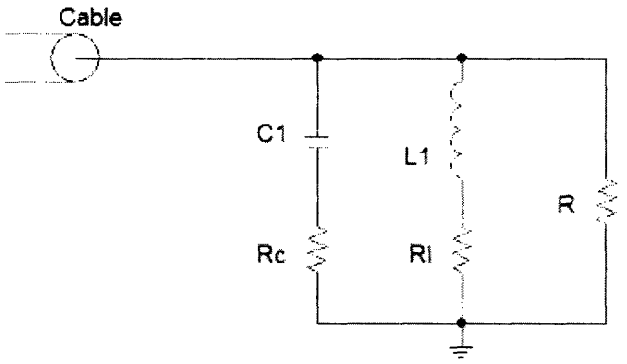

Proposed frequency-independent load termination diagram figure 20.

For very high frequencies the inductor impedance is large, while the capacitor impedance is small, therefore, the total impedance approaches R||Rc. For very low frequencies the opposite effect happens and the total impedance approaches R||Rl. Thus, it is plausible that if we choose our component values correctly, we might be able to cancel the effect of the capacitor pole with the inductor zero to get a constant impedance network if we make Rc=Rl.

To approach this situation, let's first calculate the total impedance of the network:

$$Z_{eq} = R \| \left(R_c + \frac{1}{Cs} \right) \| \left(R_L + Ls \right)$$

which, after some manipulation yields:

$$Z_{eq} = \frac{R(R_L + Ls)(1 + R_c Cs)}{RCs(Ls + R_L) + (1 + R_c Cs)(R + R_L + Ls)}$$

To simplify the equation above, define three time constants:

$$\tau_c = R_c C, \quad \tau_L = \frac{L}{R_L}, \quad \tau_x = R_L C$$

Then the impedance equation "simplifies" to:

$$Z_{eq} = \frac{RR_L(1 + \tau_L s)(1 + \tau_c s)}{RR_L Cs(1 + \tau_L s) + (1 + \tau_c s)(R + R_L + Ls)}$$

By inspection of the above equation, it is clear that setting $\tau_L = \tau_c$ makes it possible to factorize the denominator and achieve a pole-zero cancellation:

$$Z_{eq} = \frac{RR_L(1 + \tau_c s)}{R(\tau_x s + 1) + R_L(1 + \tau_L s)}$$

Finally, setting $\tau_L = \tau_c = \tau_x$ results in an additional cancellation:

$$Z_{eq} = \frac{RR_L}{R + R_L} = R \,||\, R_T \forall s$$

Thus, the impedance of the network is frequency independent and has a magnitude equal to the parallel combination of the capacitor/inductor resistor and the shunt resistance. Finally the value of inductance that would achieve this is given by:

$$L = R^2 C$$

2.5.5. Regions of operation of a transmission line

2.5.5.1. Introduction

Although the model we have developed is useful to predict the behavior of transmission lines in general, because of their distributed nature, different specific

operating conditions might lead to vastly different behaviors. For example, suppose that we could cut a transmission line down to the point that it's well modeled by a single LC network. In this case, instead of experiencing the usual Z0 input impedance for a relatively long transmission line, we would see just a simple LC divider network. The factors that determine how relatively "long" or "short" a transmission line is are its physical length and the frequency of interest. The table shown below in figure 21, extracted from the book High Speed Signal Propagation: Advanced Black Magic, shows the different regions of operation for different trace lengths (this book is focused on integrated circuit design, so instead of referring to transmission lines, it refers to traces) and frequencies of interest:

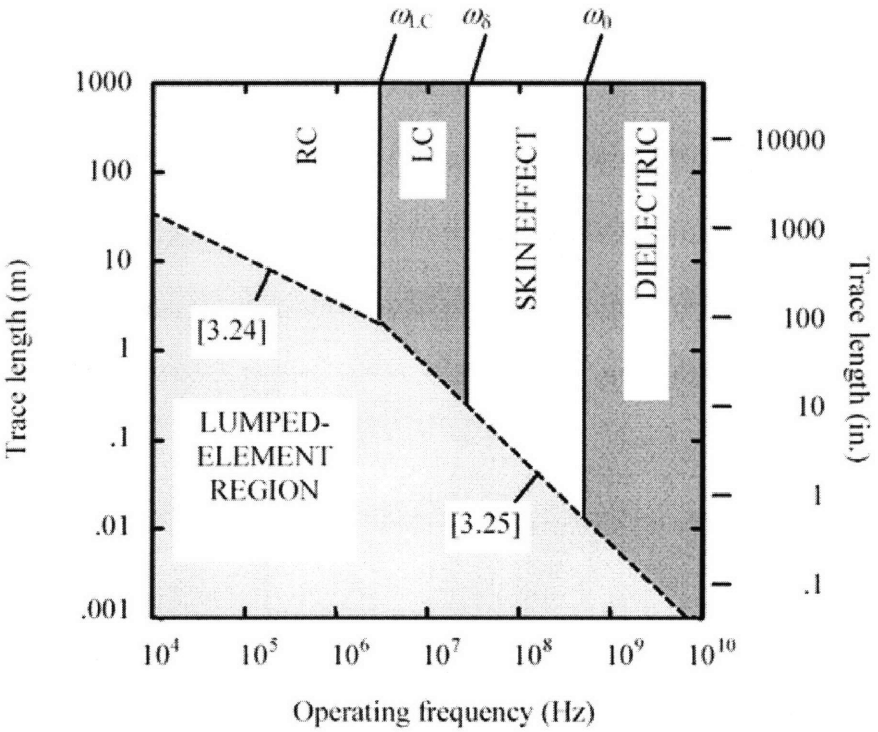

Regions of operation for different trace lengths and operating frequencies [8] figure 21.

In the following sections, we will briefly discuss the different regions of operation and their characteristics. The lumped-element region, corresponding to the combination of

frequencies and lengths which result in the transmission line behaving similarly to an LCR circuit, will not be addressed as it occurs for trace lengths much shorter than our motor cable.

2.5.5.2. RC region

For very low frequencies and long cable lengths the impedance of the equivalent series inductance of the transmission line: L(jw), becomes negligible. In this case, we can ignore the contribution of this part in our model, leaving us with a transmission line which contains only series resistance and shunt capacitance. In this case, we can restate our equation for characteristic impedance, now letting L(jw)=0:

$$Z_0^{RC} = \sqrt{\frac{R}{C_0 jw}}$$

Note that we are ignoring the conductance term, G because we are currently interested in low frequency behavior in which conductance losses are not significant. Contrary to the ideal case, in the RC region the characteristic impedance is a strong function of frequency and is not purely real. This could prove to be very troublesome if one is attempting to match the impedance of the line.

2.5.5.3. LC region

As we increase the frequency of interest, the L(jw) term in the impedance equation dominates:

$$\lim_{w\to\infty} \sqrt{\frac{R + L_0 jw}{C_0 jw}} = \sqrt{\frac{L_0}{C_0}}$$

,yielding our familiar impedance of an ideal transmission line. One of the main characteristics of the LC region is that the transmission line signal attenuation, corresponding to the real part of the propagation coefficient, is almost independent of

frequency. Because of this reason, this region is often also called the "constant loss region".

2.5.5.4. Skin-effect region

When the operating frequency is very high, non-ideal frequency-dependent conductor losses begin to appear. Usually, the first onset of these non-idealities is heralded by the arrival of the skin-effect region. Skin effect was discussed in more detail in section 2.4.2. As derived previously, skin effect contributes a series conductor resistance which increases proportionally to the square root of frequency. Thus, in this region, we can derive the characteristic line impedance as follows [7]:

$$Z_0^{SER} = \sqrt{\frac{R(w) + L_0 jw}{C_0 jw}} \approx \sqrt{\frac{L_0}{C_0}}$$

Because the series resistance term, R(w) rises in proportion to the square root of frequency while the impedance of the series inductance rises linearly with frequency, as we increase the frequency the term R(w) becomes less significant compared to the Ljw term. Therefore, in the skin-effect region, we have a characteristic impedance which is independent of frequency. The other distinguishing feature of the skin-effect region is that the transmission line signal attenuation rises with the square root of frequency for all frequencies above this region.

2.5.5.5. Dielectric loss region

For frequencies well above the threshold for the skin effect region, dielectric losses begin to dominate our attenuation. The different types of dielectric losses are discussed with more detail in section 2.4.3. According to Johnson [7], the attenuation constant corresponding to dielectric loss can be approximated as:

$$\alpha_D = \frac{\theta_0 w}{2v_0}$$

, where $\tan\theta_0$ is the loss tangent of the dielectric material at some arbitrary frequency and v0 is the wave propagation speed at this same frequency. The most important characteristic of this region is that the attenuation constant increases linearly with frequency, although, utilizing the same argument as for the previous regions, the characteristic impedance is independent of frequency. Furthermore, the attenuation constant in this region is directly proportional to line length, i.e., a 10-fold increase in transmission line length will cause a 10-fold increase in signal attenuation.

2.5.5.6. Waveguide dispersion region

The final region of operation of a transmission line is the waveguide dispersion region. In this region the frequencies of interest are so high that the signal wavelength is comparable to the cross-sectional dimensions of the transmission line. Because the signals can now "fit" in other dimensions across the transmission line, the TEM assumption does not longer hold. This region of operation is characterized by unexpected signal behavior, such as significant overshoot and ringing for matched transmission lines. The onset of this region, though, is at such high frequencies that it will be very unlikely for us to encounter any of its effects in our experiments.

2.6. Serial Communication Protocols

2.6.1. Introduction

Before we can effectively analyze any information transmission system it is important to understand the nature of the information that we wish to communicate. In

our case of interest, we are going to utilize two serial communication protocols, namely RS232 and RS485. Serial protocols, by definition transmit information in a (not surprisingly) serial manner. In other words, the whole information package is broken up into bits which are communicated one by one in order. The next few sections include brief descriptions and side by side comparisons of these two serial communication protocols.

2.6.2. RS232

2.6.2.1. General description

RS232 is a well-established and widely available serial communication protocol. Originally developed as a means of communication between a central mainframe and remote terminals, RS232 allows two instruments to utilize a single line to communicate. Furthermore, a single communication line can only be utilized by two instruments at any point. For this reason, we might call RS232 a point-to-point communication protocol, contrary to a multipoint communication network. An example of two typical RS232 connectors is shown in figure 22. The physically larger DB25 connector is generally the norm for older devices, while the DB9 connector is the more modern version. Most fairly recent PC's have at least one RS232 DB9 connector.

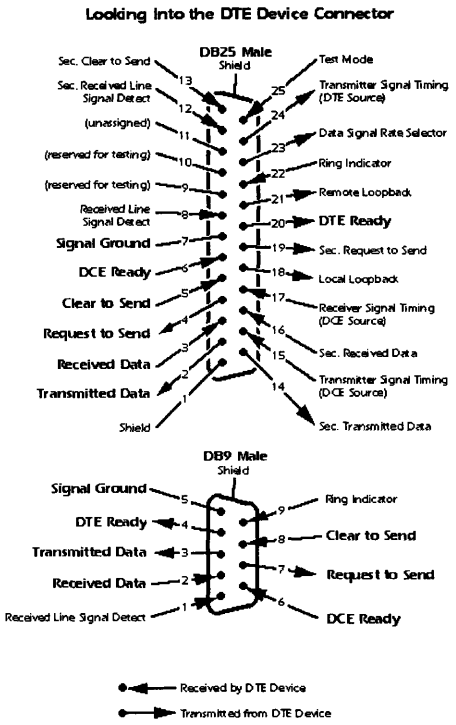

RS232 DB25 and DB9 male connectors [18]
Figure 22

The main characteristic that makes RS232 different from other serial communication protocols is, other than the fact that it only allows a single point-to-point communication, is the existence of a common signal ground pin at both ends of the communication channel. RS232 signals are all referenced to a common ground voltage, which must be effectively transmitted in conjunction to the information signals themselves. The advantage of this setup is its relative simplicity. Each bit is represented by a voltage level, ranging from -15V to +15V relative to common ground. The main disadvantage is that the need for a common signal ground greatly limits the length of the communication line for a given baud rate. This is due to the fact that long cables will present higher total capacitances, lowering the slew rate and thus the maximum communication speed. Furthermore, because of the necessity for these long ground level lines, RS232 signals are known for having level-shifting and ground loop problems.

2.6.2.2. Protocol parameters, data rate

Now, we present a table with the RS232 protocol parameters from www.rs485.com for reference:

Parameters for RS232 serial protocol

Mode of Operation	SINGLE-ENDED
Total Number of Drivers and Receivers on One Line	1 DRIVER, 1 RECEIVER
Maximum Cable Length	50 FT.
Maximum Data Rate	20kb/s
Driver Output Signal Level	+/-5V to +/-15V

2.6.3. RS485
2.6.3.1. General description

Although RS232 works efficiently for short transmission distances and low data rates, it does not offer any solutions for long distance monitoring and communication. Furthermore, it does not allow for sharing of a single communication line of several transmitters and receivers. RS485 addresses most of these issues by implementing a fundamentally different method of information transmission: twisted pair differential signal transmission.

Contrary to RS232, which requires a common signal ground between the transmitter and receiver, RS485 uses a single twisted wire pair to transmit information differentially. Bytes are transmitted and received by measuring the voltage difference between these two wires, rather than by comparing them to an absolute signal ground. By disposing of the need for a common signal ground, the RS485 also solves the

problems of level shifting and ground loops, allowing for communication over much longer distances. Furthermore, RS485 signals utilize balanced signal transmission in which the signal at some point in one of the wires composing the twisted pair is ideally exactly opposite to the signal at that same point in the other wire. Refer to figure 23 below.

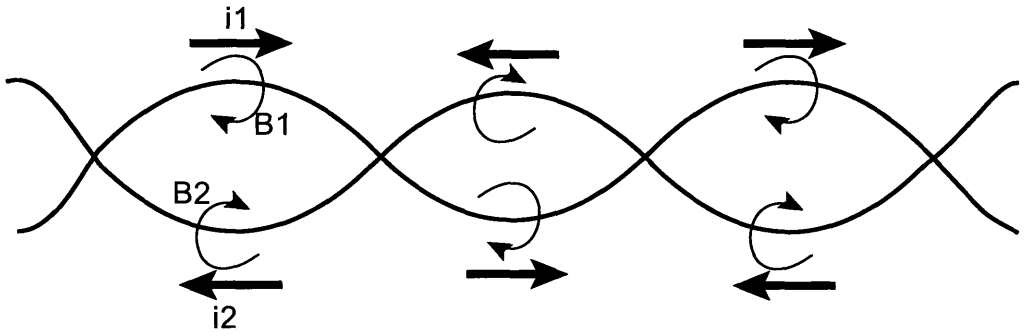

RS485 twisted cable pair showing signal currents and induced magnetic fields for balanced signal transmission
figure 23.

There are two main advantages of RS485 balanced differential signal transmission. First, radiation from the communication channel will be greatly reduced. This is due to the fact that if the currents in each wire are exactly equal but opposite in direction, they will induce exactly equal but opposite magnetic fields, resulting in very little magnetic radiation. The second advantage is that this configuration is much more resilient against unwanted signal pickup as the effective area between the twisted pair loops is very small, as long as the pair is twisted tightly. Immunity to signal pickup is not the only main difference between the RS232 and RS485 protocols.

While RS232 only allows for one set of driver and receiver per communication line, RS485 allows for the setup of truly multipoint communication, with several receivers and drivers sharing the same line. This sharing of a single communication line

is achieved by a form of time division multiplexing. Each of the devices connected to the communication line has a specific address assigned to it. Before transmission of information, the transmitting device "announces" the address of the receiver plus the bit length of the data. All other devices then wait until this communication finishes before attempting to communicate. This way, all the instruments can utilize a single line to communicate with one another while avoiding collisions.

2.6.3.2. Protocol parameters, data rate

We now present a table of RS485 protocol parameters in the same manner as we did for RS232, extracted from www.rs485.com:

Parameters for RS485 serial protocol

Mode of Operation	DIFFERENTIAL
Total Number of Drivers and Receivers on One Line	32 DRIVER, 32 RECEIVR
Maximum Cable Length	4000 FT.
Maximum Data Rate	10Mb/s-100Kb/s
Driver Output Signal Level	+/-1.5V

2.6.3.3. Advantages of RS485 over RS232

Having discussed the main characteristics of the RS232 and RS485 protocols, we can now list the different advantages of RS485 signal transmission over R232:

- Highly increased maximum communication line length
- Increased maximum data rate
- Possibility of sharing a single data line with many drivers and receivers
- Substantially reduced electromagnetic radiation

- Immunity to ground level shifting and ground loops
- Better rejection of unwanted signal pickup

Therefore, RS485 is the protocol of choice for most industrial applications in which long distance, high speed links are required. RS485 is the protocol of preference employed for the transmission of feedback data of PWM motor control systems with currently-available separate cable solutions.

2.7. Principles of Modulation

2.7.1. Introduction

Suppose we wanted to transmit a certain data string. Although it is possible in theory to just send the raw data string, in most cases this is not an efficient way of doing so. For example, if the data string is digital, transmission of the raw data string would imply sending pulses, which spread out in the frequency domain. In theory, therefore, we would need to use the full frequency spectrum for transmission. Not only does this conflict with FCC regulations, but it's a very inefficient way of using the available bandwidth. This method of utilizing energy pulses for information transmission was first developed by Marconi while attempting to demonstrate that wireless communications were in fact possible. The spark gap transmitters that resulted from these experiments operated by creating visible, very high voltage sparks. These sparks would then induce EM waves that could be detected and heard from a remote location. Although these transmitters were effective in demonstrating the feasibility of wireless communication, more than one line of communication could not be sustained, as there was no way of discerning between the sparks of different transmitters. This problem, among many others is addressed by the technique of modulation.

Modulation is defined as encoding data on a carrier by modifying its characteristics. One of the main advantages of using a carrier to transmit our information is that we can easily separate any desired signals by filtering out frequencies of interest. For our purposes, a carrier can be thought of as a sinusoidal wave:

$$f_c = A\sin(\omega t + \phi)$$

It is clear, then, that we can manipulate three characteristics of this carrier, namely the amplitude A, the frequency w, or the phase phi. Practically all of the modulation techniques currently in existence encode information by deliberately modifying one or more of the three carrier parameters mentioned. In the following sections we will briefly discuss some of these binary (one of two symbols is transmitted at any time) modulation techniques, with focus on frequency shift keying (FSK), the modulation method used in our experiments.

2.7.2. FSK Modulation

The first modulation method we shall discuss encodes binary information by shifting the frequency of the carrier. This results in a particularly simple, and, as we will explore later, robust transmission system with relatively cheap components. FSK will be the modulation method that we will use for our experiments.

2.7.2.1. Principle of operation

The main idea behind FSK is to transmit the binary data stream by using different frequency signals. Although it is possible to encode multi-bit symbols by this method, the base example of BFSK (binary frequency shift keying), where each symbol represents as single bit, is appropriate to understand the basics of operation. In BFSK a "1" or a "0"

is represented by two different frequency signals, separated by some predetermined amount, delta f. The demodulator at the receiver end can be constructed by comparing the energy detected by two different band-pass filters centered at the two symbol frequencies. Figure 24 below shows an example of this simple FSK modulator/demodulator system:

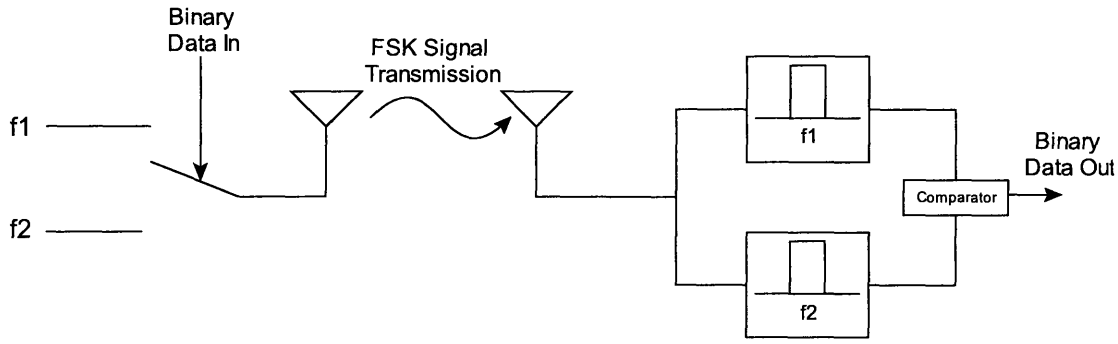

BFSK modulation/demodulation system
Figure 24

We select the carrier frequency depending on the binary data stream. This FSK signal is then transmitted to the receiver (wirelessly or otherwise). The demodulator at the receiver is composed of two filters centered at the two different symbol frequencies and a comparator. The binary data stream is demodulated by comparing the energy of the signals detected at each frequency.

2.7.2.2. Mathematical model

As discussed previously, BFSK encodes binary data signals by changing the frequency of the carrier. For most applications, the frequency of the carrier is shifted some small amount from a predetermined center frequency. Mathematically, the resulting BFSK signal can be expressed as follows:

$$f_c(t) = \sin\left(2\pi\left(fc \pm \Delta f\right) + \phi\right)$$

For example, we could choose to represent a 1 by shifting the frequency of the carrier up by an amount Df, and a 0 by shifting the frequency down by the same quantity. Usually this quantity Df is small compared to the center frequency. The magnitude of this shift Df is very important for determining how we trade off noise immunity, bandwidth efficiency and ease of implementation.

For example, suppose we choose a very small Df. This would enhance our bandwidth efficiency, because we would only need the frequency band extending from fc-Df to fc+Df. Unfortunately, this degrades our noise rejection and ease of implementation. Discerning between two carrier frequencies that are close together increases the probability of them interfering with each other, plus, it requires detection filters with very sharp cutoffs, which are expensive. To avoid these problems we could choose a very large Df, but this comes at the cost of utilizing more bandwidth.

2.7.2.3. Probability of error

Suppose we are attempting to transmit some FSK modulated signal in the presence of some sources of interference. There are two possible sources of error, a binary 0 being detected as a 1, and a binary 1 being detected as a 0. A common assumption is that the probability density functions of the interfering signals are Rician and Rayleigh. The resulting probability of error for FSK assuming that the probabilities of transmitting a binary 1 or 0 are equal is [9]:

$$P_E^{FSK} = \frac{1}{2} e^{-\frac{SNR}{4}}$$

, where SNR is the signal to noise ratio in the channel. From this exponential relation we can deduct that the probability of error increases rapidly with degrading SNR, although

the maximum probability of error is capped at ½, the same probability of error we would have if we were to guess the binary bit without considering the signal.

2.7.2.4. Data rates

The maximum possible data rate achievable with FSK is bounded by several design factors. Of course, the SNR of the transmission channel is essential as it directly correlates to the probability that information will be faithfully transmitted. Another limitation which is characteristic of practically all modulation methods, not only of FSK is that the baud rate is limited by the frequency of the carrier. In general, higher frequencies allow for faster baud rates. 900MHz FSK transceivers that run at data rates over 1Mbps are commonly available for purchase.

2.7.3. OOK, ASK, FSK ortho-normal plots

Some other simple modulation schemes include OOK and ASK. In ASK, which stands for amplitude shift keying, the amplitude of the wave is modified to carry the information. For example, for binary ASK, one could choose two different signal amplitudes, with one representing a 0 and one representing a 1. The signal could then be demodulated by comparing the received signal amplitude to some threshold. One obvious problem with this modulation scheme is that it needs some sort of adaptable threshold as the amplitude of the received signal may vary substantially if the transmission conditions change (such as if the distance between the transmitter and receiver changes).

OOK, which stands for on-off keying, is a special case of ASK. In this modulation scheme, the two binary values are represented by a non-zero signal (on) or a

0 amplitude signal (off). The problem with this modulation scheme is that it is susceptible to interference. If the signal interference is strong enough, it might be incorrectly detected as an "on" signal, independently of the transmitted value.

An easy way to compare some different modulation methods is to build their corresponding ortho-normal plots, sometimes referred to as signal diagrams. In these diagrams, the different symbols are represented by points in a Cartesian plane. The ortho-normal plots for ASK, OOK, and FSK are shown below in figures 25, 26 and 27 respectively.

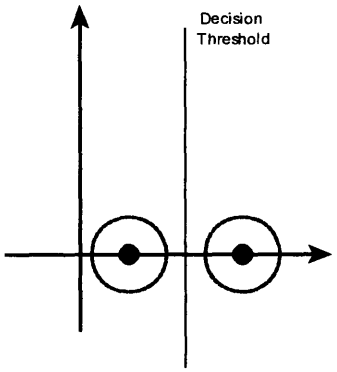

Ortho-normal diagram for BASK
figure 25.

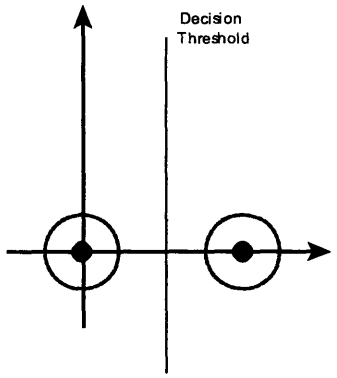

Ortho-normal diagram for OOK
figure 26.

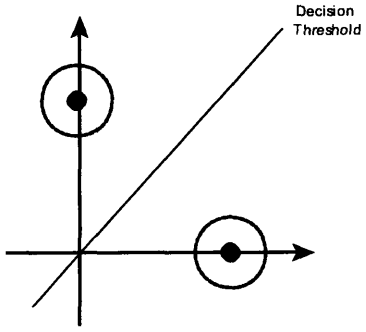

Ortho-normal diagram for FSK
figure 27.

The dark dots represent the two possible symbols, while the dotted circles are drawn to represent the smearing that might occur due to noise and interference. It is clear from these plots that FSK has at least two main advantages over the other modulation schemes. First, it does note require an adaptive decision threshold, as the strength of the received signal does not contain any data. Furthermore, we can predict that FSK will have better noise rejection for a given SNR, as the two symbols are orthogonal.

3. APPARATUS AND PROCEDURE

3.1. Description of Components and Devices

3.1.1. FT1 30m reference cable

One of the main elements in our experiment is the motor feeder cable. Motor feeder cables have slightly different constructions depending on motor specifications. For example, the number of independent conductors at the core of the cable is generally one plus the number of phases in the PWM signals, with the extra conductor used as a protective ground. The thickness of each of the independent conductors is determined by the peak amount of power that must be delivered to the motor. Because the PWM voltage levels are generally set and usually do not exceed 600V, higher power levels require higher currents. Higher currents require larger conductors to minimize resistive power loss and prevent thermal breakdown. Although thicker conductors imply lower losses in general, the reduction in signal loss is more for DC signals than for high frequency signals, due to the skin effect (see section 2.4.2.). This means that the transfer response of thicker conductors will have more of a difference between DC and high frequency signal loss. For our experiments, we chose a common, relatively inexpensive 3-phase motor cable for our experiments. We shall argue that this cable is a good general representation of most cables currently utilized for PWM motor power transmission.

The cross sectional structure of our reference cable, which we will refer to as FT1, is shown below on figure 28 below:

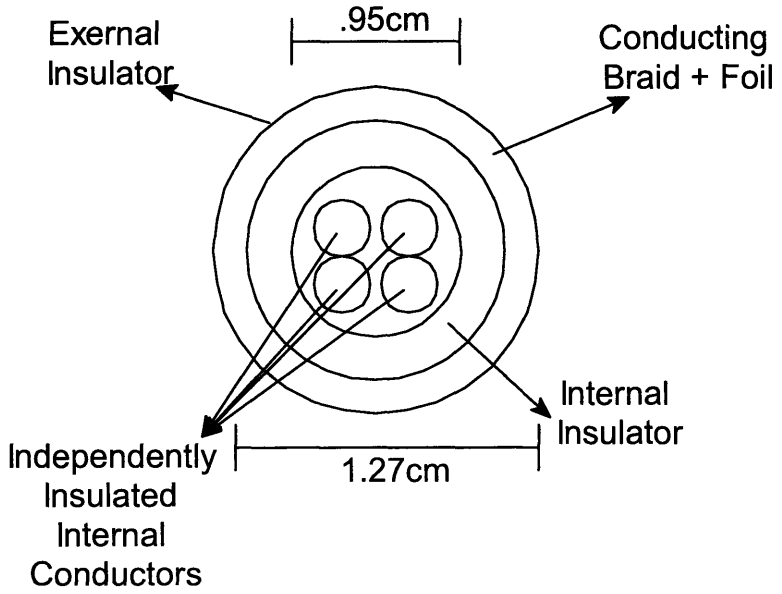

Cross-sectional figure of reference 3-phase motor feeder cable, cable FT1 figure 28.

Because our system works in three phases, our cable has four internal conductors. The four internal conductors are independently insulated and twisted together at the center of the cable. This bundle is then wrapped in an insulating material. Cable shielding is provided by an additional layer of conducting foil plus a conducting braid. The outermost layer is, of course, an insulating material. During normal operation the braid and foil are tied to protective ground at both ends of the cable, to block any radiation from the unbalanced transmission of the four internal conductors. The physical length of the cable, which is important both for determining signal propagation speed and for determining the region of operation of the cable at different frequencies (see section 2.5.5.), is measured at 30.8m. For all practical purposes, we will use 31m as a good approximation of the physical length of the cable.

3.1.2. Motor Drive

For this investigation, we will use the S200 series drive from Danaher Motion-Kollmorgen to power the motor. This drive provides the power to the motor, utilizing PWM (Pulse Width Modulation) to control some user-selectable motor state variable, such as shaft rotational speed, shaft position or motor torque. The 3-phase PWM signals achieve this feedback control by changing the widths of the square waves of one of the three phases at a time. The power delivered to the motor is proportional to the difference between the phase voltages. Thus, the narrower the pulses in one of the phases get, the greater the fraction of time that there is a non-zero difference, implying higher power into the motor.

The voltage levels of typical PWM power signals produced by the S200 can range anywhere from 15V steps up to over 100V steps. The voltage level of these signals is determined only by the power supply voltage level.

The S200 motor drive offers several options for programming and interfacing the user settings. First, there are several digital and analog ports, which can be configured such that a certain motor state variable, such as shaft rotational speed, is directly proportional to an input signal, such as an input voltage. This makes it possible to set up stand-alone motor control systems that do not need PC interfacing for adjustments. The other interfacing option is a direct PC serial connection through the PC's RS232 port. The software provided with the drive allows setting a variety of motor and drive variables, plus offering auto-refreshing data on motor status variables. For the purposes of this experiment, we shall utilize the PC interface, as it offers the most flexibility.

3.1.3. Pulse generators

For testing purposes, we will use pulse generators to simulate motor and data signals. The advantage with this kind of testing is that we are able to simulate different transmission conditions by changing the rise time and absolute magnitude of the pulse generator signals. Because our final purpose is to transmit high frequency signals through the cable in the presence of high voltage, but lower frequency components, we will use two different pulse generators running simultaneously, one for simulation of the PWM motor power signals and one for simulation of high frequency data signals.

3.1.3.1. DataPulse 101 pulse generator

The first pulse generator is the DataPulse 101 Pulse Generator. This pulse generator produces relatively low voltage signals, up to a maximum peak magnitude of 10V into 50 Ohms, but with fast rise times, in the order of 4ns. For this reason, this pulse generator will be used for two experiments. First, we will use the signals produced by this pulse generator to obtain transfer responses for our system components, the FT1 reference cable and the filters. With rise times in the order of 4ns, we will be able to obtain useful information about the transfer responses up to a frequency of about 200MHz. Additionally, we will use this pulse generator as a crude high-frequency data signal simulator, as the pulse signals have substantial spectral content at 200MHz. One disadvantage of this specific model of pulse generator is that it does not allow for adjusting the rise time. For this reason, we need another pulse generator to simulate the motor PWM signals, which have much slower rise times, and higher voltages.

3.1.3.2. HP-8005B pulse generator

The HP-8005B Pulse Generator is similar to the DataPulse 101 pulse generator in that it has maximum signal amplitudes in the order of 10V into 50 Ohms. The HP pulse generator, though, allows for adjusting the rise time from around 50ns to above millisecond range. The ability to change the rise time translates directly to adjusting the frequency content of the signal, thus allowing us to simulate the motor PWM signal spectral content. We do not expect the cable transmission system to be highly non-linear, thus, we can scale up or down the results from these experiments to better represent real PWM transmission.

3.1.3.3. Ritec SP-801 square wave pulser

The Ritec SP-801 Square Wave Pulser is a high-voltage pulse wave generator. The maximum pulse amplitude is well over 200V into 50 Ohms, which allows us to simulate high-voltage PWM motor signals. Unfortunately, the SP-801 does not feature user selectable rise times. As we will see later in the results section, the rise times of the Ritec pulse generator, are shorter than the rise times of typical PWM signals. This means that in any case, simulating the PWM signals using the SP-801 will give us a worst case result on the efficiency of our system.

3.1.4. Filters

One of our main problems boils down simply to being able to efficiently separate the PWM motor power signals from the high frequency feedback data signals. Because the PWM signals are square waves with rise times in the order of 100ns, we expect that the spectral content of these signals will have a diminishingly small magnitude for higher

frequencies. In contrast, our high frequency data signals will have most of the signal power at a very high frequency. Thus, a simple solution to the problem would be to use a filter to separate frequency wise the PWM power signals from the feedback data signals.

We have two main options for coupling in and out of the cable our data without interfering with the power transmission. The first option is to couple magnetically into the cable, which would imply using a structure similar to a transformer to transmit the data signal power through magnetic induction. The second option is to use capacitors to couple in and out of the cable, transmitting the data signal power through electric fields in the capacitor dielectric. We will focus on the second method, but future work could be done with magnetic coupling, especially if lower transmission frequencies are used.

3.1.4.1. Feed-through capacitor box

To couple in and out of the power cable, we need a structure through which our power signals can pass unaffected, but with a third terminal which is capacitively connected to the power cable conductors. This device is called a feed-through capacitor, and as described above, it is a three terminal device, two terminals are directly connected to each other, while the third one is capacitively connected to the other two. The feed-through capacitor box is composed of four of these capacitors, each connected to one of the three phases (plus ground) of the power cable. The capacitive terminals of each device are tied to each other via mounting on a common copper plate. A diagram showing the general structure of this capacitor box is shown below in figure 29:

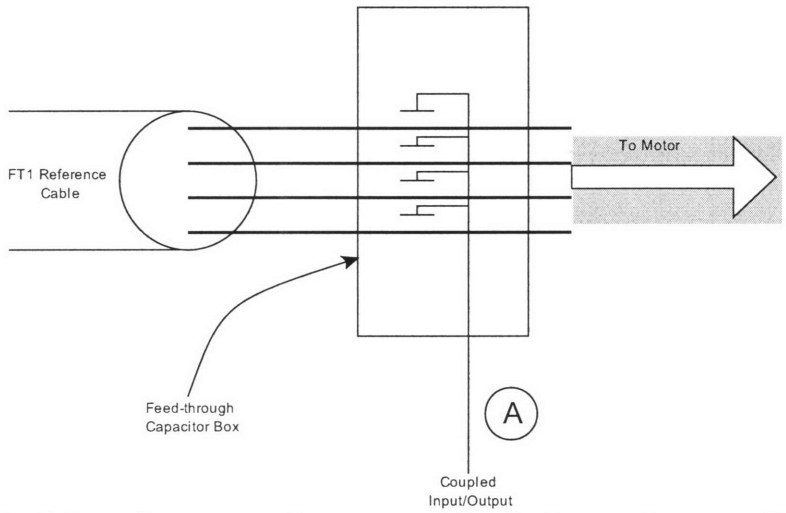

Feed-through capacitor box connected to 3-phase reference cable figure 29.

A picture of the actual feed-through capacitor box is shown below in figure 29a.

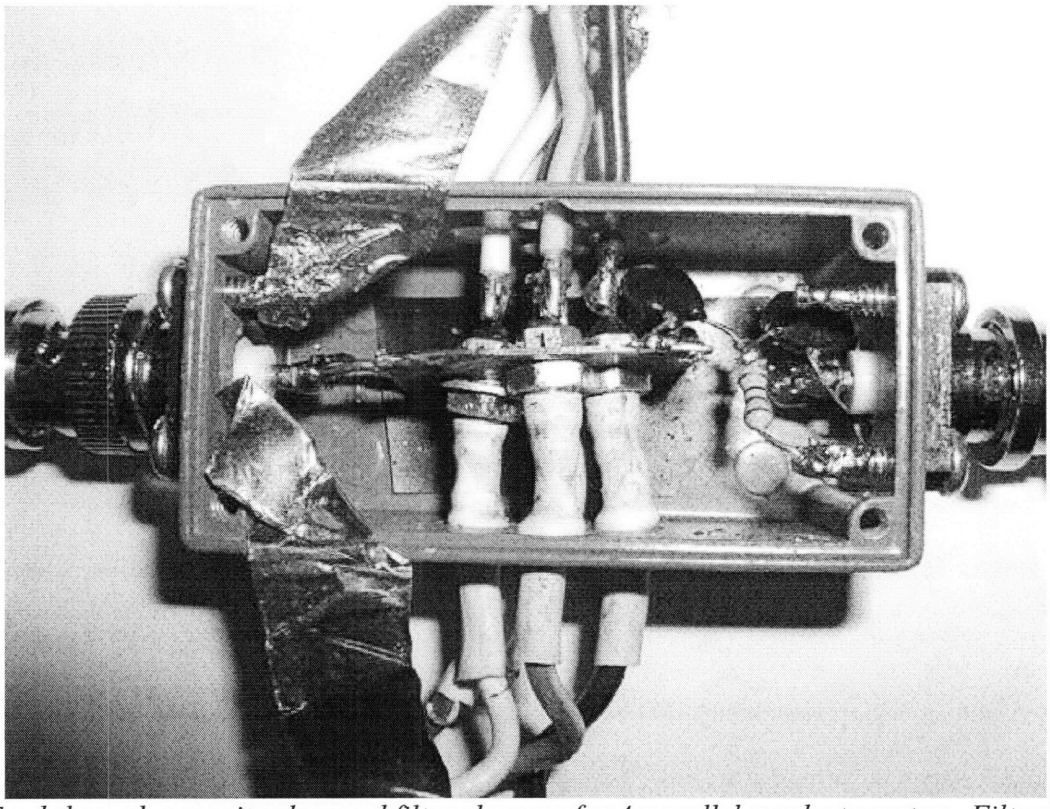

Feed-through capacitor box and filter close-up for 4-parallel conductor setup. Filter is shown at the right (two black capacitors and a resistor to common ground). The motor cable is shown at the bottom, the PWM signals come through the top and the modem is connected through the right and RF for DC power on the left.
Figure 29a.

For very high frequencies, the impedance of each of the feed-through capacitors will be negligible. Therefore, for high enough signal frequencies, the four individual conductors that compose the FT1 power cable are coupled together. The total capacitance of the capacitor box, measured from the coupled input/output terminal to the four pass-through terminals tied together is 570pF. These capacitors are RF ceramic feed-through capcitors typically used in RF equipment.

3.1.4.2. Lumped external filter

In order to set the cutoff frequencies for our feed-through capacitor box, we need to add an external resistor. By changing the value of this resistor, we can modify the -3dB frequency of our filter. Furthermore, we can add further filtering stages to achieve sharper frequency domain cutoffs, such as to separate the low frequency PWM components from the high frequency feedback data signals. The resulting equivalent circuit is shown in figure 30:

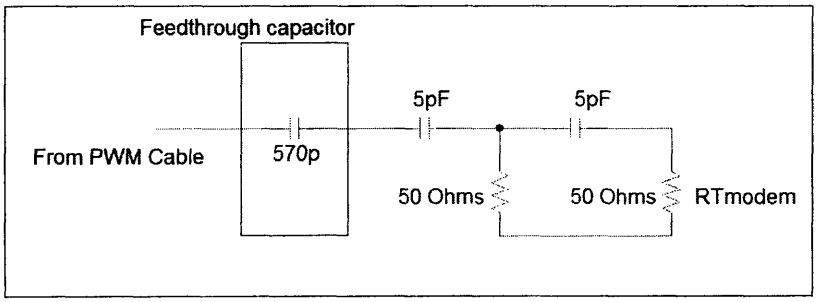

Equivalent circuit for feed-through capacitor box plus two 640MHz high-pass filter stages
figure 30.

In this figure, we chose to place the poles of this 2nd order filter at 640MHz. The pole frequencies can be adjusted by simply changing the resistor values or changing the external capacitance. Furthermore, it is possible to add additional filter stages by adding capacitor-resistor strings at the end of the circuit. Although this allows for sharper filter

cutoffs, it also brings the problem of increased filter insertion losses. For a view of the real physical external filter, refer to figure 29a.

3.1.5. 9Xtend radio modems

3.1.5.1. General description

The 9Xtend Radio Modem from Mainstsream® is a radio frequency transmitter originally developed for wireless communication of serial devices through long distances or noisy environments. The wireless frequency transmission is centered at 900MHz, which is a reasonable transmission frequency for our purposes, as it is high enough to guarantee low PWM spectral content. Furthermore, because the modems are designed to communicate through very long distances, they are designed to detect signals with very low power levels (see 3.1.4.3.), which will help us in beating signal loss through the power cable.

For our particular application, the modem output signal will not go to an antenna, but rather to one end of the PWM motor drive cable. Similarly, the receiver is connected to the other end of the PWM motor drive cable and not an external antenna. In this manner, the motor cable serves as a waveguide between the modems.

The 9Xtend radio modems use FSK (see 2.7.2.) to modulate the received data stream up to the 900MHz band. The specific type of FSK is unknown, but it is known that the FSK frequencies range from 905MHz to 925MHz. Thus, the % frequency difference between the two symbols is about 2.2%. For error checking, the 9Xtend utilizes 16-bit CRC (Cyclic Redundancy Check), a mainstream algorithm that allows detection of data corruption during transmission. There is no built in algorithm to

retransmit corrupted data, the modem will recognize that there was an error and can discard the data, but it will not automatically ask for retransmission.

3.1.5.2. Operational diagram

Instead of sending continuous streams of data, the 9Xtend sends discrete packets of user-selectable size. The process of sending a packet is shown in figure 31 below:

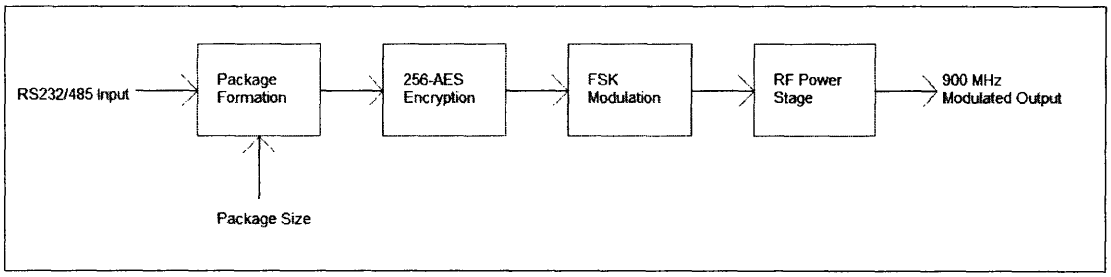

9Xtend operational diagram for data transmission figure 31.

First, the modem receives a string of data from the RS232 or RS485. This string is accumulated until it reaches the user-selected package size (or until the modem times out after waiting for additional data). Then the package is encrypted using 256-bit AES and then modulated up to 900MHz using FSK. This process is repeated in reverse order at the receiving end to finalize data transmission. . Therefore, the total delay of transmission depends on a multitude of factors. First, there will be a time delay in waiting for enough data to arrive to form a packet. This time delay will thus depend strongly on both the interface data rate (the rate at which the data is sent to the modem) and the packet size. Next, the data must be encrypted, which constitutes an additional, unknown time delay. Finally, modulation adds another delay. These are in addition to any signal path delays that are present in the circuit. Total delay times, measured from the time the data packet is completed and enters the transmitting modem until the data packet exits the receiving modem are given by MaxStream in the following table:

Manufacturer-Provided Delay Times for 9XTend Radio Modems

Interface Rate Packet Size	**115.2Kbps**	**9600bps**
1 byte	8.5mS	82mS
32 bytes	13mS	82mS

These numbers were obtained by setting the interface rate equal to the RF data rate, to avoid data overflow. Note that for slow data rates the delay is independent of packet size, which implies that in this case the data transmission is the limiting factor. For faster data rates the delay increases with increasing packet size, thus, the limiting factor is the time consumed in forming/encrypting the packet.

3.1.5.3. Manufacturer specifications

Important manufacturer specifications for the 9Xtend radio modems (such as data rates and minimum detectable power signal levels), obtained from the Maxstream® website are shown below:

9XTend Radio Modem Specs from Maxstream®

Transmit Power Output	1mW,10mW,100mW,500mW,1W, Software Selectable
Maximum Line-of-sight range (with high gain antenna)	40miles=64km
Interface Data Rate	10 - 230400 bps, Software Selectable
Throughput RF Data Rate	9,600 bps – 115,200 bps, Software Selectable
Receiver Sensitivity	-110dBm at 9,600 bps -100dBm at 115,200 bps

RF Operating Frequency	ISM 902 – 928 MHz
Spread Spectrum	FHSS (Frequency Hopping Spread Spectrum)
Modulation	FSK (Frequency Shift Keying)
Encryption	256-bit AES

Furthermore, the modems have an output impedance of 50 Ohms.

3.1.5.4. Software loop-back test

The software included with this modem provides the option of testing the connectivity of two units by using a serial loopback transmission test. It also provides a readout in dBm (referenced to 0dBm=1mW) of the Received Signal Strength Indicator (RSSI) and indicates any time there is an error in the received packet. The serial loopback transmission test works by first sending a certain string of characters to the modem. This data is sent to the receiving modem, which is fitted with a loopback RS232 connector. In short, the loopback connector ties the RX and TX terminals of the 232 port together, thus, echoing the received signal back to the source. The receiving modem now sends back the same string of characters back to the transmitting modem. If the string received is equal to the transmitted one, the connection is successful and the process starts again. If the echoed string is different from the one originally transmitted or if no data is received, the connection is unsuccessful and the process starts again. The software keeps track of the total number of successful and unsuccessful attempts and provides a cumulative percentage of good packets received. This test will be used to measure the quality of the transmission line.

3.1.6. Miscellaneous cables and connectors

In addition to the cable, modems and pulse generators, we will use several cables and connectors to create each experimental setup. These include 50-ohm coaxial cables, BNC to RPSMA and BNC to MMCX adapters, BNC male/female adapters and others. Of all these miscellaneous parts, the ones that could produce substantial inaccuracies are the coaxial cables. Because we will use these to bridge the gap between several devices, such as between the pulse generators and the cable or between the cable and our measurement system, long coaxial cables could add signal delays and reflections that could affect our measurements. The effect of these delays will only be significant if the lengths of the coaxial cables are comparable to the length of cable FT1. Fortunately, all the coaxial cables used have physical lengths under 2m, which is well below the 31m length of cable FT1.

3.2. Experimental Setup

To facilitate future reference, this section will include diagrams and short descriptions of the different experimental setups. The first part will contain the different setups which address the characterization of the different components, the second part will address our measurement system, finally, the third part will describe the setup for simulated data transmission.

3.2.1. Equipment Characterization
3.2.1.1. Drive and motor setup

To characterize typical operating conditions, we first measured motor PWM and feedback signals during operation using the currently available extra-feedback cable

solution. The drive control was set at a constant rotational speed of 500rpm, and the drive power supply voltage was 24V RMS. The setup is shown in figure 32 below:

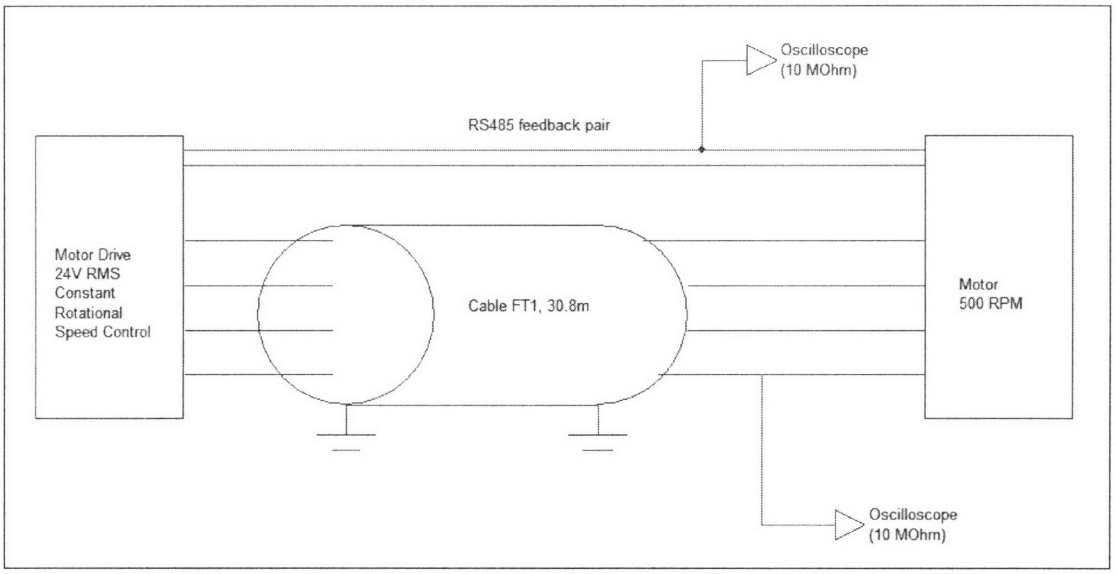

Functional motor/drive setup using external RS485 feedback cables
figure 32.

The S200 series drive and 3-phase PWM motor are shown in pictures 33 and 34 respectively.

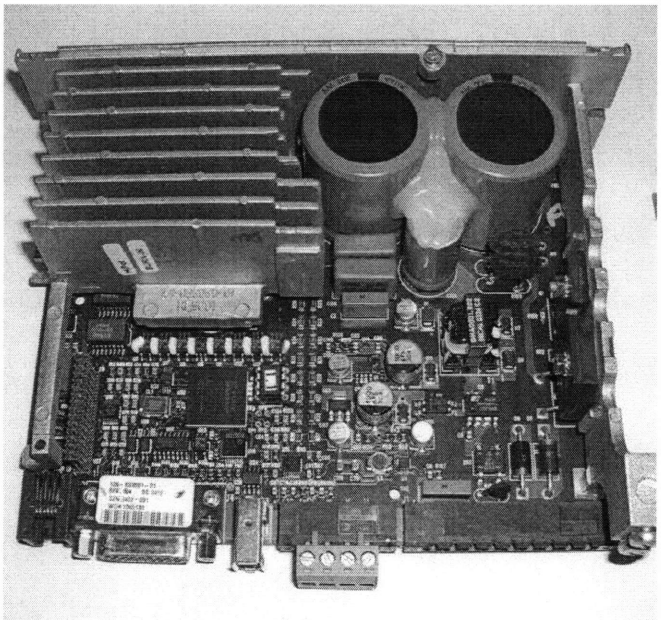

S200 series drive from Danaher® used for motor control
figure 33.

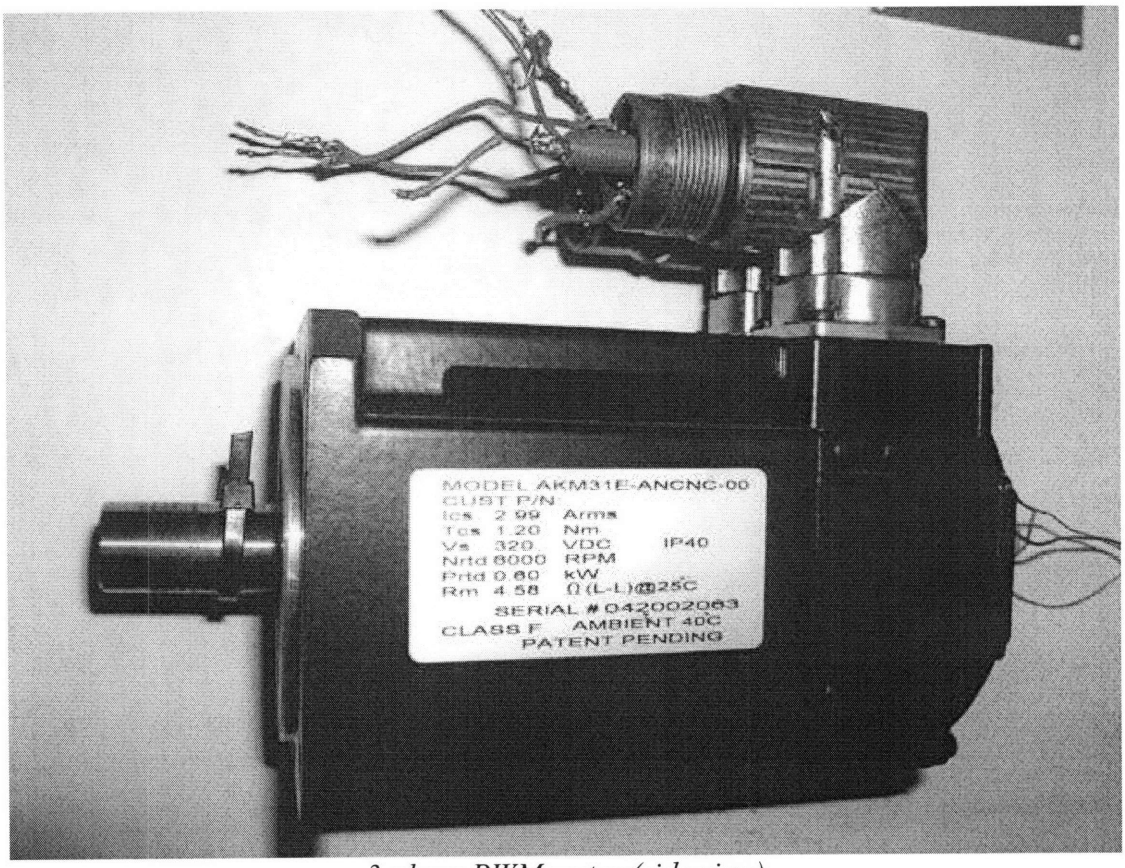

3-phase PWM motor (side view)
figure 34.

3.2.1.2. Direct FT1 cable pulse response

Before diving into frequency characterization we will characterize the time response of the cable. This will allow us to calculate and measure several cable characteristics such as signal delay and characteristic impedance. These quantities (specifically the characteristic line impedance) change considerably depending on how many conductors are used in parallel. The different configurations are shown on figures 35, 36 and 37:

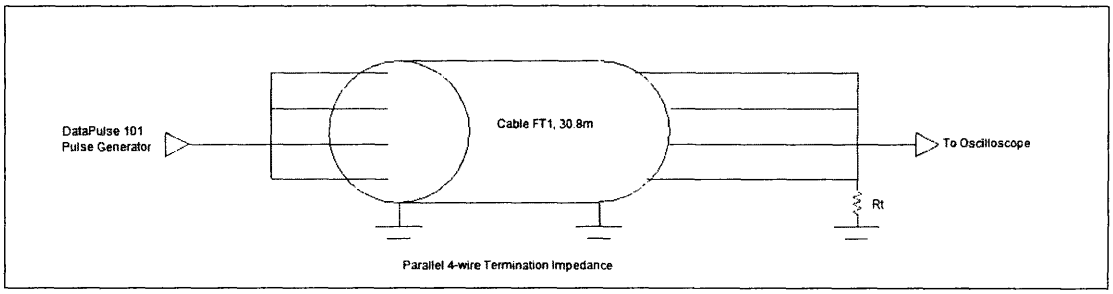

Direct time domain characterization with 4 parallel conductors and determination of characteristic impedance
figure 35.

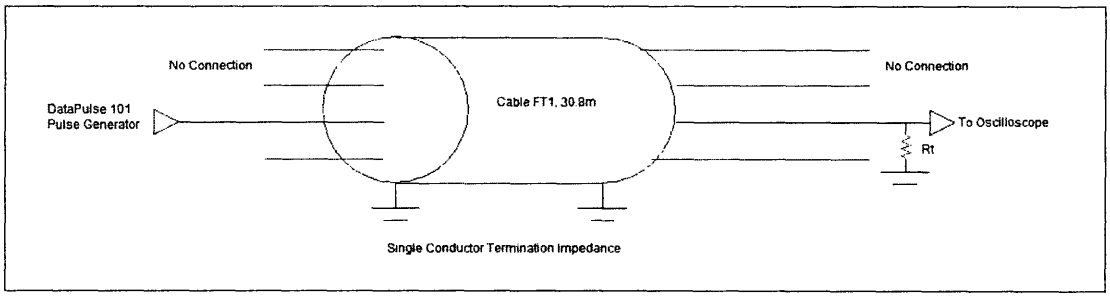

Direct time domain characterization with single connector, other connectors open, and determination of characteristic impedance
figure 36.

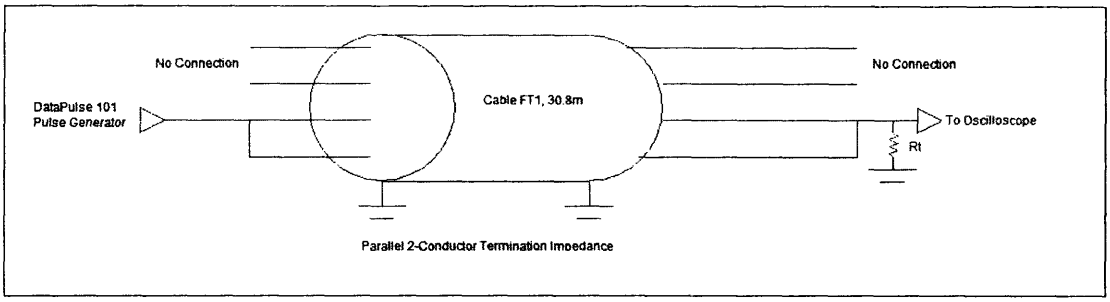

Direct time domain characterization with two parallel conductors, other conductors open, and determination of characteristic impedance
figure 37.

3.2.1.3. Filter pulse response

The filter frequency response is obtained in a similar way as the cable frequency response. The four input terminals are tied together (as they are for high frequency signals) and voltage pulses are sent through the filter network. By comparing the

frequency content of the input and output signals, one can derive a frequency response, which we can then compare with the expected frequency response based on theoretical analysis. The setup is shown in figure 38 below:

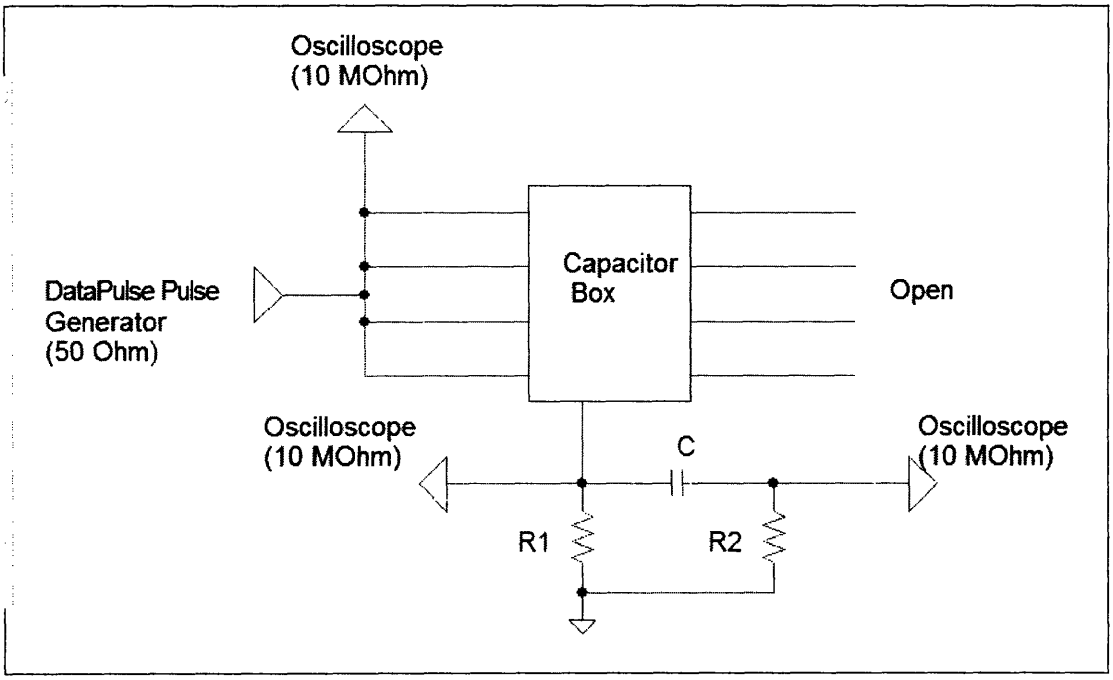

Capacitor network setup for measuring frequency response figure 38.

3.2.1.4. Coupled FT1 cable pulse response

After measuring the direct cable response as shown above, we will measure the response of the cable with the addition of the coupling feed-through capacitors. The different coupling configurations (output only, both) are shown below in figures 39 and 40:

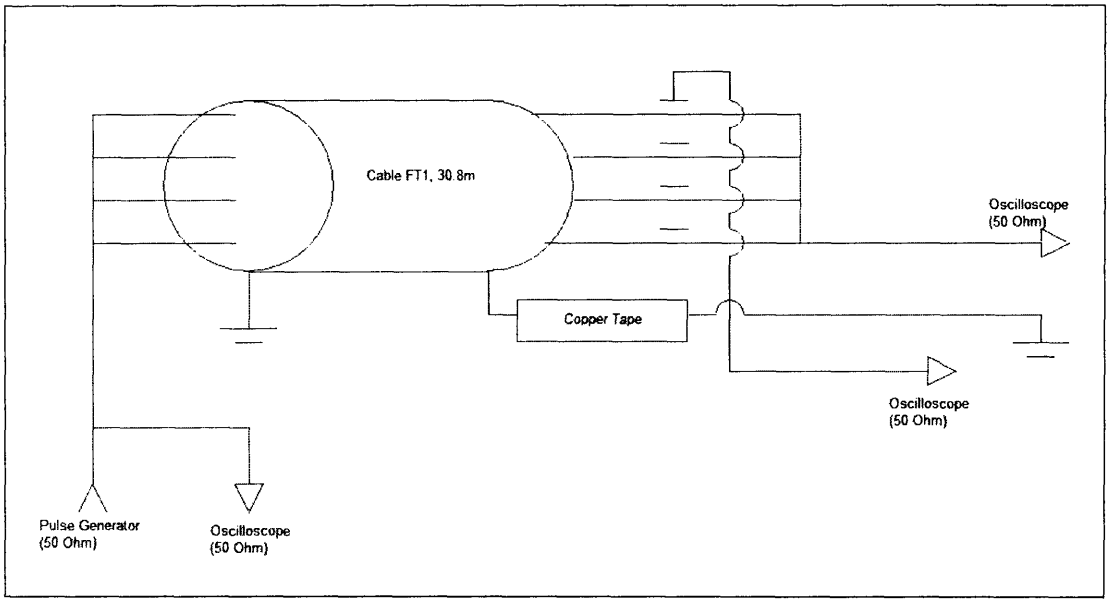

Feed-through capacitor network at output end only
figure 39.

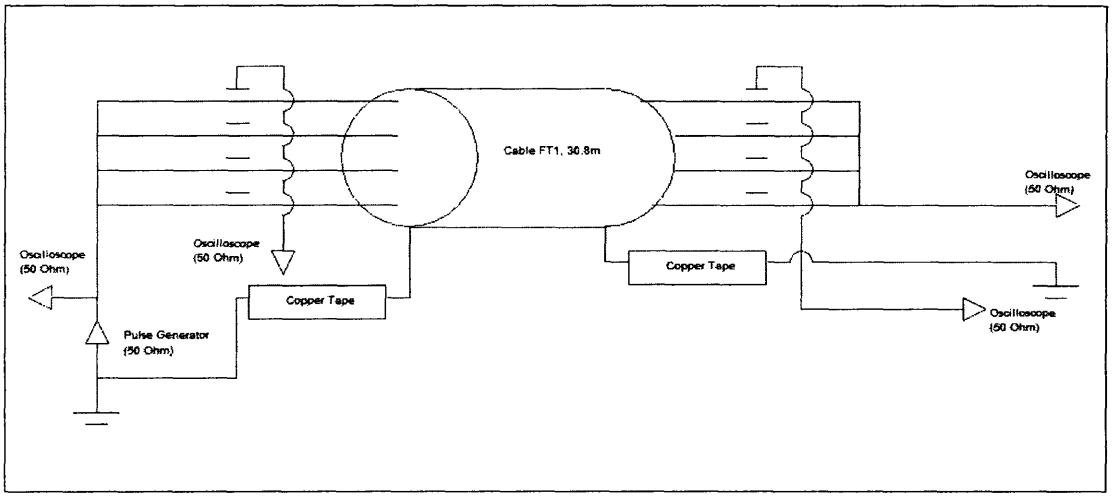

Feed-through capacitor network at input and output ends of cable FT1.
figure 40.

These setups allow for measuring the direct cable response and the signal at the coupler output simultaneously, which allows us to obtain frequency transfer responses of the coupled and uncoupled systems.

3.2.1.5. FT1 cable response at 900MHz

Because our pulse generator only allows us to obtain relevant frequency response data up to 200MHz, we will measure the cable response at 900MHz by directly connecting the radio modems in transmission mode and measuring the amplitude of the transmitted and received signals. The setup is shown in figure 41:

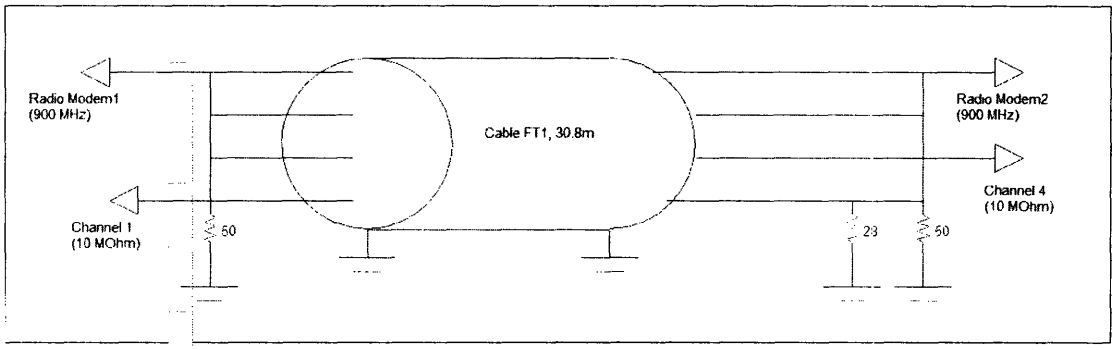

Setup for measuring cable FT1 frequency response at 900MHz figure 41.

3.2.1.6. Radio modem transmission with simulated PWM signals

The last of our experimental setups attempts to simulate information transmission in the presence of PWM motor power signals. The radio modems are coupled in and out of the system through the feed-through capacitor boxes, while the Ritec SP-801 high voltage pulse generator is used to simulate the PWM signals. The setup is shown in figure 42.

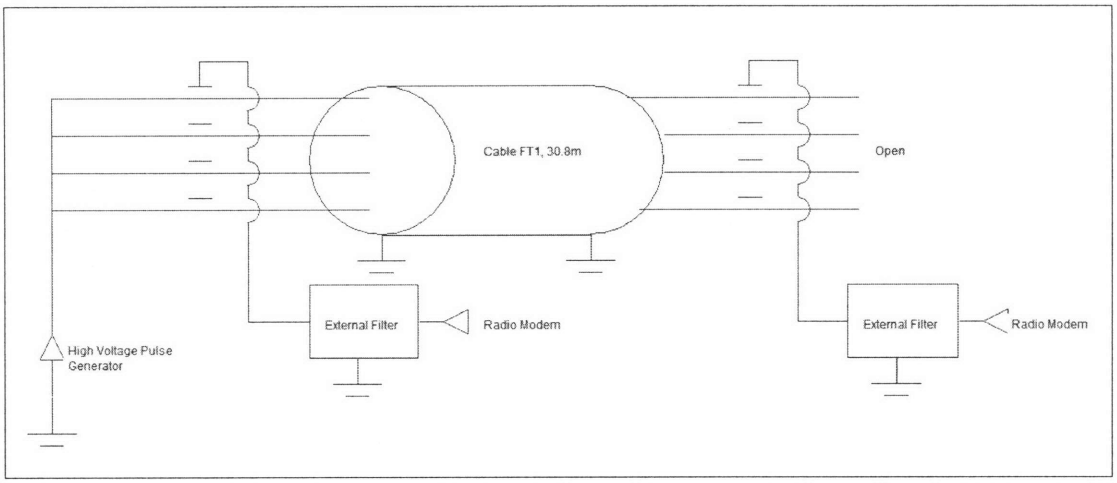

Simultaneous transmission of RF data signals in the presence of simulated PWM signals figure 42.

Figures 43a and 43b show actual pictures of the final setup.

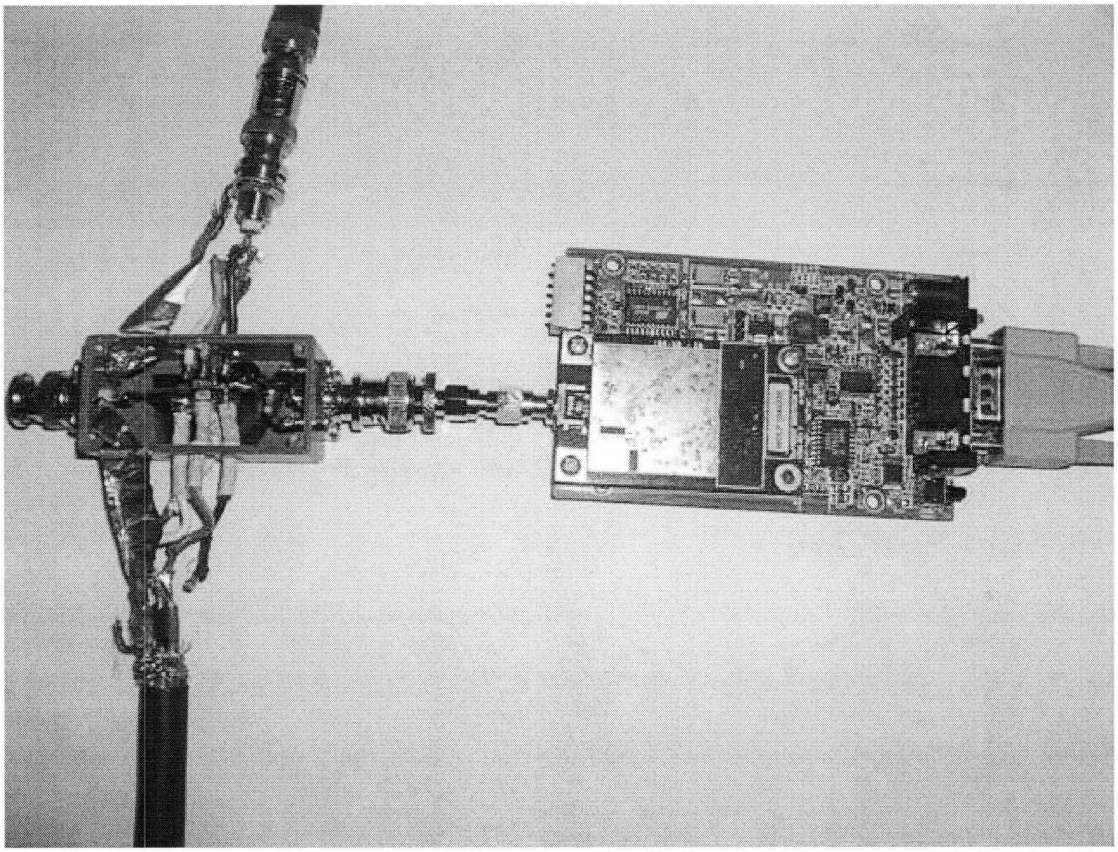

Full system setup. The motor cable is shown at the bottom, the PWM signals enter through the top, the modem is connected through the right
figure 43a.

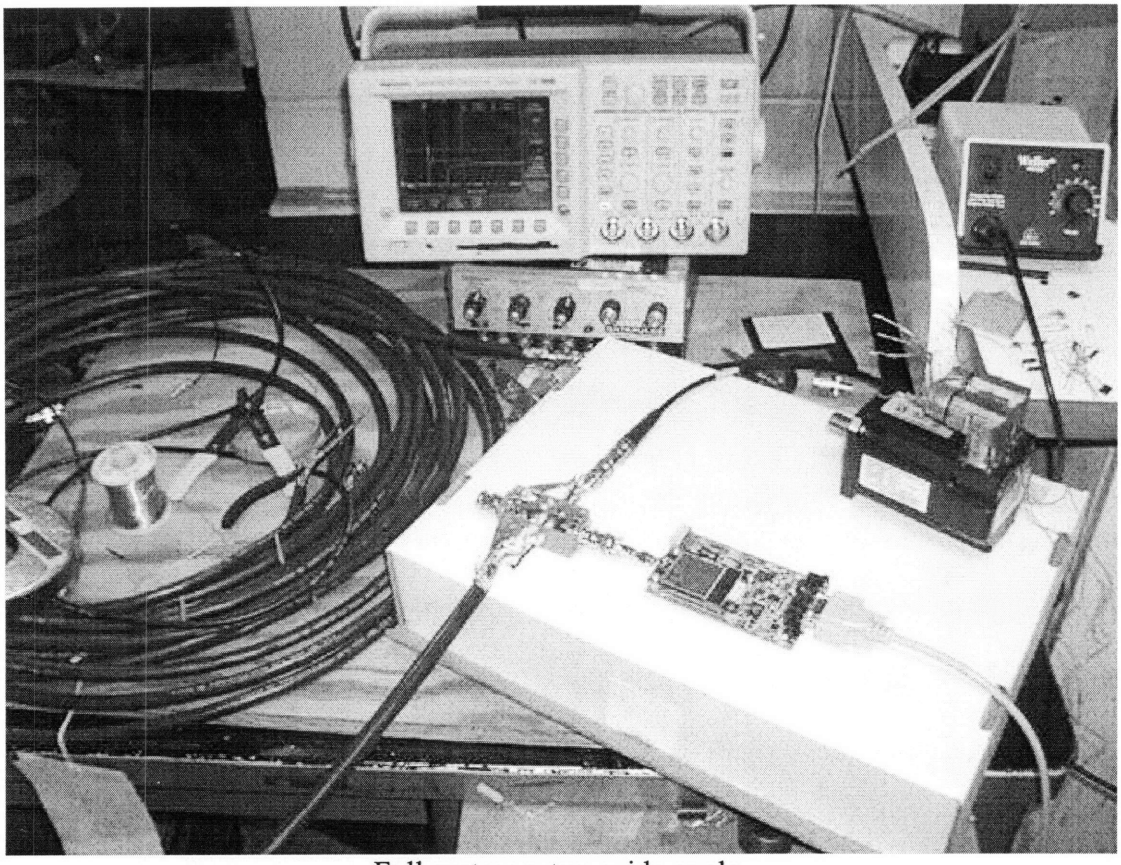

Full system setup, wide angle.
figure 43b.

Because the radio modems are originally designed for wireless transmission, the output ports are MMCX and RPSMA. These ports are connected directly to the filters through MMCX/RPSMA to BNC adapters. The end of the PWM cable in which the motor would be connected was left open circuited to simulate the motor's high frequency impedance characteristic.

3.2.2. Measurement system

In the following section we will introduce the measurement system used to obtain the experimental data. In its simplest terms, the measurement system is composed of four main elements, a signal source (or pulse generator), an oscilloscope which collects the

raw data, a data acquisition software which is used to interface from the oscilloscope to the computer, and finally analysis software used to get frequency domain information from the time domain measurements.

3.2.2.1. Tektronix TDS 3054B 4-channel oscilloscope

The oscilloscope used for all measurements is the Tektronix TDS 3054B 4-channel oscilloscope. This oscilloscope allows for simultaneous collection of data from four different sources. Furthermore, it includes the option of averaging the received signals as a noise-reduction technique (see 3.2.2.3.), with a maximum sample size of 512 averages. With high-bandwidth probes or direct connections, the maximum bandwidth of the scope is 500MHz. The maximum number of samples per second is 5Gs/sec. The number of data points per signal capture is 10,000, independent of time scale.

3.2.2.2. Acqumen data acquisition software

The Acqumen software interfaces with the oscilloscope and allows for collection, averaging and saving of oscilloscope data in data sheet formats. The most important feature of this software is that it permits further averaging of data signals read from the oscilloscope (which are already averaged with a sample size of up to 512), thus allowing us to accurately measure small amplitude signals while rejecting random noise and pickup.

3.2.2.3. Noise reduction by averaging

As we have mentioned before, averaging is a powerful tool which allows us to measure signals with relatively small amplitudes while rejecting random noise and pickup. To better understand how this works, suppose we wish to measure some signal represented by s. When measuring this signal, we also get some additive noise, which is

represented by the random variable N. The total measured signal, S will then be given by the simple equation:

$$S = s + N$$

Suppose that the noise has some variance v, such that:

$$\text{var}(s + N) = \text{var}(s) + \text{var}(N) = v$$

Now, suppose we instead take an average of measurements of n samples. The resulting data and the calculated variance of the data in terms of the sample size are derived as follows:

$$S_{avg} = \frac{1}{n}\left(S_1 + S_2 + \cdots + S_n\right) \Rightarrow$$

$$\text{var}\left(S_{avg}\right) = \text{var}\left[\frac{1}{n}\left(S_1 + N_1 + S_2 + N_2 + \cdots + S_n + N_n\right)\right]$$

$$= \frac{1}{n^2}\text{var}\left(N_1 + N_2 + \cdots + N_n\right)$$

$$= \frac{1}{n^2} n\,\text{var}(N)$$

$$= \frac{v}{n}$$

The variance of the resulting quantity is reduced by a factor of n. Now, assuming that the noise is purely random (centered at 0), we can calculate the equivalent reduction in noise magnitude that would result in a measured signal variance equal to v/n:

$$S = s + \frac{N}{k} \Rightarrow \text{var}\left(S\right) = \frac{1}{k^2}\text{var}(N) = \frac{v}{k^2}$$

$$k = \sqrt{n}$$

Therefore, a reduction by a factor of N in the variance corresponds to a reduction in the magnitude of the noise equal to $\sqrt{N}$. Thus, although more samples in averaging will

always result in better signal resolution with less noise, the effect suffers from diminishing returns as the number of samples is increased.

4. RESULTS, ANALYSIS AND MODELING

4.1. Motor PWM signals

To determine the needs for the data signals it is first necessary to know the characteristics of the motor drive signals such as magnitude, speed of transitions and frequency content. We must also be able to overcome the problem of differentiating between data signals and PWM spectral content contributions. In the following sections, we will describe typical PWM motor power signals, both in the time and frequency domains.

4.1.1. Motor PWM signals in time domain

The way 3-phase PWM motor feedback control works is by feeding three different signals to the motor at any point in time. In general, two of these signals will be equal, while the third one will resemble a pulse train. The motor then effectively sees as its input signal the difference between these signals. Thus, by changing the width of the third signal, one can control the energy delivered to the motor at any point. Therefore, there are two different possible PWM motor signals, one that resembles a square wave with a 50% duty ratio, and another one which is represented by a square wave with a variable duty ratio. Figures 44 and 45 show the waveform of this third wave for constant speed control at 100rpm and 500rpm with the drive operating at 24V AC, 60Hz power input:

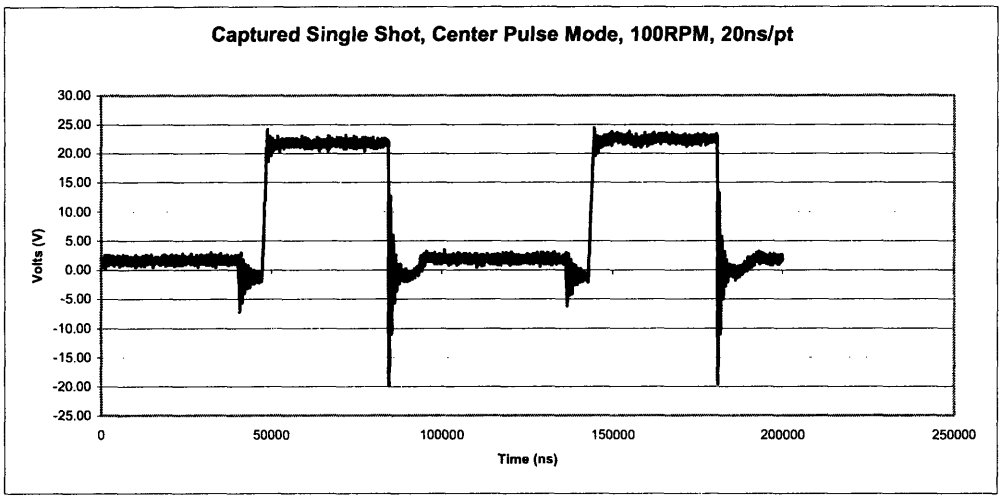

Variable PWM duty ratio waveform for constant rotational speed control at 100rps, 24V AC drive power
figure 44.

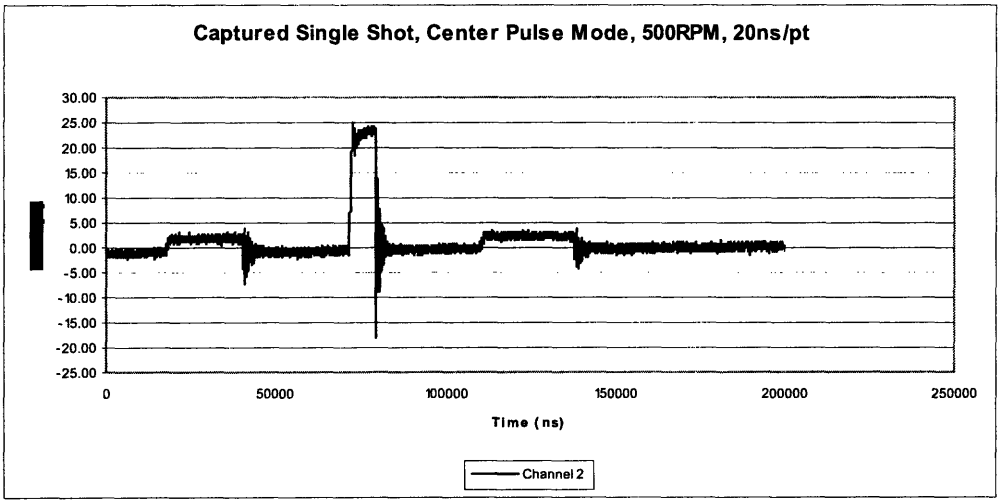

Variable PWM duty ratio waveform for constant rotational speed control at 500rps, 24V AC drive power
figure 45.

As the width of the pulses in this waveform increases (as the duty ratio approaches that of the other phases), the fraction of time in which there is a non-zero voltage difference at the motor decreases. This translates into lower average power into the motor. Thus, we observe that for constant speed control we get narrower pulses for higher speeds, as higher speeds require higher power levels.

The averaged PWM signals (figure 46) show what at first might appear to be odd behavior:

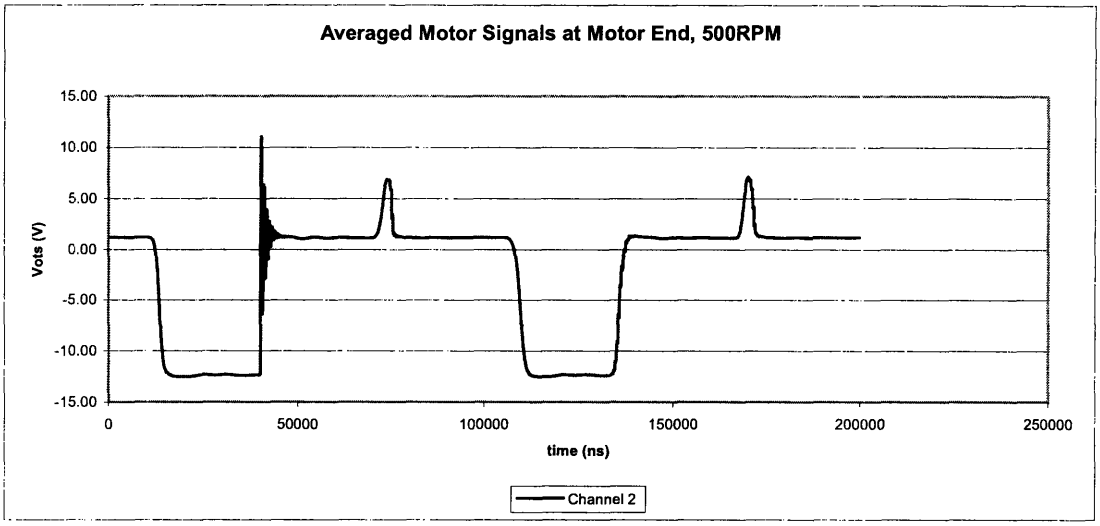

Averaged motor PWM signals at a single motor phase, 24V AC drive power figure 46.

The little peak at the middle of what would otherwise be a square wave is due to the fact that each phase is sometimes a square wave and sometimes a pulse train. Averaging these two signals in time results in a square wave with a "peak" at the center of each pulse. The other feature of interest in this response is the dramatic ringing which appears at the rising edge of the waveform. Figure 47a shows this ringing in more detail:

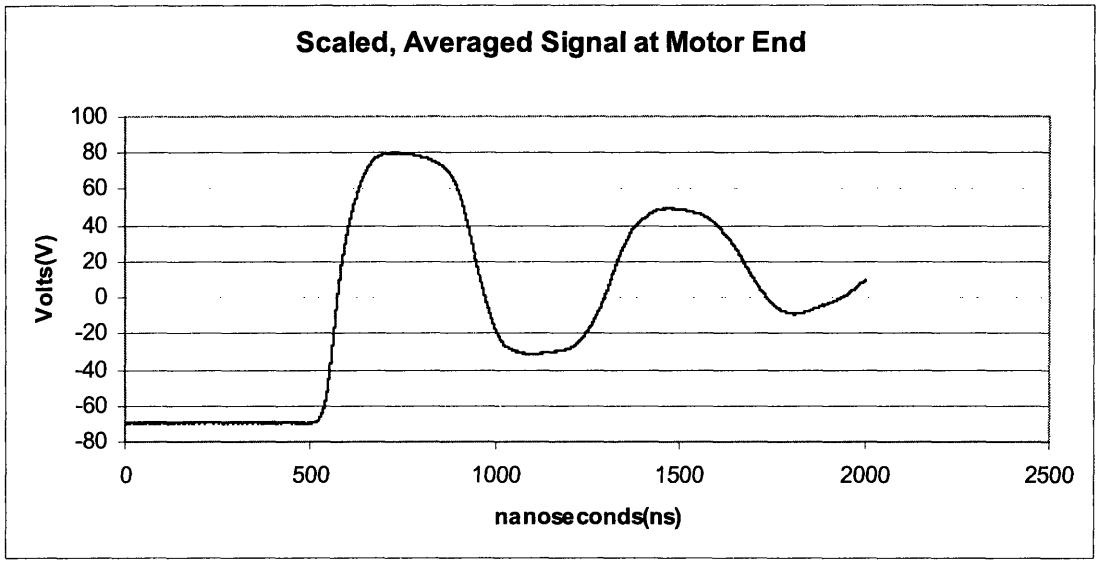

Motor drive signal at motor end with 31m cable.
figure 47a.

The period of this oscillation is close to 700ns. The cause of this ringing was pinpointed to be the cable itself and its reflections. Recall that the one-way travel time across the length of cable FT1 was measured to be 170ns. When the PWM wave first arrives at the motor end, it is reflected back towards the drive. This wave is in turn reflected at the drive back towards the motor. When this wave arrives back at the motor, we get a negative dip in the oscillation. The total wave travel time needed for this situation is twice a one-way trip, or 340ns. Therefore, we would expect the oscillations caused by cable reflections to have a period of twice 340ns, or 680ns. This corresponds exactly to the oscillations we observe at the motor end.

The PWM waveforms at the drive end are similar to those at the motor end, except with much greater damping (provided by the impedance of the driver) and therefore cable oscillations are less perceivable, as shown below in figure 47b:

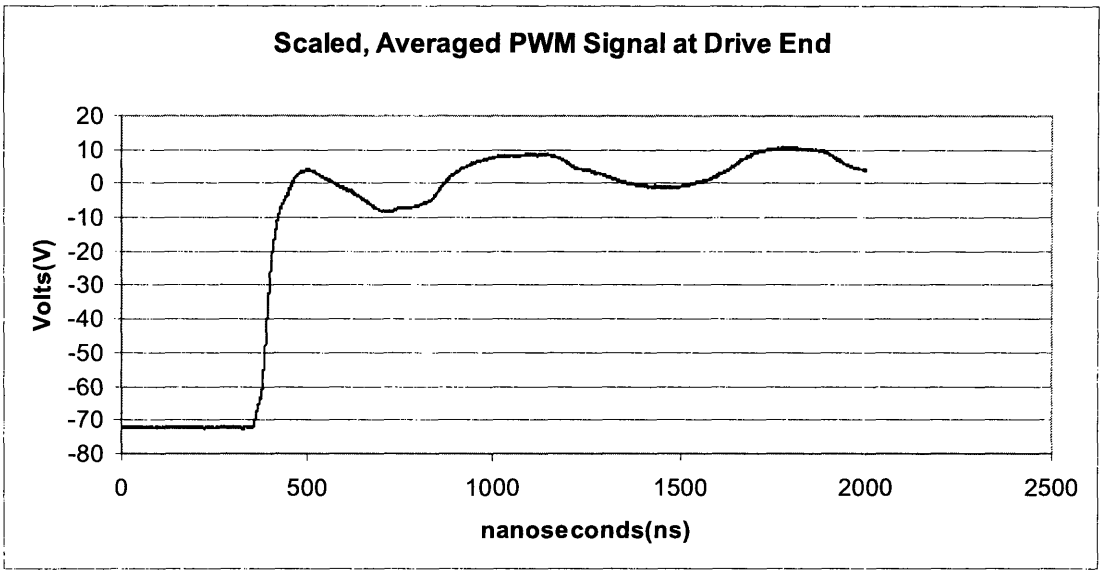

Motor drive signal at drive end with 31 cable.
figure 47b.

Another important piece of information we can obtain from observing this reflections is that the impedance of the motor must be very high compared to the characteristic impedance of the cable. The PWM signal overshoot is almost the same as the magnitude of the PWM step, thus, the reflection coefficient must be nearly 1, which corresponds to a load impedance which is much greater than the characteristic impedance of the transmission line. This is to be expected, as the load presents an inductive load, which for these fast transitions (which correspond to high frequencies), appears as a complex impedance of great magnitude. The Q of the resonance is about 7.

4.1.1.1. Rise time, fall time, pulse width

To be able to simulate the PWM motor signals with pulse wave generators, we need to measure typical rise and fall times, as well as pulse widths of PWM signals. Figures 48 and 49 show the rising and falling edges of typical PWM signals:

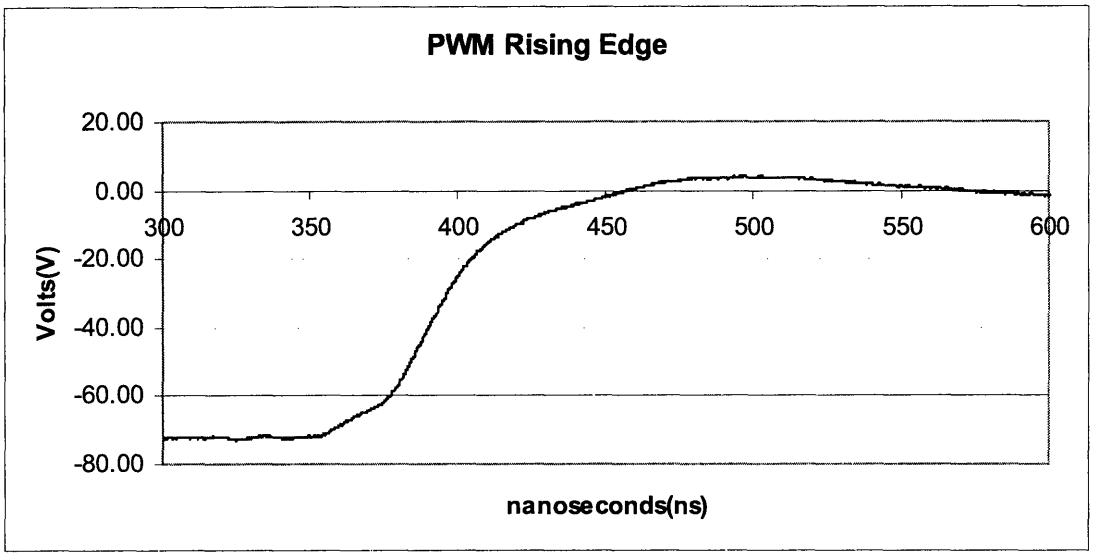

figure 48.

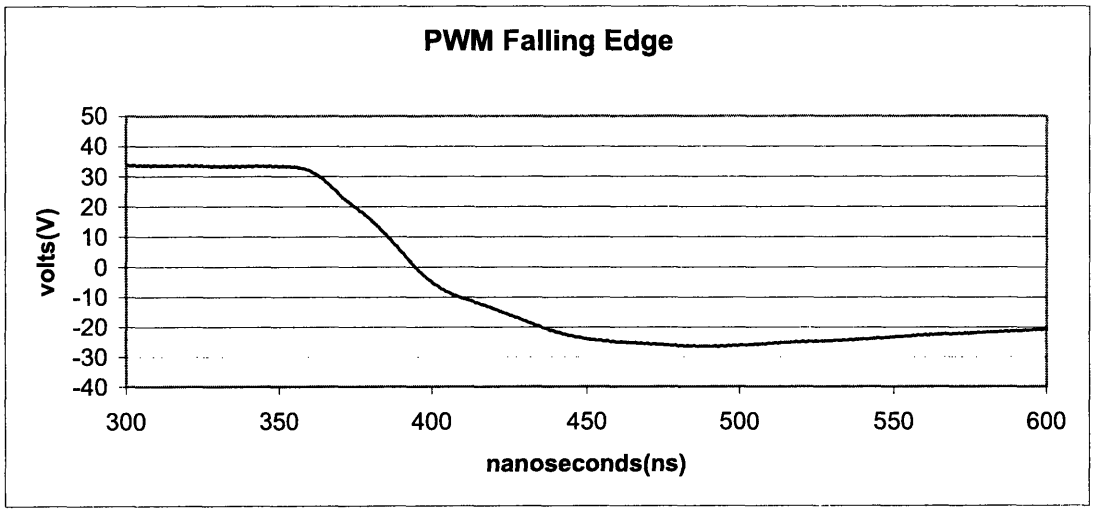

figure 49.

The rise and fall times of the PWM signals are similar and both approximately 120ns. The fact that the rise and fall times are symmetric allows us to restrict the frequency domain measurements to rising edges only, as the frequency content depends on the magnitude of the slope of the wave and not on the polarity of the transition.

The maximum frequency of the PWM waves is 10KHz and the width of the 50% duty ratio waves is therefore 50us.

4.1.2. PWM signals in frequency domain

The spectral content of the PWM signals will give us insight into what will be the magnitude of the "noise" they will contribute to our data transmission operation. The spectral content plots are obtained by calculating FFTs of the time-domain signals using RespMstr®.

4.1.2.1. Spectral content

The calculated spectral content for PWM signals at the drive and motor end are shown in figures 50 and 51:

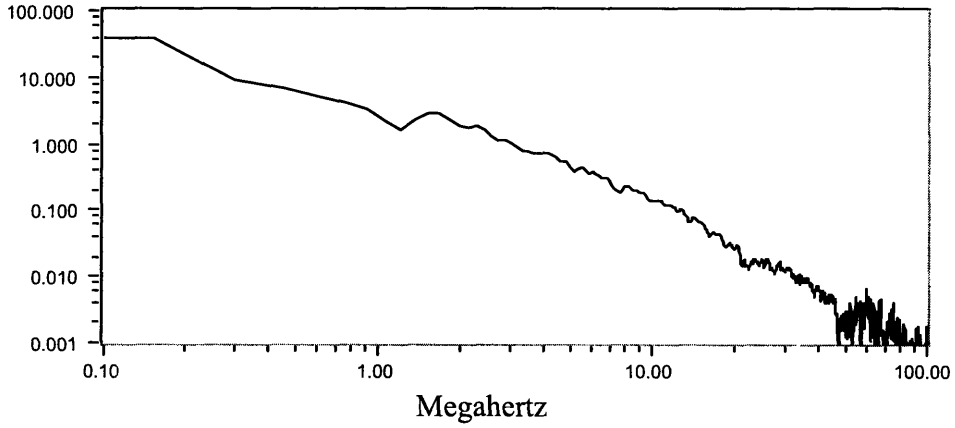

Spectral content of PWM signals at drive end (see figure 47b.) with 120V AC supply to motor drive
figure 50.

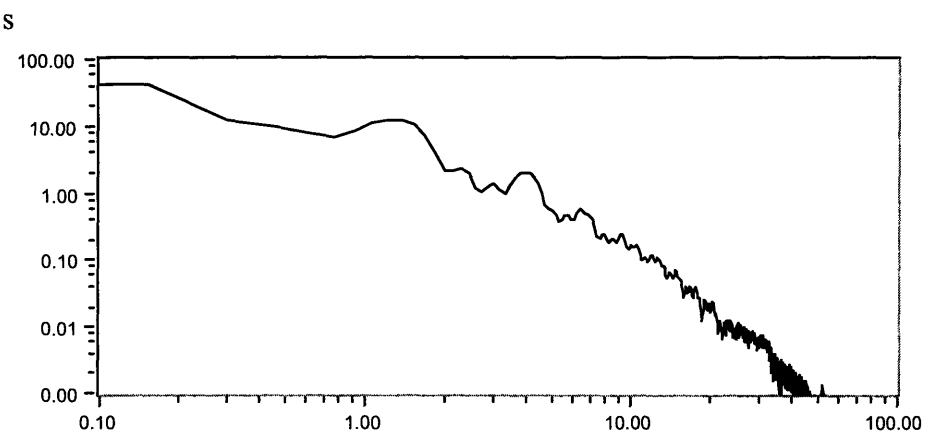

Spectral content of PWM signals at motor end with PWM absolute step magnitude of 15V (averaged signal)
figure 51.

The magnitude peaking that is observed in the spectral content of the signals at the motor end corresponds to the cable oscillation, which has a natural frequency of 1/(4*cable propagation delay)=1.4MHz.

The roll-off rate of the spectral content of these PWM signals is about -40dB/decade for frequencies above 10MHz. The approximate absolute value of the spectral content at 900MHz (our proposed data transmission system) will be in the order of 1e-12 to 1e-13 Volts. For full-voltage motor signals, which are about 10 times higher than the ones we tested, the expected spectral content at 900MHz should then be between 1e-10 and 1e-11 Volts. In any case, motor PWM signals are expected to have very little energy in the 900MHz frequency band. However, it is still necessary to limit the lower frequency voltage from the PWM that could reach the RF circuitry to avoid damage to these components.

4.1.2.2. Ideal PWM spectral content

PWM signals in the ideal case are perfect square waves. In the worst case, these signals will have a spectral content equal to the spectral content of a voltage step. The

Laplace Transform of a voltage step of value V is given by V/s. Therefore, the ideal spectral content of the PWM signals should be given by V/2pif, where f is the frequency in hertz. The main difference between the expected ideal spectral content and the real spectral content is that the roll-off rate of the spectral content of the real PWM signals is greater than -20dB/decade for higher frequencies. This is mainly due to the fact that real PWM signals have a finite rise time, which implies lower high frequency spectral content. Fortunately, this works to our advantage as the energy of real PWM signals will be lower than ideally expected at 900MHz.

4.1.3. Simulated PWM Signals

For the purposes of our investigation, rather than utilizing a running motor with PWM signals produced by the motor drive, over which we have very little control, we will use a high voltage pulse generator (see 3.1.3.3.), which allows us to more easily control the magnitude of the PWM pulses. In this section we will present typical signals from our high voltage pulse generator to justify that these in fact impose equal or more stringent requirements on our designs than real motor PWM signals would.

4.1.3.1. Simulated PWM in time domain

The Ritec high voltage pulse generator produces negative square waves with relatively fast rise times. A typical voltage signal produced by this pulse generator in time domain is shown below in figure 52:

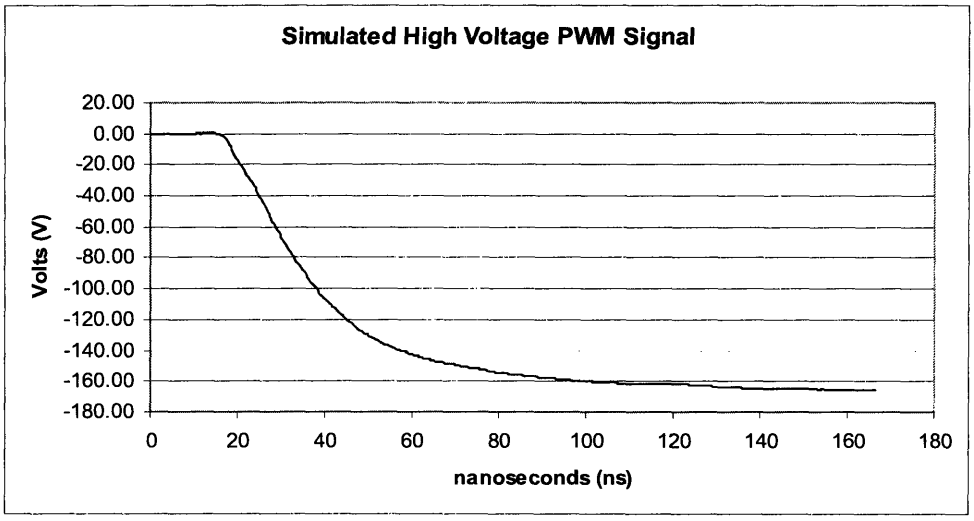

Typical simulated PWM signal in time domain
figure 52.

The maximum absolute slope of this waveform is 5.78V/ns, slightly less than double that of the maximum absolute slope of typical motor signals, 3.55V/ns at the drive end and 2.51V/ns at the motor end. Because faster changing waveforms have more high frequency content, we expect the simulated PWM signals to have a greater spectral content than the real motor signals for high frequencies.

4.1.3.2. Simulated PWM signals in frequency domain

The spectral content of the high voltage pulse generator signal shown above in figure 52 is shown below in figure 53:

E-6 V*s

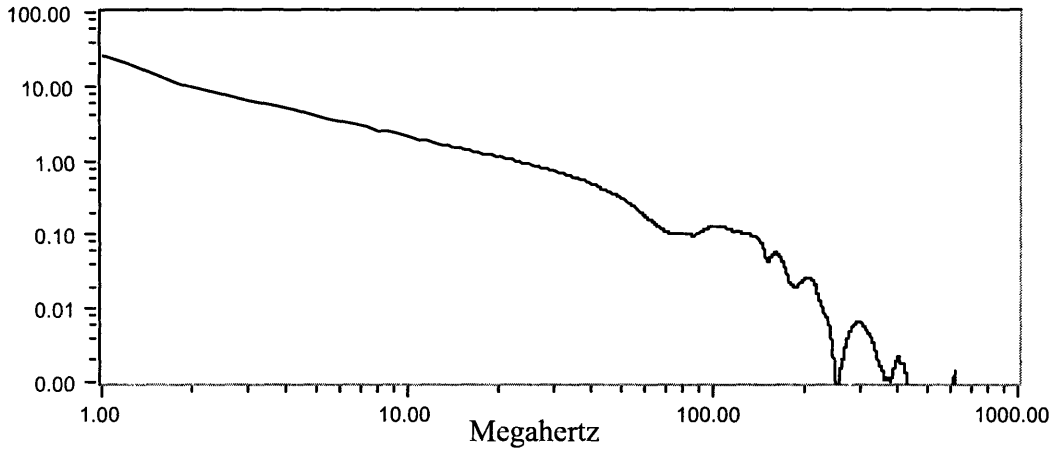

Simulated PWM signal spectral content
figure 53.

The spectral content shows a 1/s roll-off for frequencies below 100MHz. Furthermore, the magnitude of the spectral content of the simulated PWM signals is about 10X greater than the magnitude of the spectral content of real drive signals.

4.1.3.3. Contrast with real motor PWM signals

The simulated PWM signals present more severe conditions to our system than real PWM signals would. There are several reasons why this is true. First, the simulated signals have a faster rate of change (time derivative) than the real signals by a factor of ~ 2. Second, the simulated signals have greater amplitude than the real signals (160V vs. 60V). Finally, simulated PWM signals have more high frequency content (up to 400MHz) than real signals (up to 50MHz). Because of these reasons, we can argue that our test presents very rigorous conditions for operation. Therefore, testing using the simulated signals will give us a "worst-case scenario" with substantial leeway for real-world conditions.

4.2. Feedback data RS485 signals

To justify the need for modulating data signals before sending them concurrently with the PWM signals through the feeder cable, we need to understand the nature of typical motor feedback signals. Feedback signals utilize the RS485 communication protocol (see section 2.6.3). If these signals were sufficiently distinguishable from PWM signals, then we could just couple in these signals directly into the cable without the need for high frequency modulation. In the next few sections we will show that typical feedback signals and PWM signals have similar spectral contents, making the case for high frequency modulation.

4.2.1. Motor RS485 signals in time domain

A typical feedback signal is shown in figure 54:

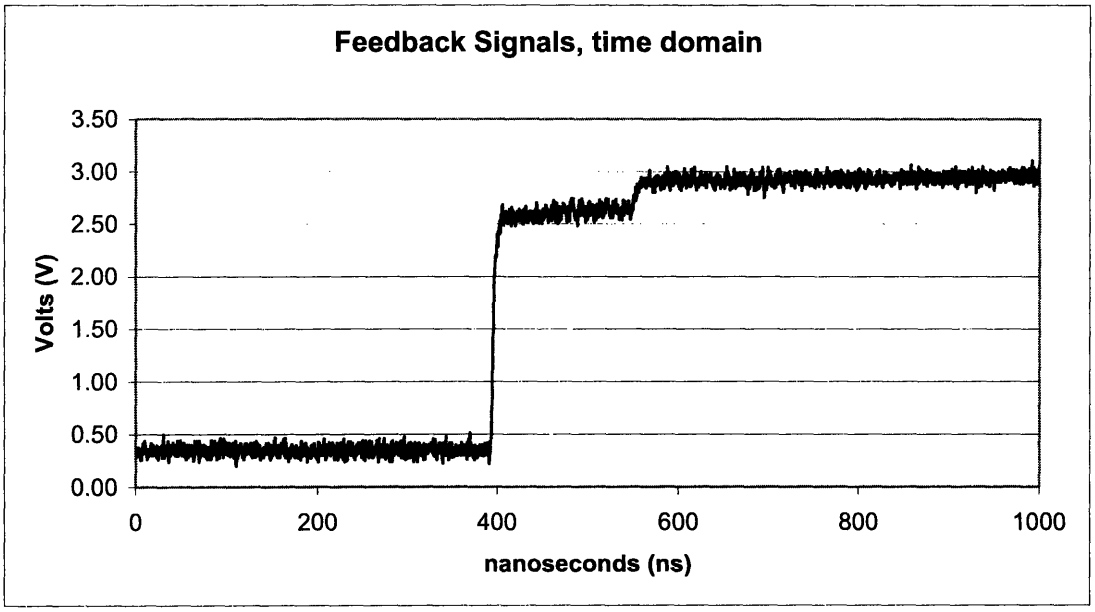

RS485 motor feedback signals in time domain, one wire to earth ground figure 54.

The RS485 sample signal shown was measured from one of the terminals to common ground, contrary to measuring the differential signals from terminal to terminal. Because the RS485 protocol utilizes balanced signal transmission, the real differential signal will be very nearly twice the amplitude.

The fact that the feedback signals are square pulses immediately points towards what will make direct transmission through the cable concurrently with PWM signals difficult if not impossible without some kind of modulation. PWM power signals are also square pulses, but with much greater amplitudes; PWM pulses can have amplitudes as high as 150V, while feedback signals have a maximum amplitude of about 5V. Thus, it will be very difficult to differentiate the relatively small feedback pulses from the high voltage PWM power signals.

4.2.2. Motor RS485 signals in frequency domain

We have already seen how RS485 feedback signals would be hard to detect in the presence of PWM signals because of their similar time-domain waveforms. We can get further insight by observing and comparing the spectral content of these signals.

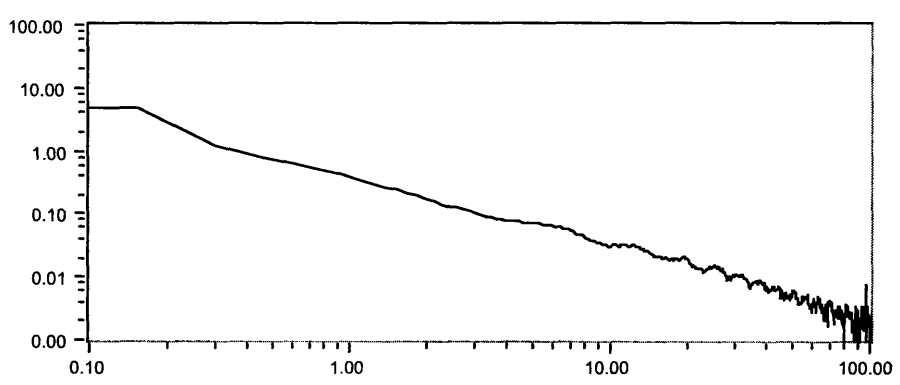

Spectral content of RS485 signals
figure 55.

As expected, the spectral content of the RS485 signals intersects unavoidably with the spectral content of the PWM signals. Furthermore, the spectral content of the PWM signals has a much higher magnitude. Therefore, it is not practical to attempt to send feedback signals concurrently with PWM signals, if we wish to be able to distinguish between the two.

4.3. FT1 cable signal propagation response

To better understand and design our system, we must first understand and characterize the four conductor motor feeder cable that is at its core. We will focus on obtaining parameters such as characteristic impedance, signal delay and magnitude frequency response. All these parameters can be obtained by applying a voltage step at one end of the cable and measuring the input and output relations of the resulting signals.

4.3.1. Characteristic impedance

One of the most important parameters of the cable is its characteristic impedance. As explained in 2.5.2.3., the characteristic impedance is the equivalent, purely real impedance that any sufficiently long transmission line presents to any driving source. An equivalent condition is that this is the equivalent impedance seen by a fast changing signal, such as a pulse or a step.

Although the most commonly known expression for the characteristic impedance of a transmission line depends on indirect parameters which are hard to measure, namely, the capacitance per-length and inductance per-length, there is a rather simple way to determine this impedance directly. As seen in 2.5.4.2, a voltage signal traveling down a

finite transmission line will be reflected at the termination end if and only if the termination impedance is different from the line's characteristic impedance. Therefore, to determine empirically the characteristic impedance of a transmission line, one just needs to terminate the transmission line with a certain purely resistive termination and observe any wave reflections. When there are no perceivable reflections on the line, the impedance of the external termination must match the characteristic impedance. We tested three different configurations; (1) only one active conductor with foil and shield grounded, (2) two active conductors with foil and shield grounded, and (3) four active conductors with foil and shield grounded. The resulting impedances are:

Reference cable FT1 characteristic impedance

Configuration	Characteristic Impedance (Ohms)
1 active conductor, 3 floating conductors, foil and shield grounded	47
2 active conductors, 2 floating conductors, foil and shield grounded	27
4 active conductors, foil and shield grounded	18

4.3.1.1. Single conductor active

The following are three measured voltage waveforms for a single active conductor of the 4 conductor cable active while the other 3 conductors are left open. Figures 56a-c show responses at the drive end (which has a fixed impedance of 50 Ohms) and at the termination end for termination impedances of 10 Ohms, open circuited and 47 Ohms respectively. The results show that the behavior of this setup is approximated very well by that of a finite transmission line with characteristic impedance equal to 47 Ohms.

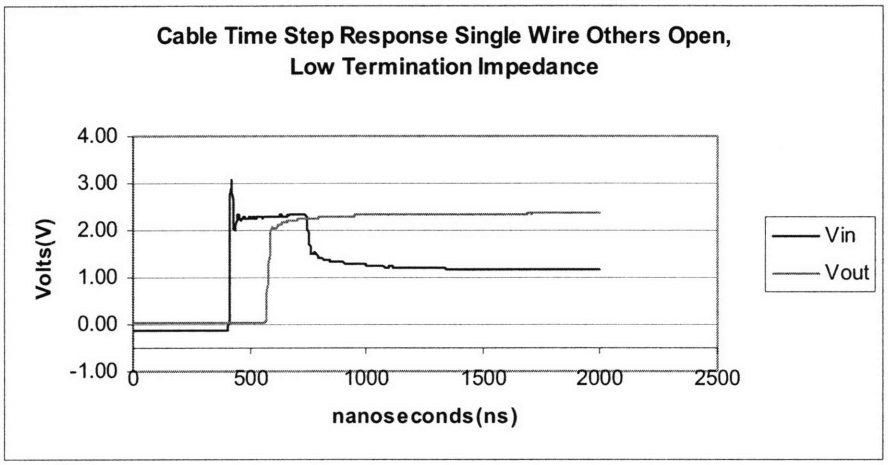

(a)

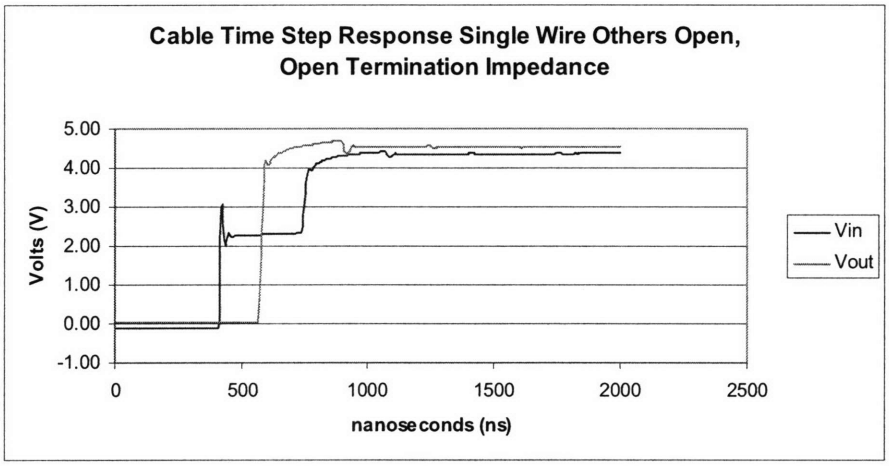

(b)

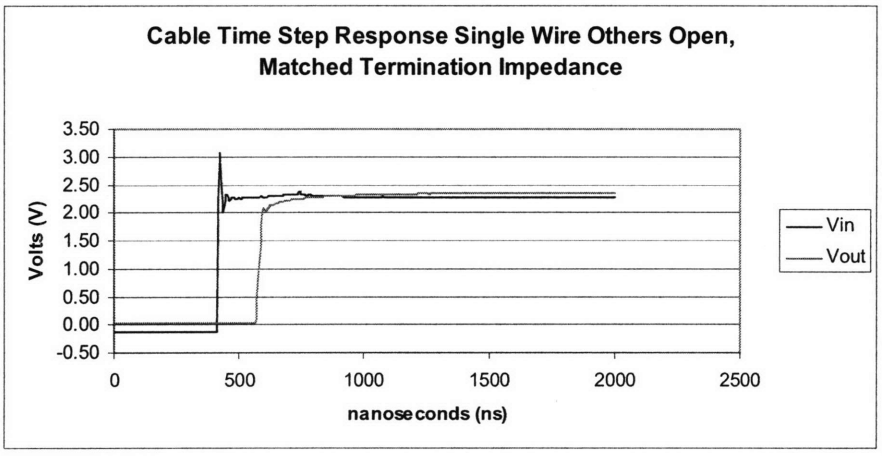

(c)

Step propagation for single conductor, all others open, foil and shield grounded. Source impedance is 50 Ohms, termination impedances of 10 Ohm(a), open(b) and 47 Ohm(c) figures 56a-c.

4.3.1.2. Two conductors active

Similarly as we did for the one active conductor setup, we measured the step responses at the drive and termination end for two active conductors. Figures 57a-b show responses for white and black conductors tied together with others open while figures 58a-b show responses for white and red conductors tied together with others open. Again, the behavior is very well approximated by a finite transmission line, with, in this case, a characteristic impedance of 27 Ohms. Furthermore, the responses for white+black and white+red are almost identical. This implies that pair-wise combinations of conductors yield very similar transmission lines, something that could be of great importance when investigating differential, balanced data signal transmission.

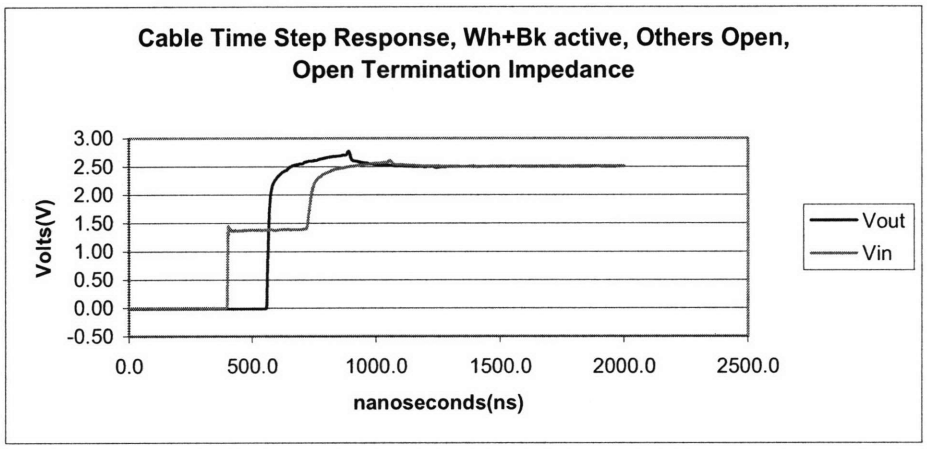

(a)

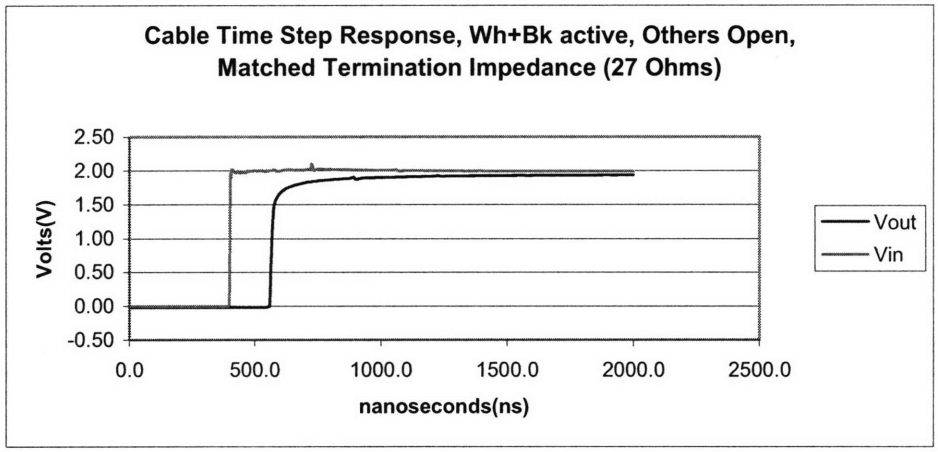

(b)

Step propagation for white and black conductors active, foil and shield grounded. Source impedance is 50 Ohms, open termination(a) and 27 Ohm termination (b) . figures 57a-b.

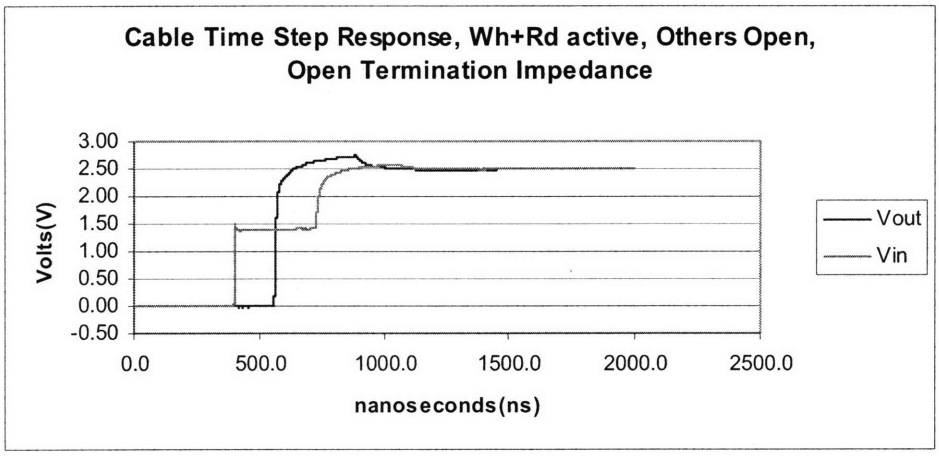

(a)

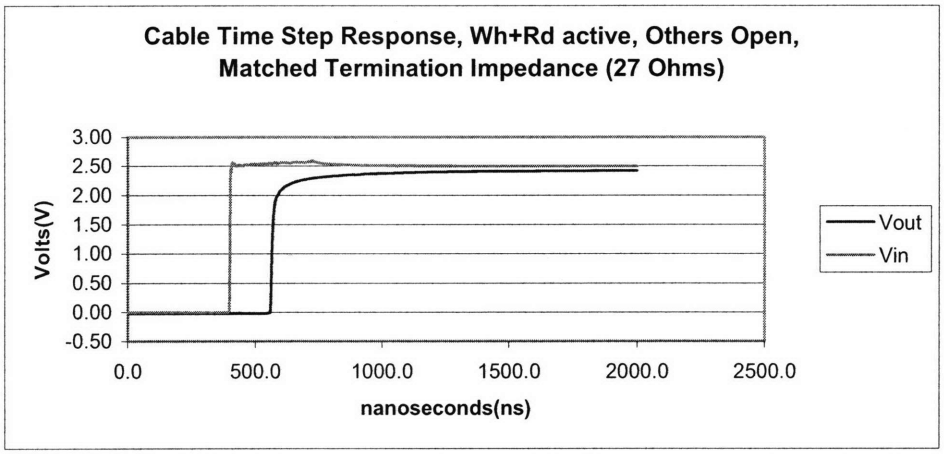

(b)

Step propagation for white and blasck conductors active, foil and shield grounded. Source impedance is 50 Ohms, open termination(a), 27 Ohm termination(b).. figures 58a-b.

4.3.1.3. Four conductors active

Finally, we test step transmission through the motor cable when all four conductors are connected in parallel. Figures 59a-c show measured voltage signals at the drive and termination end for termination impedances of 5 Ohms, 18 Ohms and open circuit respectively. Again, we observe that the conductors behave like a finite-length transmission line. The additional reflections observed for low termination impedance are mostly due to the fact that our pulse generator's output impedance of 50 Ohms does not

nearly match the characteristic impedance of the 4 conductor setup, which is 18 Ohms. This produces reflections back and forth down the transmission line as the waves reach both unmatched terminations.

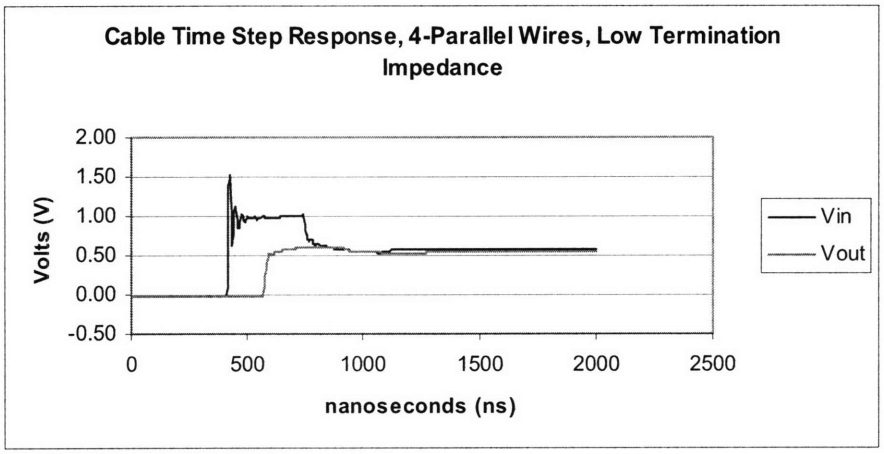

(a)

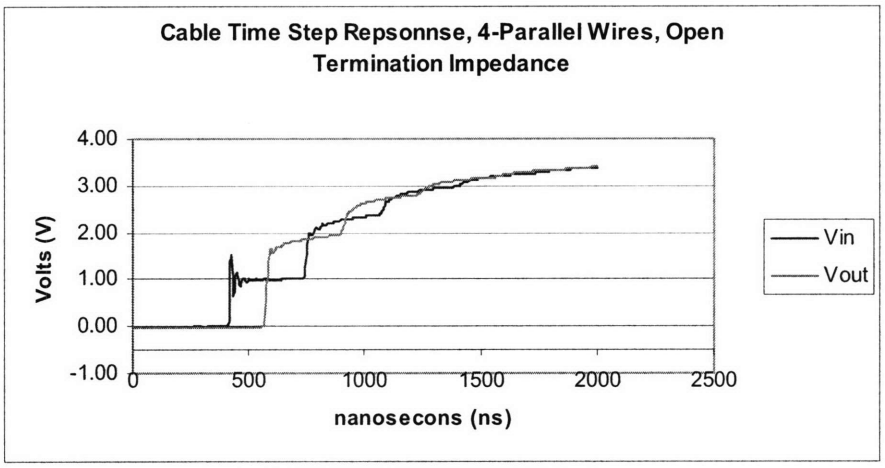

(b)

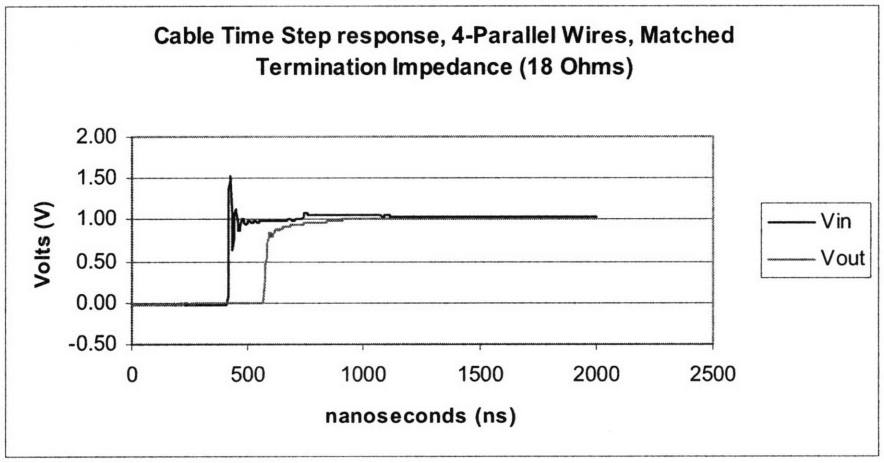

(c)

Step propagation for 4 parallel conductors, foil and shield grounded. Source impedance is 50 Ohms, termination impedances of 5 Ohms (a), open (b), and 18 Ohms (c). figures 59a-c.

Using more active conductors reduces the characteristic impedance, as expected. This can be justified in several ways. First, using more active conductors implies a larger cross sectional area, thus, a lesser per-length inductance and greater surface area, thus a higher capacitance per unit length. Because the characteristic impedance is proportional to the ratio of inductance to capacitance per-length, the characteristic impedance should decrease. Another conceptual way of predicting this behavior is to consider each of the four conductors as an independent transmission line, thus, using several active conductors results in a total equivalent characteristic impedance proportional to the parallel combination of the individual characteristic impedances of the four independent transmission lines. Of course, the real equivalent characteristic impedance will not equal the parallel combination of the four individual characteristic impedances because these are not independent transmission lines and coupling will occur.

4.3.2. Propagation delay, capacitance and inductance

The propagation delay is defined as the time a voltage signal takes to travel the length of the transmission line. The propagation speed is a characteristic quantity determined by the transmission line parameters. The propagation delay can be measured empirically with the same setup we used for determining characteristic impedance. Obtaining the propagation speed is just a matter of measuring the physical length of the cable and dividing the propagation delay by this number. We will design our system to operate with four active conductors (to minimize signal loss), so we shall focus on this setup.

The resulting step response of the cable with 4 active wires is shown in figure 60:

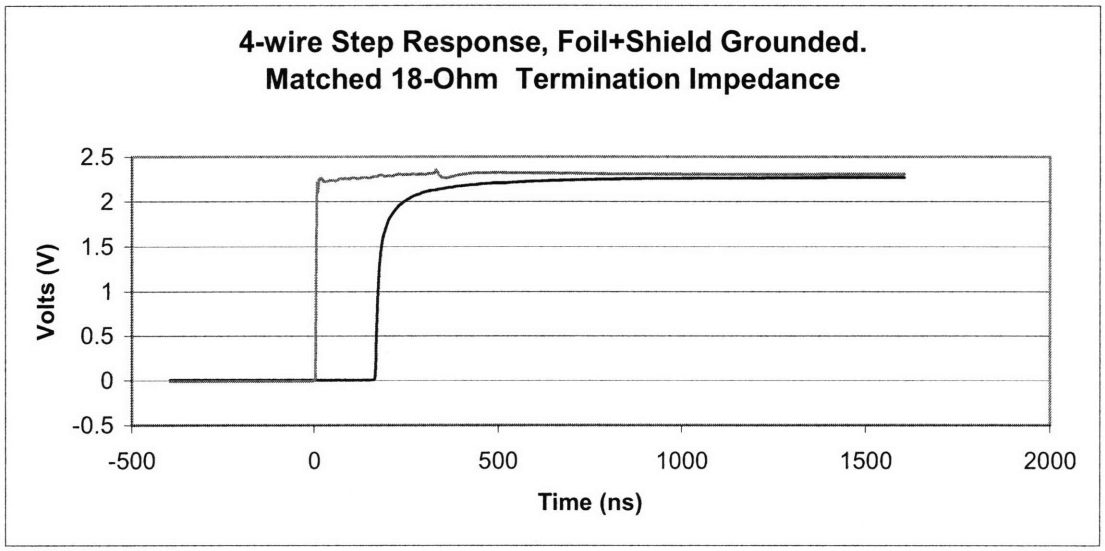

Step response for 4 active conductors with foil and shield grounded.
figure 60.

There are several things to point out about this response. First, we can observe the time delay between the input (the step function) and the output response (the rounded step). Furthermore, because we are testing the matched condition, there are no perceivable signal reflections. Finally, the slightly rounded response points towards some important frequency-domain characteristics of the cable.

Returning to our original goal of measuring the time delay, it is simple to obtain the equivalent time delay just by measuring the time between the input and the output reaching 50% of their final value. The measured time delay is thus: 170ns. The physical length of cable FT1 is 30.8m. Therefore, the signal propagation speed is given by: 1.811e8 m/s, or 0.60434c, where c is speed of light constant (c=299,792,458m/s).

Assuming that our reference cable is nearly ideal, we can now calculate approximate values for capacitance and inductance per-length. (see section 2.5.2.):

$$Z_0 = \sqrt{\frac{L_0}{C_0}} = 18$$

$$v = \frac{1}{\sqrt{L_0 C_0}} = 1.811e8 \Rightarrow$$

$$v = \frac{1}{Z_0 C_0}$$

Therefore, we obtain C0=3.07e-10F/m, L0=9.94e-8H/m. To verify the validity of these results, we also measured the total capacitance of the transmission line by using an impedance meter. The total capacitance from the 4-active conductors in parallel to ground was 12.16nF, which corresponds to a capacitance per-length of 12.16e-9/30.8=3.95e-10F/m. The two values differ by about 20%.

For reference, the capacitance per-length of the 1 active conductor configuration was measured to be 1.43e-10F/m using the impedance meter.

4.3.3. Cable frequency response

4.3.3.1. Transfer response

One of the most important barriers that we must overcome when designing our system is the levels of high frequency signal loss through the motor feeder cables. As previously discussed, motor feeder cables are not designed for high frequency signal propagation, thus, they are not normally designed to avoid high frequency loss effects such as skin effect and dielectric loss. Using the same pulse-generator setup as before, we can measure the frequency response of the cable by using RespMastr® software to perform FFT on the input and output voltage time responses, which we can then use to calculate the frequency response. The magnitude response is shown below in figure 61:

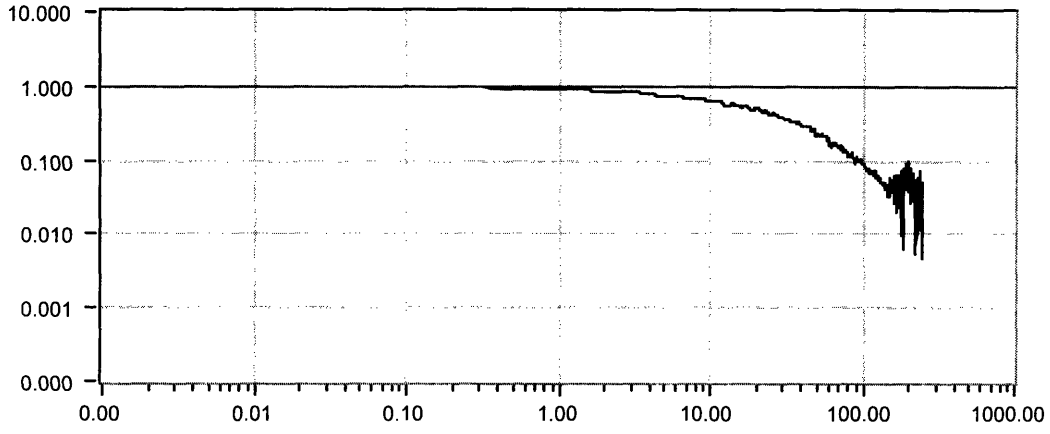

Frequency magnitude response for FT1 Cable in 4-active conductor setup with foil+shield grounded
figure 61.

The cable behaves much like a non-ideal transmission line (see regions of operation in section 2.5.5.), with a magnitude response which approaches 1 for low frequencies and then drops off at higher frequencies. Note that we do not get any relevant data above frequencies of 200MHz. This is mostly due to the fact that the rise time of our input step voltage is finite, which means that the frequency content of the input signal is limited. Because the magnitude of the frequency spectrum of the input signal is too low for frequencies above 200MHz, the transfer function shows an erratic behavior, which corresponds to a computational artifact resulting from "divide by zero" situations.

It is the rate at which the frequency response drops for high frequencies which will give us more information about what will be the expected signal losses at transmission frequencies, plus allowing us to characterize the region of operations of the transmission line model of cable FT1.

4.3.3.2. Mathematical model

To develop a rough mathematical model for the high frequency behavior of the cable, we can begin by observing the general shape of the empirical transfer response and

then attempt to match this to what we know about the different regions of operation of a transmission line (2.5.5.). If we observe the high frequency behavior of this transfer function, we can observe that the magnitude decays with a slope of more than -20dB/dec, but less than -40dB/dec. Let's assume that we can model the transfer function with a single nth order pole:

$$H_{cable}(s) = \frac{1}{\left(\frac{1}{(2\pi)f_c}s + 1\right)^n}$$

The corner frequency, fc will depend on the estimated slope of the transfer function at high frequencies, and thus, on the value of n. Depending on the region of operation, n could have a value of 3/2, 2 or 5/2. The table below shows some possible transfer functions, including the expected magnitude at 900MHz, our desired transmission frequency. Because skin effect causes a $1/\sqrt{s}$ response, we expect n to be close to 3/2. Figure 62 below shows the frequency response of the motor cable including the data point at 900MHz corresponding to direct measurement of cable loss for direct modem transmission.

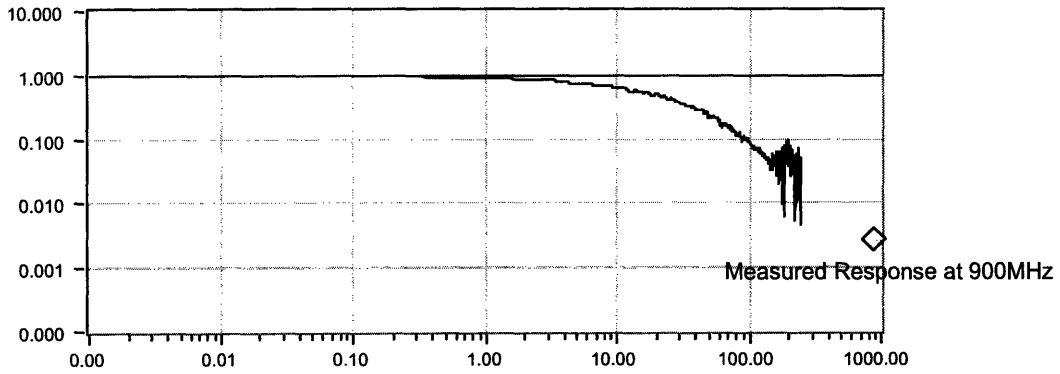

Motor cable frequency response including measured data point at 900MHz. figure 62.

Possible Mathematical Models for Cable Frequency Response

n	fc (MHz)	H(s) (w in Mrad/s)	|H(2pi900j)| (dB)
3/2	21	$\frac{1517}{(s+132)^{\frac{3}{2}}}$	-49
2	35	$\frac{48400}{(s+220)^{2}}$	-56
5/2	41	$\frac{1.06e6}{(s+257)^{\frac{5}{2}}}$	-67

The magnitude response of each of these proposed functions is shown in figure 63:

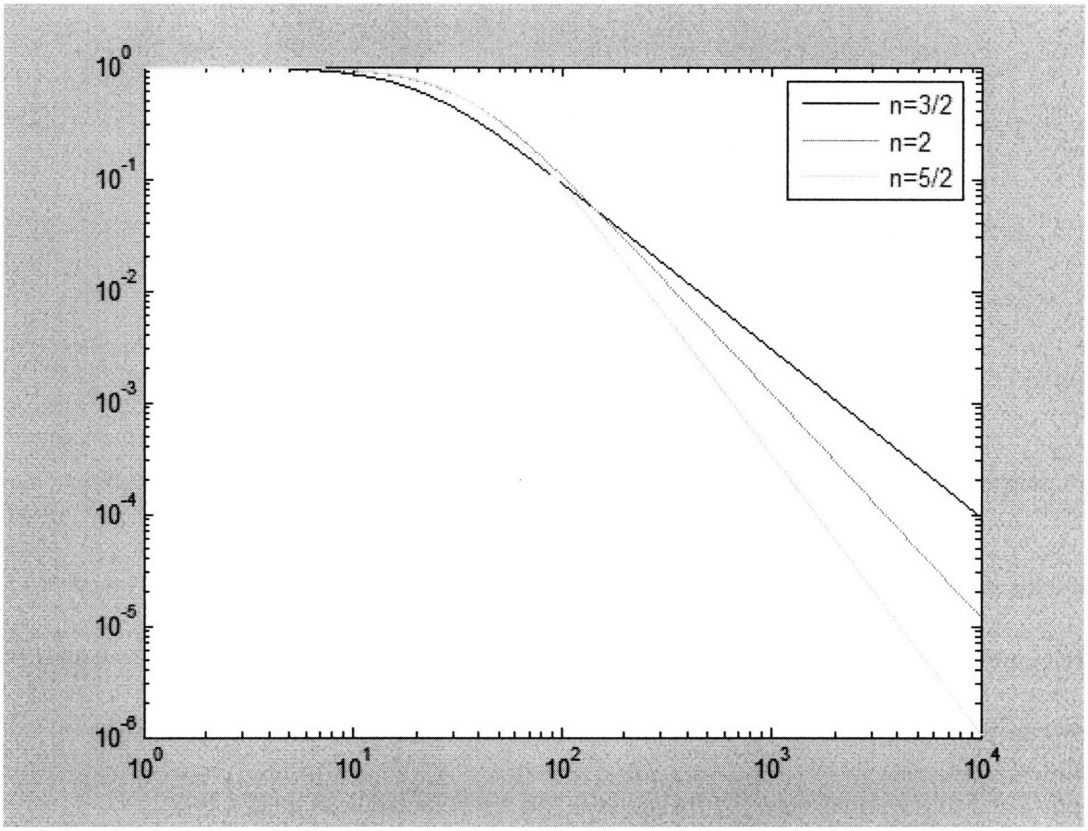

Log-log magnitude frequency response for three theoretical models for cable FT1 figure 63.

4.3.3.3. Region of operation analysis

As discussed before, the value of n, which corresponds directly to the rate of decay of the transfer response, will depend on the region of operation of the transmission line. The region of operation will be determined mostly by the length of the transmission line and the frequency of operation. Recall figure 21:

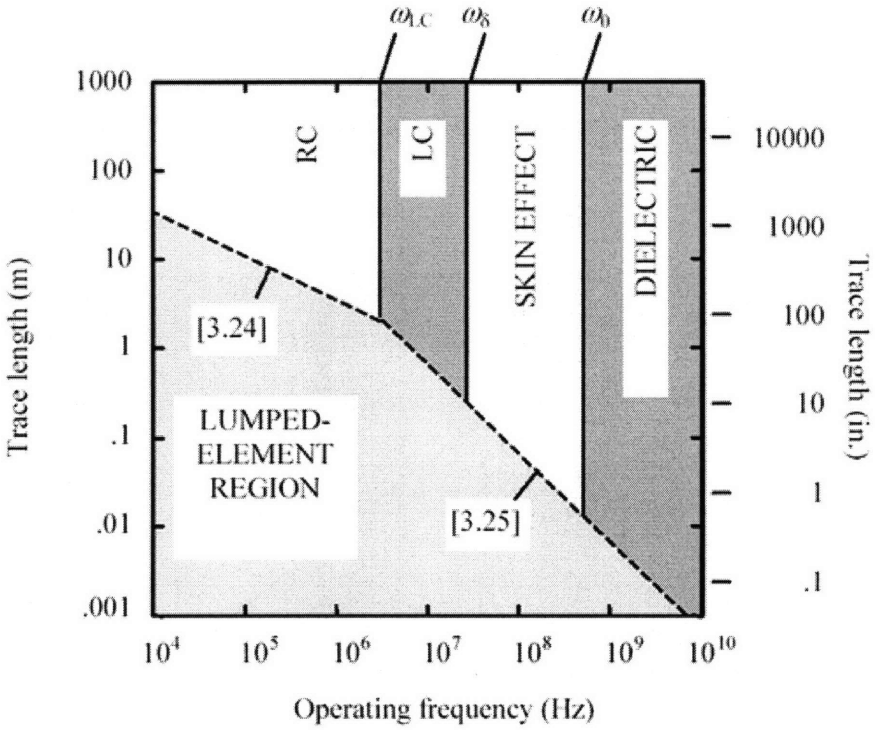

Regions of operation for different trace lengths and operating frequencies [7] figure 21, revisited.

Note that an operating frequency of 900MHz and a line length (trace length) of 31m, corresponds to the threshold between the skin effect region and the dielectric loss region. This would, in turn correspond to a value of n between 3/2 (skin effect adds a loss proportional to the square root of frequency) and 2 (dielectric loss adds a loss proportional to frequency).

4.3.4. 900 MHz cable characterization

One of the problems we encountered when characterizing the frequency transfer response was not being able to get any relevant data for frequencies above 300MHz because of the finite rise time of our pulse generator. The radio modems allow us to measure the frequency response of the cable at 900MHz. The information provided by this extra data point will allow us to determine which mathematical model best suits the cable for high frequencies.

4.3.4.1. 900MHz cable response at different power TX levels

One of the RF modems was connected to one end of the cable, and the resulting input and output signal amplitudes at 900MHz were measured for different transmission power levels. The resulting data is shown below:

900MHz Measured Frequency Response for 4 Active Conductors

TX power level	Vin(p-p), V	Vout(p-p), mV	Vout/Vin	dB signal loss
1mW	0.140	unreadable	unreadable	unreadable
10mW	0.457	1.5	.003	-49.7
100mW	1.2	2.3	.002	-54.3
500mW	1.900	7	.0037	-48.6
1W	1.907	8	.004	-47.5

The average cable loss at 900MHz is -50dB. Note that the input signal amplitude did not increase when the transmission power level changed from 500mW to 1W. The reason for this flattening out of amplitude voltage is current limiting in our RF modems. These modems are designed to drive antennas, whose impedance is in the order of 50Ohms.

Our feeder cable has a characteristic impedance which is lower than this (20Ohms), and thus requires higher current levels.

4.3.4.2. Cable mathematical transfer function at 900MHz

With the high frequency data point at 900MHz, we can decide which of the proposed mathematical transfer functions best describes our cable setup. Because the measured signal loss at 900MHz is approximately -50dB, we must choose the model with n=3/2 (see section 4.1.3.2.). Thus, the mathematical model for our cable setup, 4-active conductors with foil and shield grounded is:

$$H_{4-wire}(s) = \frac{1517}{(s+132)^{\frac{3}{2}}}$$

where w is in Mrads/sec.

4.4. Filter time response

The main purpose of the external lumped filter is to separate the high frequency data signals from the lower frequency, but much greater magnitude PWM power signals. Another purpose of the filter is to protect the delicate RF circuitry from voltage spikes caused by PWM signals. Figure 64 below shows a typical voltage spike seen at the output of the feed-through capacitor box when the output resistance is set at 50 Ohms.

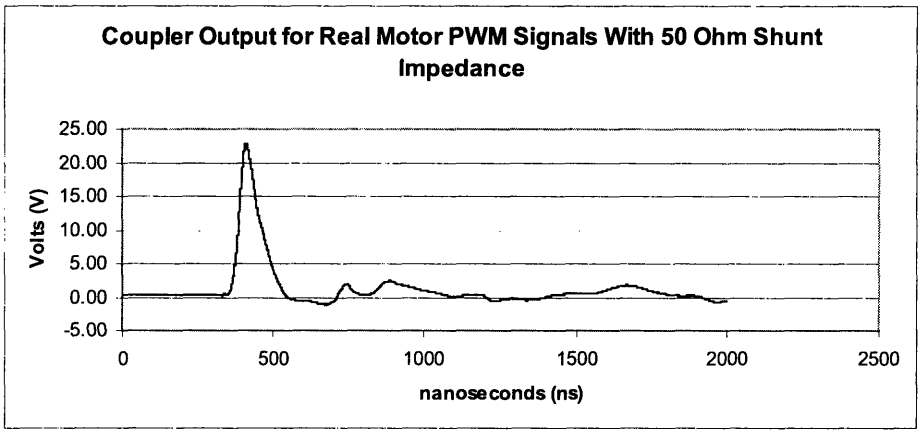

Typical voltage waveforms at feed-through capacitor box output with 50 Ohm output resistance.
figure 64.

The 20+ volt spikes shown are much too great in magnitude for our RF circuitry. The external lumped filter serves to substantially cut down on the magnitude of these spikes, making them much more manageable.

Because we are planning to use 900MHz as the modulation frequency for feedback data, we need a high-pass filter to block the low frequency content of the PWM signals while allowing the 900MHz signals to pass through. We chose a simple 2nd order filter (composed of two RC branches) with a double pole at 640MHz. The final filter circuit design is shown in figure 65.

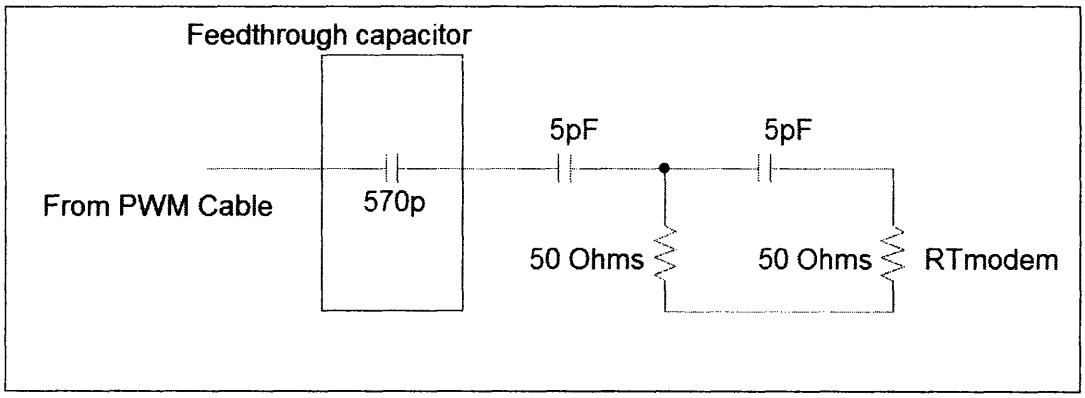

Double pole filter with high frequency poles at 320MHz
figure 65.

The resulting time-domain responses are shown in figures 66 and 67:

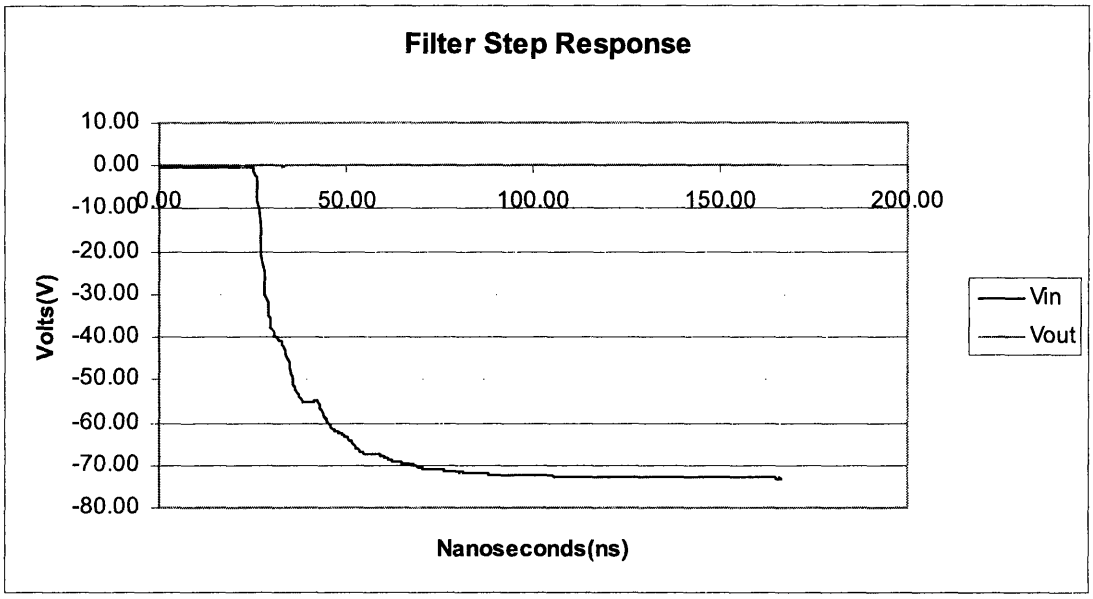

Step response of double pole filter with high frequency poles at 640MHz (output waveform is not visible, see figure 66.)
figure 66.

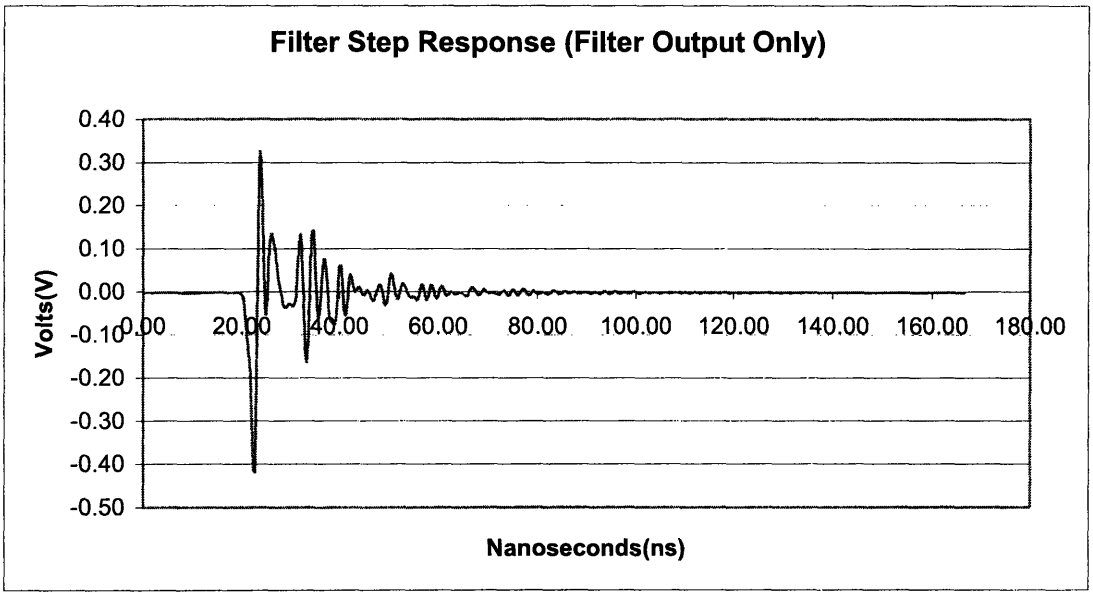

Double pole step response showing output waveform only
figure 67.

The resulting time domain step response is as we expected in the time domain.

Vout corresponds to a scaled version of the second derivative of Vin.

4.4.1. Filter frequency response
4.4.1.1. Transfer response

The filter frequency response is obtained from the time domain step response, again, by using the RespMastr® software. The calculated response from Vout to Vin is shown below in figure 68:

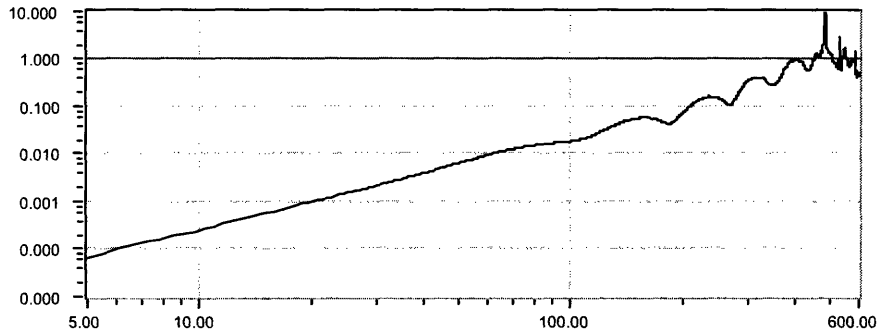

Filter magnitude frequency response figure 68.

The frequency response of the filter shows an expected roll-off of -40dB/dec for frequencies below 400MHz, while the magnitude of the transfer function rapidly approaches 1 for frequencies above it. Thus, this filter should attenuate PWM signals and their low frequency spectra while transmitting 900MHz data signals without much attenuation. The ringing observed in the calculated response at frequencies above 20MHz is most likely caused by the parasitics of the discrete lumped filter components.

4.4.1.2. Ideal Response

The ideal transfer function for the filter above (figure 62.) can be calculated as follows:

$$\frac{Vout}{Vin}(s) = \frac{R}{R + \frac{1}{Cs}} \frac{R \| \left(\frac{1}{Cs} + R \right)}{R \| \left(\frac{1}{Cs} + R \right) + \frac{1}{Cs}}$$

If we make the simplifying assumption that the two stages are independent, then the transfer functions boil down to:

$$\frac{Vout}{Vin}(s) = \left(\frac{RCs}{RCs + 1} \right)^2 = \frac{s^2}{(s + 4e9)^2}$$

The magnitude plots of this transfer function is shown in figure 69 below:

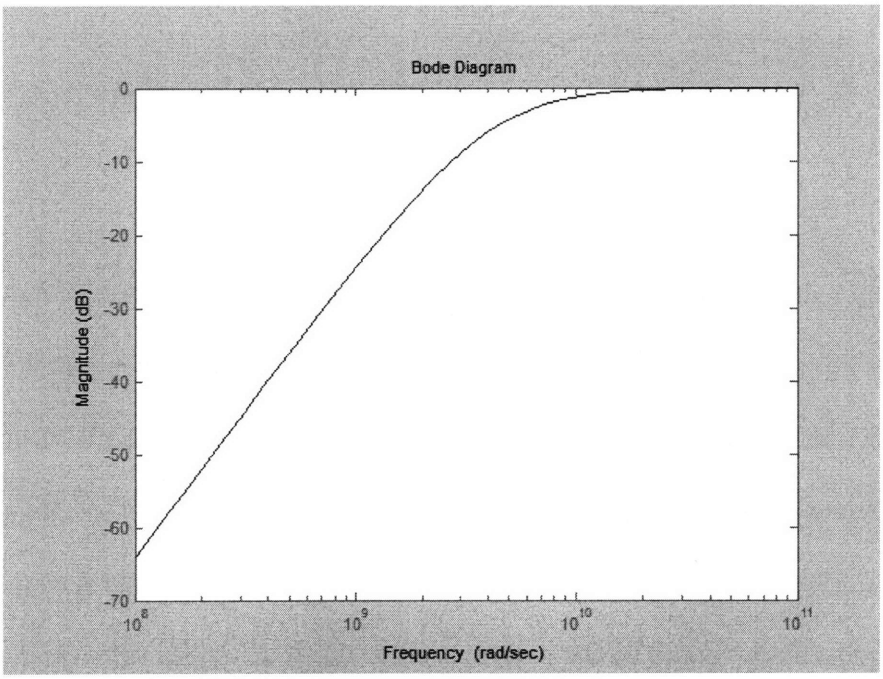

Ideal filter transfer function with double pole at 640MHz
figure 69.

4.5. Model system demonstration

For the purposes of this experiment we will not be testing under real operating conditions, but instead, we will build a model system which will behave similarly to the

real system regarding parameters which are relevant to our investigation. The main difference between our proposed model system and a real motor system is that in our model we have replaced the motor drive with a high voltage pulse generator. The idea is to simulate the motor PWM signals with the pulse generator signals, concentrating mostly on matching the frequency content of the two (which translates to matching the rise and fall times in the time domain). The end of the cable in which the motor would be attached is left open-circuited, to simulate the high impedance presented by the motor. The feed-through capacitor boxes in conjunction with the external lumped filters are installed at each end of the cable, to allow for coupling in and out of the power cable. To simulate high-frequency data transmission the modems are connected through the filter/coupler circuit at each end of the cable. Real feedback signals travel from the motor end of the cable to the drive end of the cable, therefore, the radio modem at the open circuit end will be the transmitter while the radio modem at the pulse generator end will be the receiver.

Now that we have characterized the model system, it is time to characterize its data-transmission capabilities. In this section we will present and discuss the results obtained from data transmission for different setups.

As described in section 3.1.4.4, our RF modems have a built in operation called the software loop-back test. We use this feature to measure the relative reliability of a communications channel. The way this test works is by sending an information package of user-defined size to a remote modem. This other modem, equipped with a loop-back serial adapter will then echo back this same package back to the other modem. If the package sent is the same as the package received, we get a successful transmission. For

our testing purposes we will choose a data package size of 32 bytes. To get statistically significant data, we run this test 100,000 times and then record the total successful and unsuccessful transmissions.

4.5.1. Direct modem-to-modem transmission

To measure the characteristic error rate of our modems, we connected them directly, through a 35dB attenuator. The results are shown in the table below:

Success Rates for Direct Modem-to-Modem Transmission

Power TX level	Good Packages	Bad Packages	Success %	RSSI(dBm)
1mW	99987	13	99.987%	-40
10mW	99990	10	99.990%	>-40
100mW	99989	11	99.989%	>-40

Therefore, our modems have a maximum success rate of 99.99% for the most ideal of conditions. This .9999 success rate is shown as a solid line in all figures.

4.5.2. Transmission on 50 Ohm (matched) coaxial cable

To better understand the relevance of the data we obtain for our system, it is important to compare it to a "control" system which is well known and characterized. For the purposes of this investigation, we shall compare our model system with transmission through a coaxial cable with the addition of 20dB or 35dB attenuators to simulate the losses of our reference motor cable. We use a 50 Ohm, 25m Belden® 8262 coaxial cable. The nominal serial loss of this model cable is given by the manufacturer: 20dB/100ft at 1GHz. Thus, we expect our coaxial cable to have ~ 20dB loss at 900MHz.

The 50 Ohm characteristic impedance of our coaxial cable results in very ideal conditions for our test. This results from the fact that our modems also have 50 Ohm impedance, and, therefore, by the maximum power transfer theorem, this setup will result in the modems transmitting maximum power. The data obtained from this "ideal" setup is shown below in figures 70 and 71 for 20dB and 35dB attenuators:

Success Rates for 50 Ohm Coaxial Cable + 20dB Attenuator Transmission

Power TX level	Good Packages	Bad Packages	Success %	RSSI(dBm)
1mW	99982	18	99.982%	-45
10mW	99991	9	99.991%	>-40
100mW	99990	10	99.990%	>-40

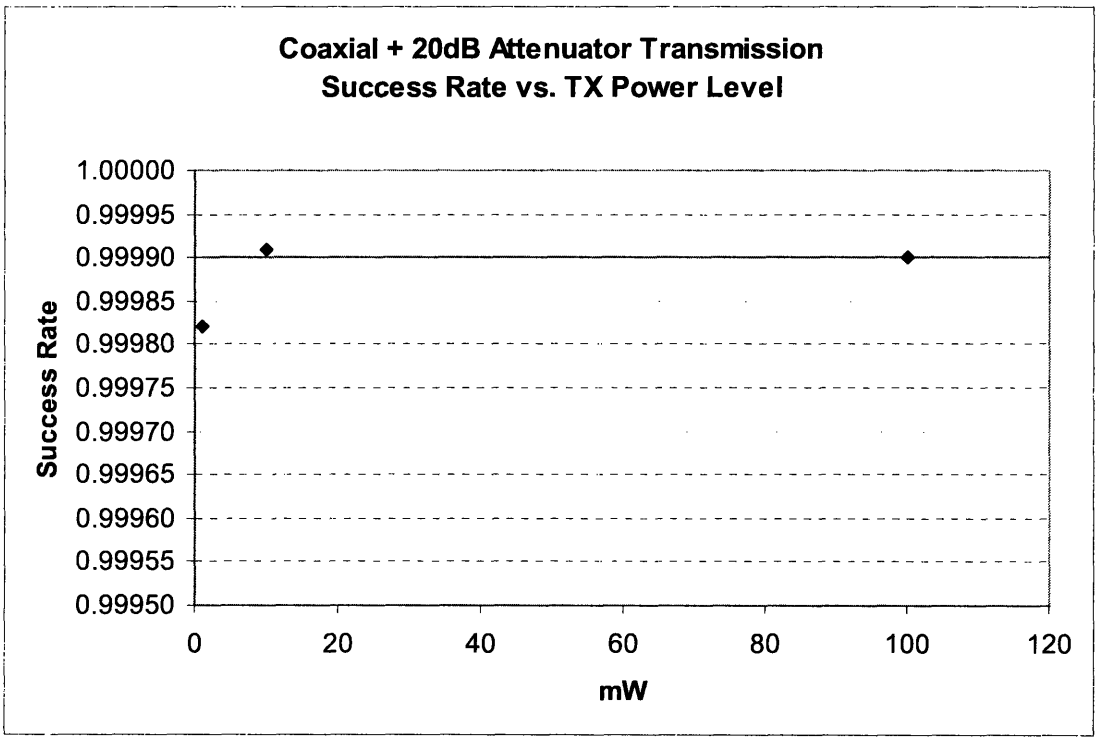

Success rate vs. TX power level for direct transmission through 50 Ohm coaxial cable plus 20dB attenuator. Solid line = measured modem limit.
figure 70.

Success Rates for 50 Ohm Coaxial Cable + 35dB Attenuator Transmission

Power TX level	Good Packages	Bad Packages	Success %	RSSI(dBm)
1mW	99981	19	99.981%	-60
10mW	99982	18	99.982%	-50
100mW	99987	13	99.987%	-40

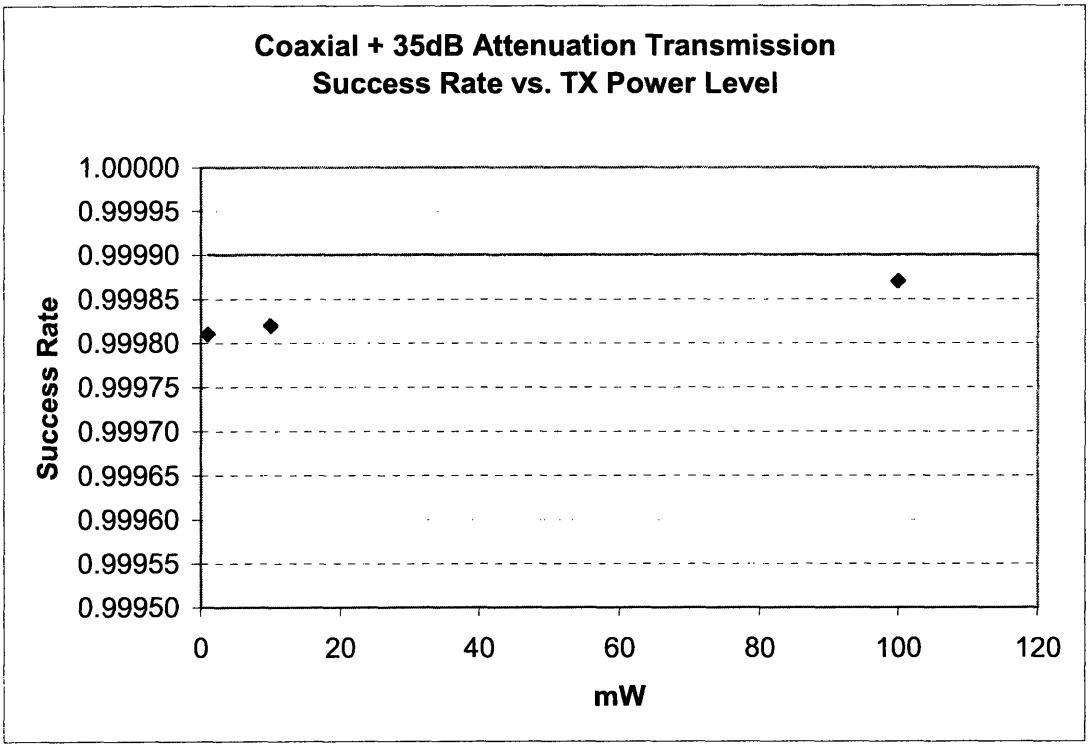

Success rate vs. TX power level for direct transmission through 50 Ohm coaxial cable plus 35dB attenuator. Solid line = measured modem limit.
figure 71.

We can observe that the success rate vs. TX power level curve is roughly logarithmic. Furthermore, the success rate for the more highly attenuated setup, with 35dB additional attenuation is slightly less than that for the less attenuated one, with only 20dB additional attenuation. Finally, as expected, the success rate of the matched coaxial cable setup for power levels above 10mW is at the modem maximum.

4.5.3. 900MHz transmission on quiet power cable

The first step on evaluating the possibility of sending high frequency data through the system is to test the data-carrying capabilities of the motor power reference cable, FT1. In this section we will present the results obtained from the software loop-back test (see section 3.1.4.4.) by connecting the RF modems directly to the reference cable without the use of any coupling circuits or PWM signals.

The results obtained for the direct cable setup are shown in the table below:

Success Rates for Direct Motor Cable Transmission

Power TX level	Good Packages	Bad Packages	Success %	RSSI(dBm)
1mW	99960	40	99.960%	-70
10mW	99976	24	99.976%	-60
100mW	99983	17	99.983%	-50

Graphically, one can see the relation between power level and success rate (figure 72):

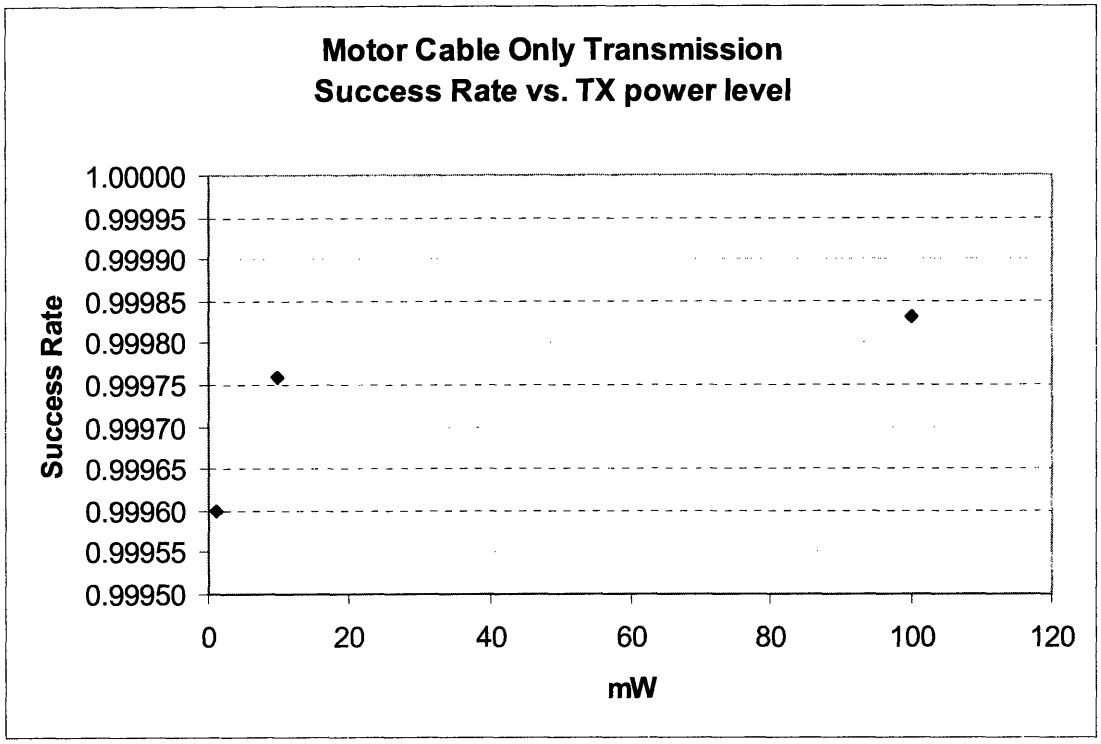

Success rate vs. TX power level for direct motor cable transmission .
Solid line = measured modem limit
figure 72.

As we would expect, an increase in the TX power level causes an increased in the measured success rate. The relationship between these two quantities approaches a logarithmic/bounded exponential function for this particular setup. The success rate at the highest measured TX power level is almost that of the modem limit.

4.5.4. 900 MHz coupled transmission on quiet cable

After measuring the error rates for direct cable transmission we move on to testing the effectiveness of our coupling circuits. Because we only want to test the effectiveness of the couplers in efficiently transmitting 900MHz waveforms plus any effect they might have in mismatches and power transmission, we will not activate the simulated PWM signals.

The results for coupled cable transmission are shown in figure 73 below:

Success Rates for Coupled Transmission Through Motor Cable

Power TX level	Good Packages	Bad Packages	Success %	RSSI(dBm)
1mW	99537	463	99.537%	-90
10mW	99844	156	99.844%	-80
100mW	99882	118	99.882%	-70

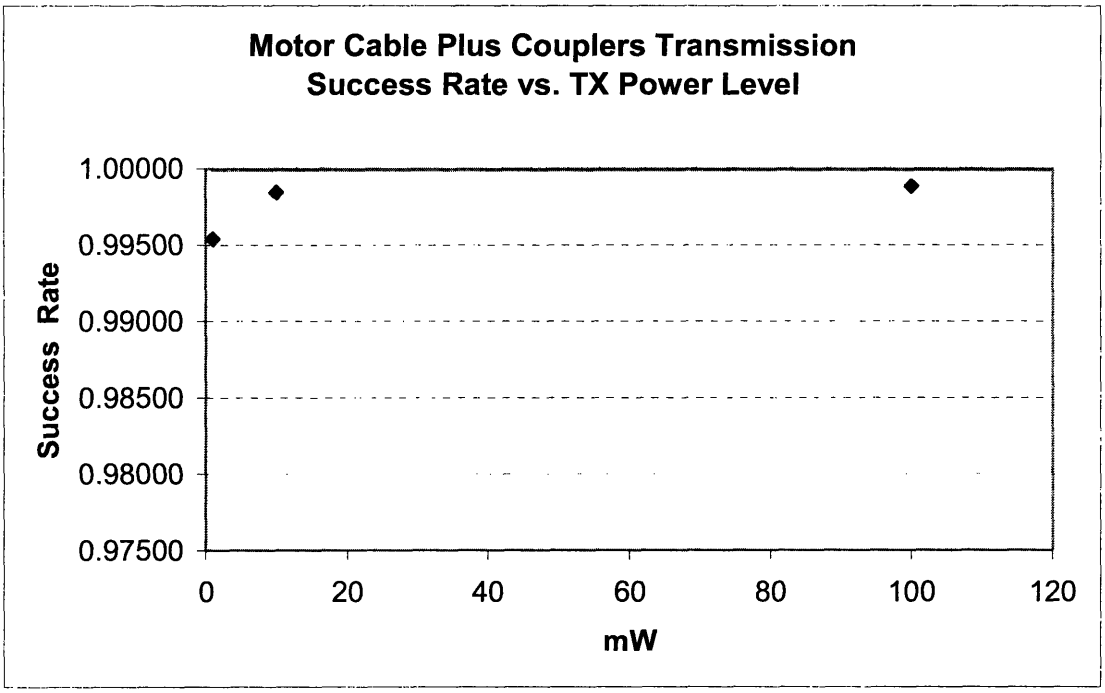

Success rate vs. TX power level for direct cable+couplers transmission. Solid line = measured modem limit
figure 73.

Again, the success rate increases with increasing TX power. Furthermore, the success rate is lower than that for non-coupled systems. The most probable reason for this decrease in success rate is mismatch produced by the shunt filter resistor. By the maximum power transfer theorem, the lower impedance presented by the filter plus cable (compared to the 50 Ohm impedance of the modem), implies lower efficiency. This

decrease in power transmission efficiency can also be deduced from the fact that the RSSI numbers dropped by about 20dBm.

4.5.5. 900MHz coupled transmission with simulated PWM Signals

The final setup is one that simulates the real system, with coupled transmission in the presence of high voltage PWM signals. As previously stated, we will use a high voltage pulse generator to simulate the motor PWM signals because this way we can more easily control the magnitude and rise time.

4.5.5.1. Contrast between PWM simulated signals and real measured motor signals

For our model system to have any real significance, we must show that the simulated PWM signals impose conditions which are as severe or worse than those that would appear with real motor signals. The relative severity of the PWM signals boils down to the amount of high frequency content they contain, because we are using high-pass filters with a high cut-off frequency of 600MHz for data transmission. Therefore, interference with data signals will occur if the PWM signals have enough frequency content in the 900MHz band. As stated before, the spectral content of the simulated PWM signals is at least 10x the magnitude of real motor signals, mostly due to the fact that our simulated PWM signals are of greater magnitude and of greater rising/falling rate. Therefore, our simulated PWM signals impose *very* severe conditions, and should give a most pessimistic, worst-case scenario result.

4.5.5.2. Error rates vs. power level

The results from the full system test are shown in figure 74 below:

Success Rates for Full System Transmission

Power TX level	Good Packages	Bad Packages	Success %	RSSI(dBm)
1mW	97998	2002	97.998%	-90
10mW	99783	217	99.783%	-80
100mW	99881	119	99.881%	-70

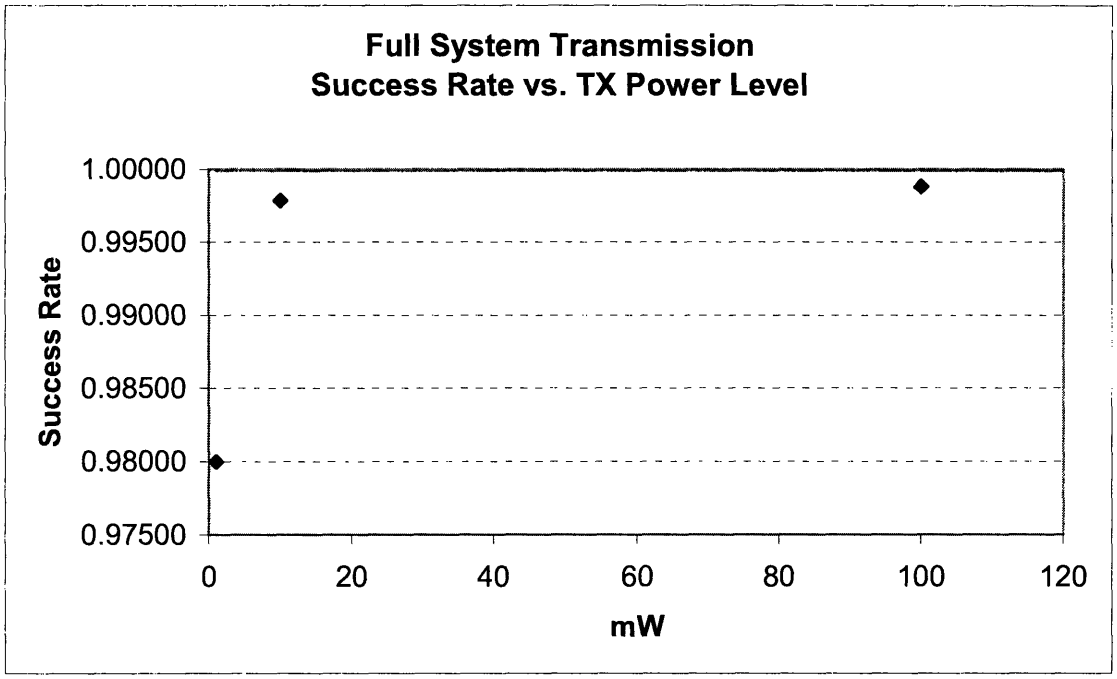

Success rate vs. TX power level for full system transmission (with simulated PWM signals). Solid line = measured modem limit.
figure 73.

One interesting result is that turning on the PWM signals has a drastic adverse effect for 1mW TX power, but almost no perceivable effect for TX power of 10mW or above. For TX power of 10mW or above, the RF data signals are much stronger than the PWM signals, and adding these into the system has little or no effect in data transmission.

4.5.6. Analysis and summary of results
4.5.6.1. Error rates vs. RSSI

Although plotting success rates vs. TX power levels is useful in establishing some trends, RSSI gives us a better measure on the real power that is being delivered at the

receiver end. For this reason, we also present success rates vs. RSSI readings in figure 75 below:

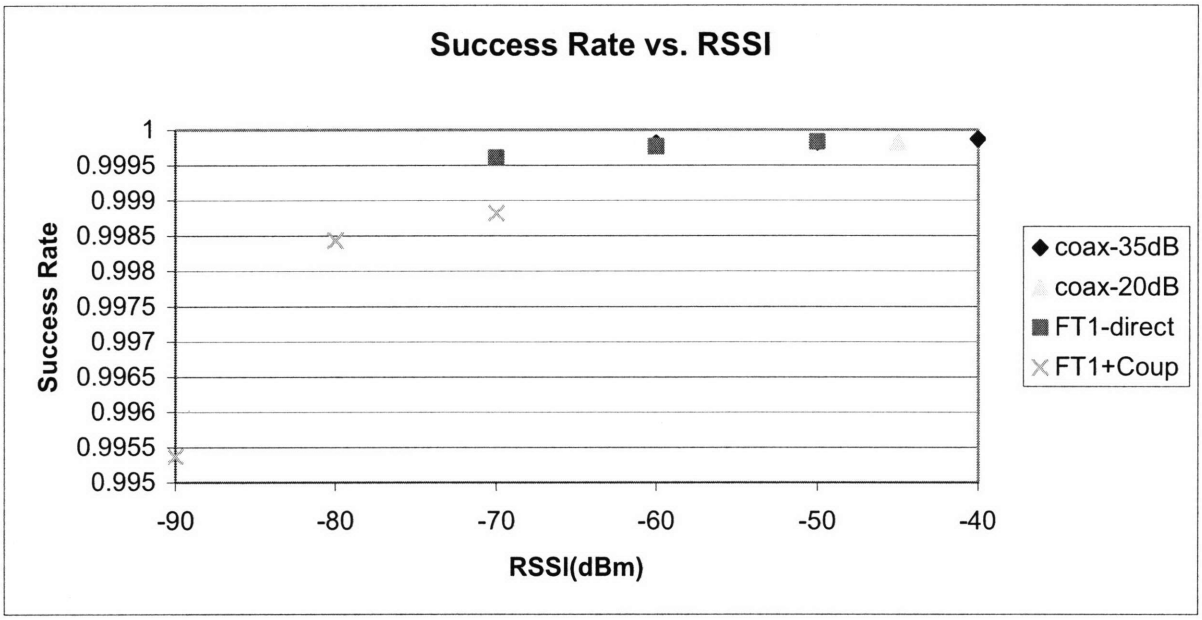

Success rates vs. RSSI readings for different setups
figure 75.

Figure 76 below shows the average success rate vs. RSSI across all setups:

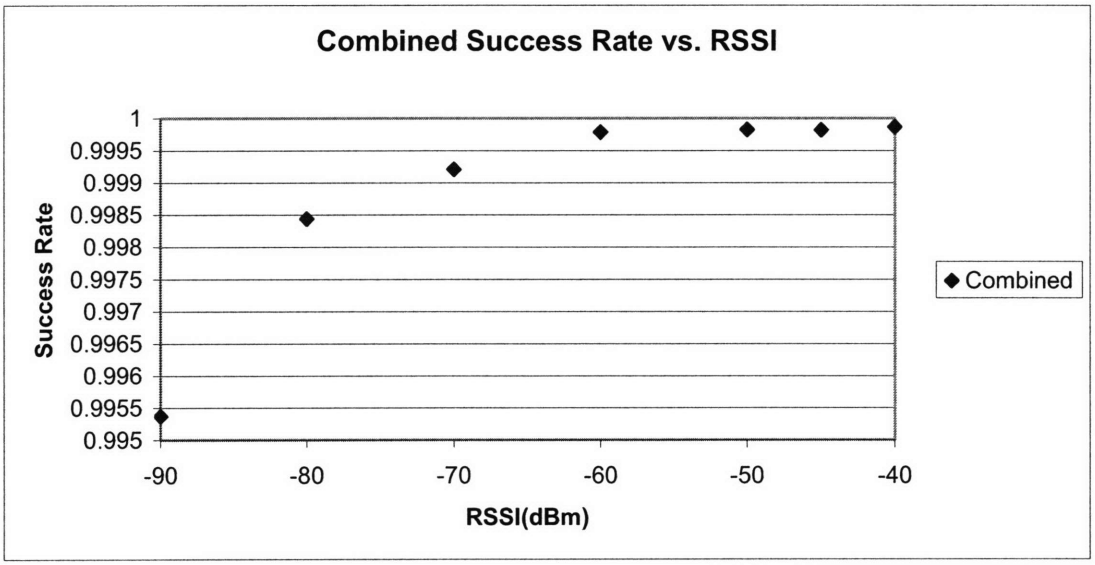

Average success rate vs. RSSI for all setups
figure 76.

The combined success rate vs. RSSI shows a very clear logarithmic/bounded exponential relationship between Success rate and RSSI. This agrees with theoretical error rate (see 2.7.2.3.) expectations, which predict a bounded-exponential curve for success rate (1-error rate).

4.5.6.2. Error rate analysis

The lowest error rates were for the setups with the direct 50 Ohm, matched coaxial cable, direct motor power cable, and direct modem-to-modem connections. Furthermore, all these setups had very similar absolute error rates. The fact that the direct modem-to-modem connection yielded an error rate of about .013% bad packages implies that our modems (or perhaps the serial connection between the PC and the modem) impose a limit on the maximum success rate. The error rate for coupled transmission through the motor power cable was higher than that for direct transmission. When the simulated PWM signals were turned on, the error rate was unchanged for TX power levels higher than 10mW, although the error rate increased by a factor of 5 for TX power level of 1mW. This implies that the spectral content of the PWM signals in the 900MHz band is swamped by signal power levels over 10mW.

RSSI readings give us an insight into why the coupled transmission through the power cable yielded higher error rates than the direct transmission. At 900MHz, our coupling circuit appears as a shunt 50 Ohm impedance. This impedance appears in parallel with the motor cable impedance and thus degrades the matching between the modem output impedance and the total impedance seen by the modem. The maximum power transfer theorem indicates that for ideal efficiency, the internal impedance of the modem must match the impedance seen at the modem's output. Thus, our couplers have

the effect of decreasing the efficiency of the system, decreasing RSSI ratings and increasing the fraction of signal power which is reflected back to the modem and not transmitted through the motor cable. By increasing the matching between modem and other impedances, for example, by using an impedance transformer, we could boost RSSI ratings and thus increase success rates (see figure 76.).

It is important to note that the error rates we have presented here are package error rates and not bit error rates. During the test, we send 256-bit packages down the cable and then echo them back the same way, comparing whether the package received is the same as the package sent. Thus, if *any* of the 256 bits in the package is corrupted, all 256 bits are counted as bad. Therefore, the error rate data presented here is very pessimistic, giving us an upper bound on what the error rate is.

Another important factor to consider is that we are sending the data package twice for each trial. For the purposes of our application, i.e. sending data down from the motor end to the drive end, we only care about one-way error rates. If we assume that the system is completely symmetric, we can obtain an approximation of what is the one-way error rate:

$$P_e^{2-way} = 2P_e^{1-way} + \left(P_e^{1-way}\right)^2$$

This simple equation stems from the fact that there are 3 possibilities when we detect a 2-way error; an error was introduced during transmission, an error was introduced during re-transmission, or an error was introduced both during transmission and re-transmission. We are ignoring the remote possibility that an error happens twice on the same bit. Using this equation we can solve for the 1-way error rate. Calculated 1-way error rates vs. RSSI levels are shown in figure 77 below:

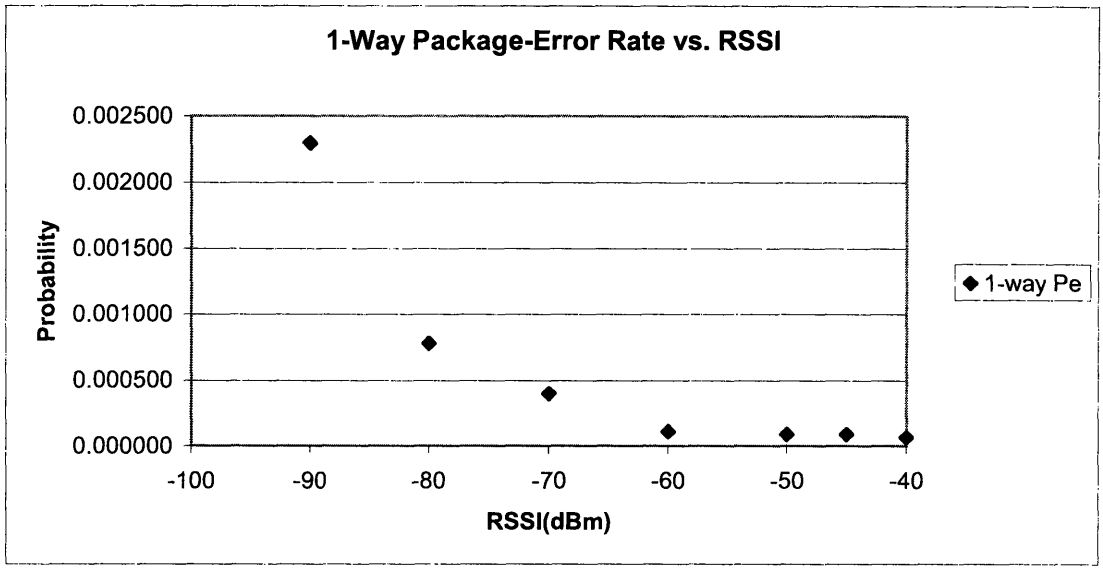

1-way package probability of error vs. RSSI readings figure 77.

This chart gives a worst-case measurement of bit-error rate, as every time a package is bad all 256 bits are automatically counted as errors.

To approximate the 1-way *bit*-error rate (rather than package-error rate), we can, again, ignore the possibility of errors occurring twice on the same bit. Then, we can state:

$$P_e^{256-bit} \approx 1-\left(P_{success}^{1-bit}\right)^{256} = 1-\left(1-P_e^{1-bit}\right)^{256}$$
$$\Rightarrow P_e^{1-bit} = 1-\sqrt[256]{1-P_e^{256-bit}}$$

, where all the probabilities shown are 1-way. Figure 78 below shows calculated 1-bit error rates vs. RSSI.

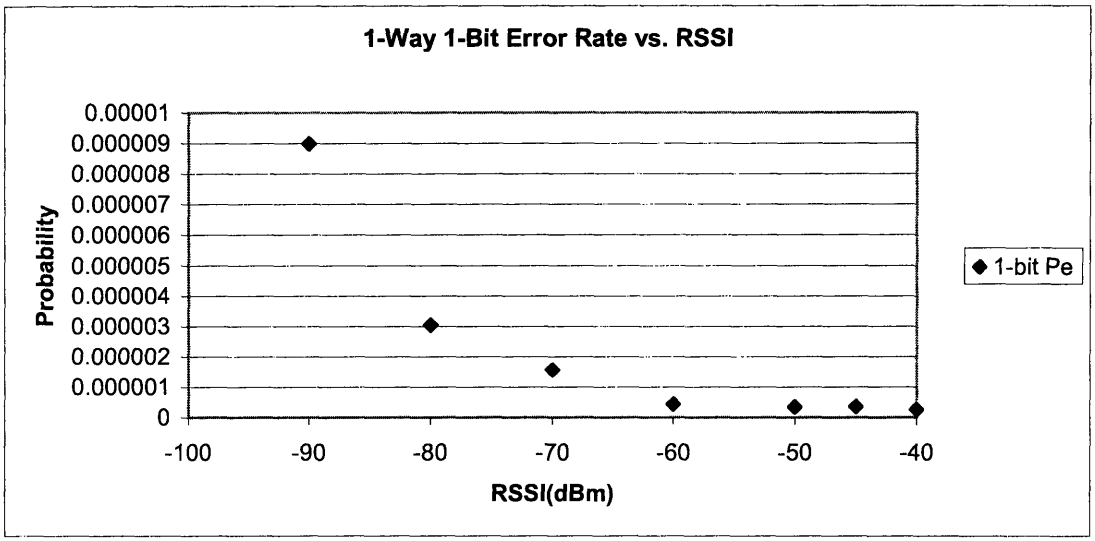

1-way bit-error rate vs. RSSI readings
figure 78.

The highest calculated 1-bit 1-way error rate is .0009% at -90dBm RSSI. The lowest (limited by our modems) 1-bit error rate is .000025% which is the modem limit achieved for all setups with RSSI higher than -60dBm.

4.6. Transmission of power for motor feedback electronics

4.6.1. Introduction

In developing our proposed zero-wire solution for feedback control, we have not yet addressed the problem of supplying power for motor feedback circuitry. By eliminating the external feedback cable we also eliminate the cables that supply DC power to these components. In this section we will propose a method for transmission of power which is in many ways analogous to our solution for data transmission; we choose an intermediate frequency to transmit the power and extract/inject it through appropriately designed filters.

4.6.2. Proposed solution and design

In developing our proposed solution for power transmission we will follow a similar methodology as we did for transmission of feedback data signals. We will choose to transmit the power signal at a different frequency from that of the PWM signals and from our 900MHz feedback data signals. For this reason, we choose 1MHz as a good compromise between separation from PWM and feedback spectra.

The requirements for our particular system ask for delivering 1W of continuous power to the motor feedback electronics, while, of course, avoiding interference with PWM and feedback data. Our proposed solution is to use a 1W 1MHz oscillator to inject a carrier into our motor cable at the drive end which can then be extracted and rectified at the motor end to power the feedback control. The generalized system is shown below in figure 79:

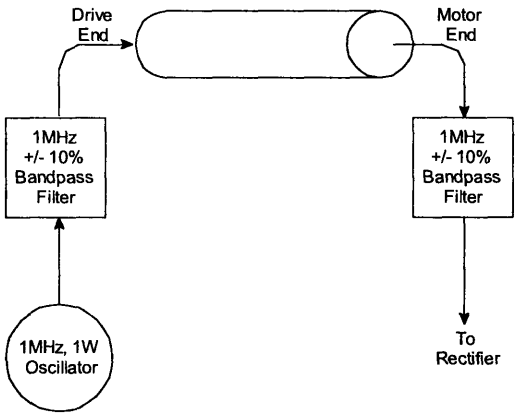

Proposed solution for power delivery to motor feedback electronics figure 79.

The band-pass filters at the injection and extraction end serve to isolate our power signal carrier while presenting very high impedances for other frequencies, thus avoiding loading effects for frequencies in the range of PWM or feedback data signals.

The main design issue is the band-pass filter. For the purposes of this simulation, we propose using a simple 2nd order band-pass RLC filter. The feed-through capacitances will serve as the "C" in our filter, while an external inductor and resistor will complete the circuit. The proposed circuit is shown in figure 80 below:

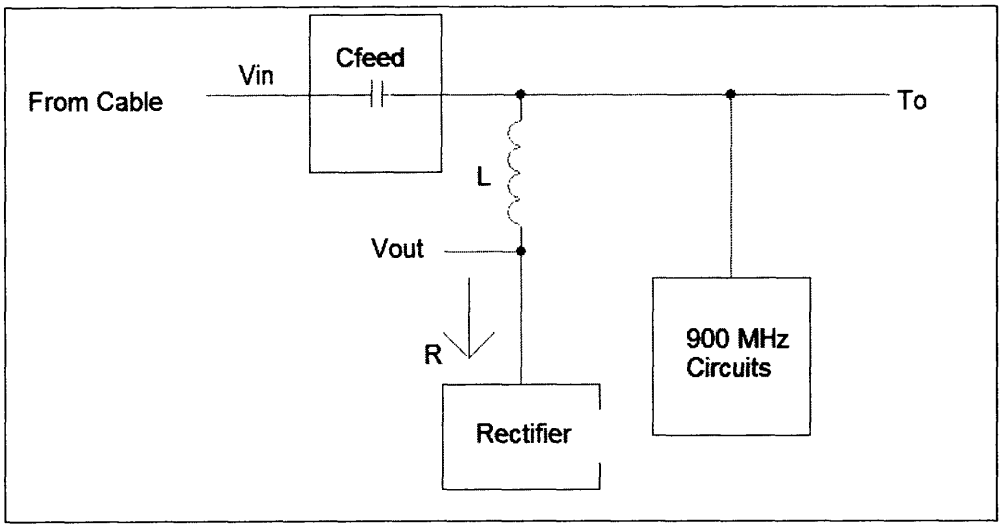

RLC band-pass filter for 1MHz power extraction figure 80.

Conceptually, the circuit works as follows. For very high frequencies (say 900MHz), the feed-through capacitors act as a virtual short circuit, thus allowing the 900MHz electronics to communicate. Our external inductor, though, with impedance that increases with frequency, will act as a virtual open circuit, thus decoupling the power circuitry for very high frequencies. The opposite happens for very low frequencies (in the PWM realm), with the feed-through capacitors acting as an open circuit. The design issue is to set the center frequency, at which the inductor and capacitor impedances cancel each other, at our desired carrier frequency.

Mathematically, we can analyze the circuit by using frequency domain techniques. The transfer function Vout/Vin is given by:

$$\frac{V_{out}}{V_{in}} = \frac{R}{R + Ls + 1/Cs} = \frac{RCs}{LCs^2 + RCs + 1}$$

Some simple algebra leads to the better known 2nd order system form:

$$\frac{V_{out}}{V_{in}} = \frac{R/L\, s}{s^2 + R/L\, s + 1/LC}$$

The general 2nd order system form is given by:

$$H(s) = K\frac{s}{s^2 + \omega_0/Q\, s + \omega_0^2}$$

, where w0 is the natural frequency (frequency of maximum transfer response) and Q is the quality factor, a measure of the sharpness of the frequency domain cut-off.

By comparing our transfer response with the general form, we conclude that:

$$\omega_0 = \frac{1}{\sqrt{LC}}$$

$$Q = \frac{1}{R}\sqrt{\frac{L}{C}}$$

For the purpose of our design, we need the center frequency, w0 be our power carrier frequency, 1MHz. Furthermore, because this frequency is separated from PWM and feedback spectra by at least several orders of magnitude, we do not need a very high Q, so we arbitrarily choose Q=5 as a good compromise. The capacitance of our filter is set by the total feed-through capacitance, 570pF, so we have two degrees of freedom L and R, to set two values, w0 and Q. Plugging our desired values, we obtain that the resulting components are R=55 Ohms and L=44uH. Our design is shown in figure 81 below:

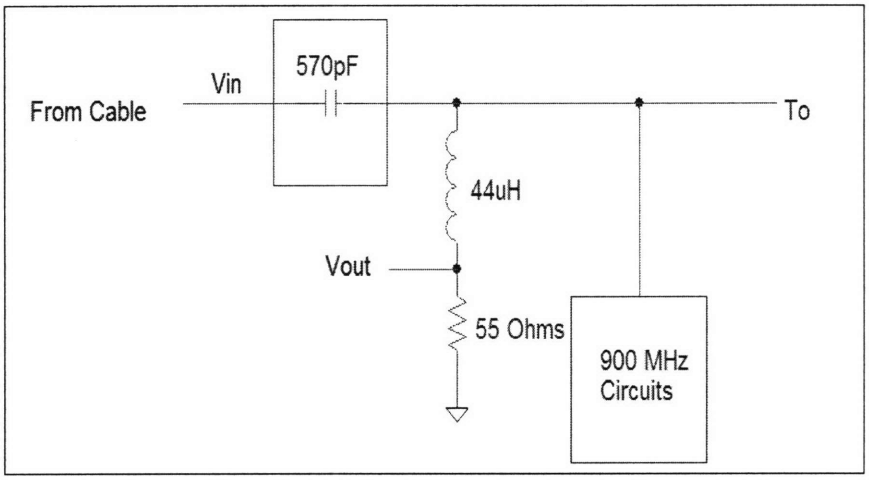

Band-pass filter design for 1MHz power signal transmission figure 81.

4.6.3. Simulation results

We use Matlab® to simulate the frequency response of this system. The resulting magnitude bode plot is shown below in figure 82:

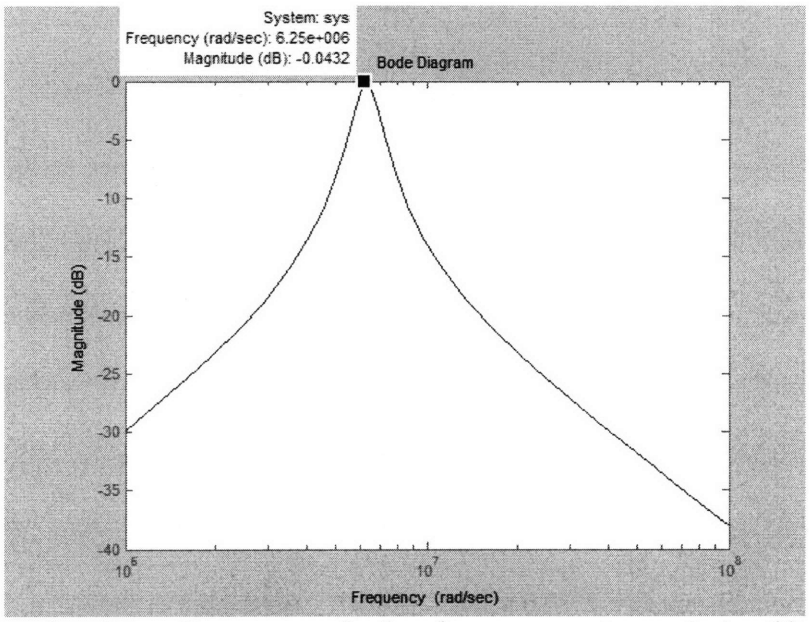

Simulated transfer response for band-pass power transmission filter figure 82.

The ideal transfer response shows a peak magnitude at 6.25Mrad/sec = 1MHz, as desired. Furthermore, the attenuation for frequencies in the realm of PWM or 900MHz feedback data is greater than 40dB. Higher attenuations could be implemented, if needed, by employing a higher order band-pass design topology.

4.6.4. Rectification of power for feedback electronics

Although we have simulated transmission of AC power through a 1MHz carrier signal for our feedback electronics, we still need to address the fact that we still need to produce a DC voltage. To obtain a DC voltage source from our 1MHz power signal, we propose a full-wave rectifier. Using a full-wave rectifier allows us to extract energy from the signal in positive and negative cycles, increasing efficiency. Furthermore, a full bridge rectifier requires less filtering at the output to fulfill maximum voltage ripple requirements. The general rectifier circuit is shown in figure 83 below:

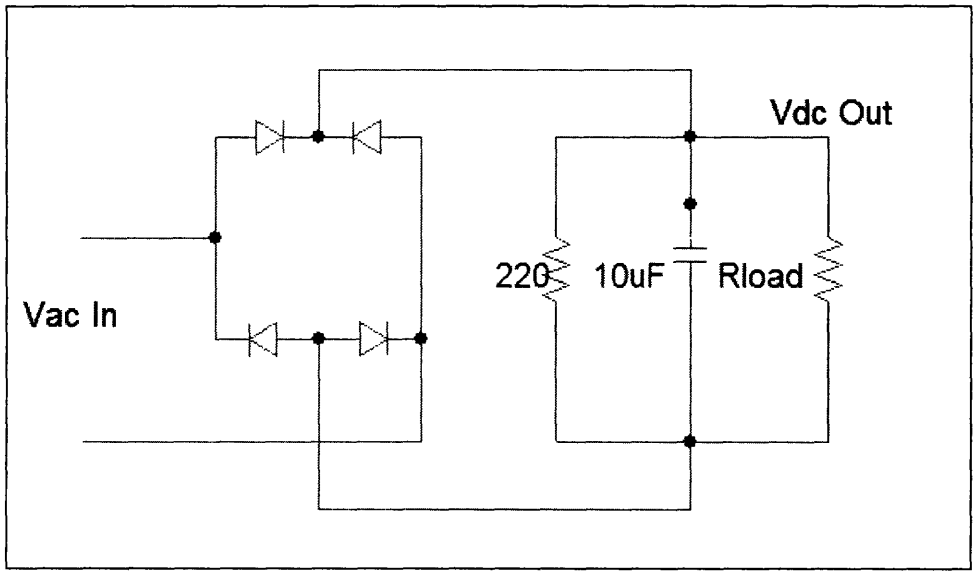

Full-wave bridge rectifier circuit with RC output filtering figure 83.

Note that this circuit requires a differential voltage signal Vac In. To obtain this differential signal we just use a transformer. This will serve several purposes. First, the transformer will allow us to step up or down the AC voltage to get a desired output DC value. Secondly, the transformer provides electrical isolation from the PWM power line. This serves as an added safety measure to prevent from shock or fire, which is an important factor when designing real-world systems.

The ripple voltage at Vdc can be decreased as desired by increasing the value of C. Another option available to decrease the voltage ripple is to use an inductor in series with the parallel RC network, creating a second order filter.

It is easy to get some preliminary values of what these components should be. We are inserting 1W of power at 1MHz into a transmission line with 18 Ohm characteristic impedance. Therefore, the voltage amplitude of our sinusoid must be:

$$P = \frac{V_{RMS}^{\ 2}}{Z} = \frac{(.707A)^2}{18} = 1$$
$$A = 6V$$

If our feedback circuitry operates off of a 5V supply, we don't need any voltage stepping, as the diode drops in the rectifying circuit will add up to close to 1V, yielding our required 5V. If we were not this fortunate, we would need to add a step-up or step down transformer before the rectifying stage.

The output voltage ripple can be expressed in terms of the output current I and the period of the AC signal T (which is 1/10^6 for our 1MHz case):

$$I = C\frac{dV_c}{dt} \Rightarrow \frac{I}{C} \approx \frac{\Delta V}{\Delta t}$$
$$\Delta V = \frac{I}{C}\Delta t = \frac{I}{C}\frac{1}{2T}$$

The factor of 2 in the period T is due to the fact the full-wave rectifying topology is utilizes both halves of the sinusoid. The current I can be approximated by assuming that our feedback circuitry is always operating at full power (pessimistic approximation), such that IV=1W -> I=.2A. Therefore;

$$\Delta V = \frac{1e-7}{C}$$

For example, if we use a 10uF capacitor, the voltage ripple will be .01V, or 0.2% of our 5V supply. A final design might include a voltage regulator to control the voltage output much more precisely.

5. CONCLUSIONS

5.1. Overview of Results

We proved that reliable data transmission through a typical motor power cable is in fact possible. Furthermore, by using simple filtering and coupling techniques, we were able to transmit information through the power cable in the presence of high-voltage simulated PWM signals. By using simple passive filters our system separated the PWM spectral content from the 900MHz FSK modulated data for simultaneous transmission on the same conductor.

The maximum data rate achieved was limited by our choice of transceiver, a ready to use radio modem. Although we only tested data rates of 115 Kbps, 1Mbps 900MHz FSK transceivers are readily available in the market which would comply with the required data throughput rate.

The measured data rates show that our modems impose a limit on how reliable the communications channel is, independent of our motor cable, PWM signals or coupling circuits. For strong RF signals with RSSI (Received Signal Strength Indicator) values above -60dBm, minimum error rates were limited by internal constraints of the RF modems to 0.01%. The error rates became progressively worse as the RSSI values decreased, such as under reduced signal transmission power levels or under increased attenuation. The lowest error rates for our full system test were in the order of .12%. It was observed that error rates did not increase with or without the presence of PWM power signals when RSSI values exceeded -80dBm. This indicates that the total spectral

power of the PWM signals in the 900MHz band should be substantially less than -80dBm. A low spectral power value is consistent with our cable loss measurements.

We proposed a solution for transmission of DC power for feedback motor electronics and RF transmitter power by using a similar approach as we did for data transmission, using 1MHz as a 1W power carrier at an intermediate frequency between PWM and feedback data spectra. The 1MHz power carrier is then rectified to obtain DC power for feedback electronics. Simulations show that our proposed solution is feasible. The chosen rectification topology is efficient so heat generation should not be a problem.

5.2. Review of thesis objectives

We have achieved the goals for this investigation outlined in section 1.5. We measured and characterized typical PWM motor power signals and feedback signals both in the time and frequency domain. We also characterized the high-frequency behavior of our reference motor power cable. Furthermore, FSK at a carrier frequency of 900MHz was chosen as the modulation technique for data transmission. Then, we designed, built and tested high-pass couplers to inject and extract the data signals by using feed-through capacitors. We used a high-voltage pulse wave generator to simulate a worst case (worse by a factor of 10) scenario for real PWM motor waveforms. Successful data transmission in the prescence of PWM type power pulses was demonstrated. In addition, we proposed a design for transmission of DC power for motor feedback electronics by use of an intermediate frequency power RF signal, while at the same time addressing electrical isolation and safety issues. Finally, we tested our proposed system under different

conditions for data transmission error measurements and found promising results for the proposed design approach.

5.3. Future work

Some topics of interest to be investigated for future work on this subject include:

- Optimization of the system for cost/performance
  - Replace RF modems with modulation transceivers
  - Explore different modulation techniques
  - Implement a higher order filter design to reduce insertion loss/increase cutoff sharpness
  - Improve RF matching for more efficient data transmission
  - Explore non spread-spectrum technologies for higher data rates
- Explore different modulation frequencies, such as 450MHz, 2.4GHz
- Investigate 2 pair differential transmission to reduce ground-loop effects
- Increase DC power transmission spec to ~1.5W for motor feedback electronics + transceivers
- Implement and demonstrate DC power transfer in the presence of PWM power signals
- Miniaturization of the system to fit inside small motor casings
- Demonstrate system performance with real motor/drive systems
- Enable asymmetric data transmission from drive to motor (slow speed) for control variable setup.

References:

1. Deutsch, A., et al. 1990. High-speed signal propagation on lossy transmission lines. *IBM J. Res. Develop,* 34 (4), 601-615

2. Sekizawa, M., 1998. Power Lines Used for Data Communications. *Transmission & Distribution World*, 1 October 1998.

3. Butler, L., 1989. Transmission Lines and Measurement of their Characteristics. *Amateur Radio*, October 1989.

4. Pavlidou, N., et al. 2003. Power Line Communications: State of the Art and Future Trends. *IEEE Communications Magazine*, April 2003.

5. Tang, L.T., et al. 2003. Characterization and Modeling of In-Building Power Lines for High-Speed Data Transmission. *IEEE Transactions on Power Delivery*, 18 (1), 69-77.

6. Hanher, T., Mund, B., 1998. *Screening of Cables in the MHz to GHz Frequency Range Extended Application of a Simple Measuring Method* [online]. Available from: http://www.bedca.com/pdf/mcsstech/TRIAXHM6n.pdf [Accessed 29 January 2006]

7. Johnson, H., 2003. *High Speed Signal Propagation: Advanced Black Magic.* Prentice Hall.

8. Lesurf, J., *Skin Effect Internal Impedance and Types of Wire* [online]. University of Saint Andrews. Available from: http://www.st-andrews.ac.uk/~www_pa/Scots_Guide/audio/skineffect/page1.html [Accessed 29 January 2006]

9. Anthes, J., *OOK, ASK and FSK Modulation in the Presence of an Interfering Signal* [online]. RF Monolithics, Dallas, Texas. Available from: http://www.rfm.com/corp/appdata/ook.pdf [Accessed 29 January 2006]

10. Moreira, A. F., et al., 2002. High-Frequency Modeling for Cable and Induction Motor Overvoltage Studies in Long Cable Drives. *IEEE Transactions on Industry Applications*, 38 (5), 1297-1306.

11. Bulington, E., et al., 1998. *Cable Alternatives for PWM AC Drive Applications* [online]. Available from: http://bwcecom.belden.com/college/techpprs/capwmtp.htm [Accessed 29 January 2006]

12. Horak, R., 2005. *Access Broadband over Power Line* [online]. Available from: http://www.commweb.com/howto/164300852 [Accessed 29 January 2006]

13. Collier, S. E., 2004. Delivering Broad Band Internet over Power Lines: What You Should Know. *IEEE Conference Papers*, No. 04-A1, 1-11.

14. AARL, 2006. *Broadband over Power Line (BPL) and Amateur Radio Scientific Papers and Studies* [online]. Available from: http://www.arrl.org/tis/info/HTML/plc/scientific-studies.html [Accessed 29 January 2006]

15. Roberts, R., *Introduction to Spread Spectrum* [online]. Available from: http://www.sss-mag.com/ss.html#tutorial [Accessed 29 January 2006]

16. Watson, B., 1980. FSK: Signals and Demodulation [online]. *The Communications Edge*, 7 (5). Available from: http://www.wj.com/pdf/technotes/FSK_signals_demod.pdf [Accessed 29 January 2006]

17. Johansson, J., Lundgren, U., 1996. *EMC of Telecommunication Lines*. Thesis , (M.S.). University of Luleå.

18. Strangio, C. E., 2006. *The RS232 Standard; A Tutorial with Signal Names and Definitions* [online]. Available from: http://www.camiresearch.com/Data_Com_Basics/RS232_standard.html#anchor1154232 [Accessed 29 January 2006].

19. HW-Server, *RS-232 – overview of RS-232 standard* [online]. Available from: http://www.hw-server.com/rs232 [Accessed 29 January 2006].

20. Skibinski, G., et al., 1997. *Cable Characteristics and Their Influence on Motor Over-Voltages* [online]. Available from: http://iecxplore.ieee.org/iel3/4379/12569/00581441.pdf?arnumber=581441 [Accessed 29 January 2006]

21. Ran, L., et al., 1998. Conducted Electromagnetic Emissions in Induction Motor Drive Systems Part II: Frequency Domain Models. *IEEE Transactions on Power Electronics*, 13 (4), 768-776

APPENDIX I

Summary, Goals and Targets for Position Control System
Danaher Project

C.M. Cooke, MIT
Sept 30, 2004

2b

Project Goals:

Reduce cost by reduction in the number of wires and connectors in the cable between drive and motor, such as might be achieved by changes to the communications protocol. The changes should maintain present performance, satisfy present constraints, and allow flexibility for future product enhancements.

Issues and Constraints:

1. three required electrical connections between drive and motor
   - a) motor power (100 watt to 10K watt shaft power)
   - b) sensor power
   - c) data protocol and transmission

2. four Modes of Operation:
   - I) full power, all ON
     - i) handle power failure, 100 sec coast down
     - ii) independent drive mechanical brake
   - II) no motor power, full 'brain' power
     - i) all sensors and analysis fully functional
     - ii) report ID info on 'brain' power-up
   - III) wires connected, but Mains Power OFF
     - i) coarse turn position measured and retained
     - ii) no reporting of info
   - IV) wires disconnected
     - i) keeps ID info
     - ii) still measure and retain coarse position (future only, desired if possible to do)

3. 1 watt power needed by existing conventional sensors/electronics
   - a) power, especially for resolver sensor or optical encoder
   - b) lowest level that might work is 0.1 watt

4. human safety barrier; CE = 'reinforced insulation' (line to human touch)
   - a) 3750 v high pot
   - b) 5.5 mm creepage

5. $ cost ≤ present 4 wire for FB/sensors
   - a) connectors at $15 motor end, and $5 at driver end
   - b) cable at $1/m
   - c) retained position function adds about $15 more.

Issues and Constraints: (cont.)

6. system application options
    a) point-to-point motion with retained position (example is robotic arm motion)
    b) point-to-point without retained position
    c) rotation only

7. accuracy, speed
    a) 20+ bits / rev
    b) about an arc-min absolute position
    c) bandwidth about 1 kHz to 10 kHz
    d) about 32 bit per data packet (includes 5 bit CRC)
    e) always absolute position within motor electronic cycle
    f) 400Hz sampling during power failure coastdown

8. data rate of about 2Mbaud, due to accuracy and speed

9. high signal integrity
    a) low error rate
    b) low latency, (30 μsec max with 5 μsec uncertainty)

10. temperature and humidity
    a) -20°C to +120°C is desired
    b) minimum possible is 0°C to 100°C
    c) humidity: 10% to 90% non-condensing

11. space limited: at motor
    a) 30 to 40mm diam, 15mm thick

12. possible production quantity: 10K to 100K per year

13. Future implementation, Mode IV-ii (see item 2 above)
    a) know number of shaft turns (coarse) made by manual turns
        i) read motor shaft at up to 600 rpm
    b) save value and report at power up
    c) system already has EE prom ID info
        i) last forever
        ii) read typically at power up
    d) all report of stored info only under full power mode

14. cable properties
    a) lengths range from 0.1 to 50 meters
    b) lightly twisted, stranded motor drive wire
        i) typical surge impedance ~ 20 ohms
        ii) other wire type limits, wire size (#18?) etc.
    c) keep flexible

15) more cable properties
    a) needed shielding
        i) FCC specs
        ii) meet industry standard conventions
        iii) inside-to-outside and also out-to-inside.
    b) cross-talk specs
        i) need info about motor drive signals
        ii) model for motor drive noise
    c) existing standard cables
        i) quantified shielding
    d) existing special cables
        i) for RS485, require < 0.1 volt noise peaks
    e) grounding requirements

16) connectors
    a) at least two types; std 8-pin and Molex (not shielded)
    b) may use terminal block barrier strips at Drive End

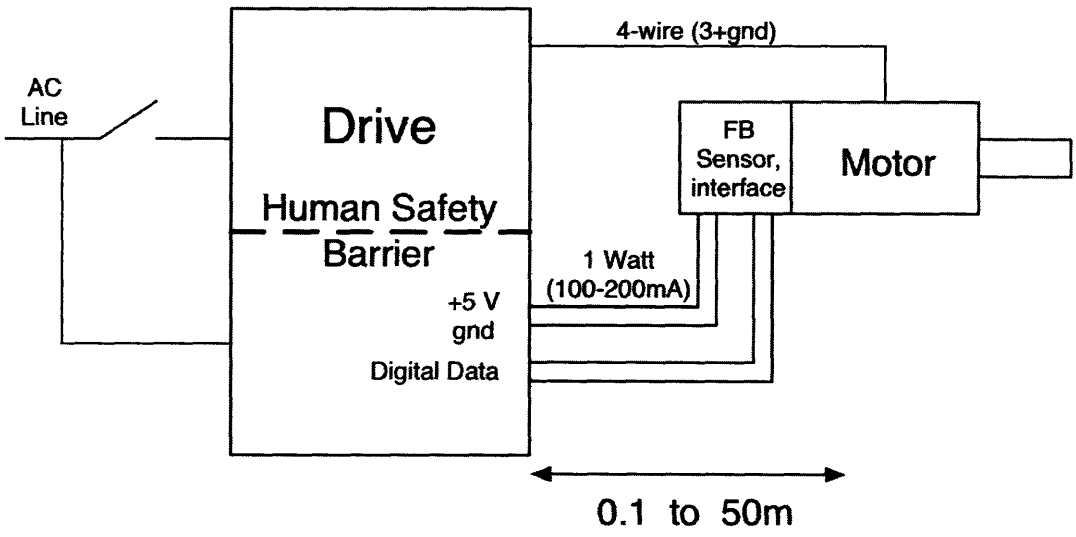

Reference diagram for position control system, base on "4-wire" FB and sensors, plus 4 wire drive.